

Self and Tracer Diffusion of Polymers in Solution

George D. J. Phillies*

Department of Physics, Worcester Polytechnic Institute, Worcester, MA 01609

The literature on self-diffusion of polymers in solution, and on tracer diffusion of probe polymers through solutions of matrix polymers, is systematically reviewed. Virtually the entirety of the published experimental data on the concentration dependence of polymer self- and probe-diffusion is represented well by the same functional form. This form is the stretched exponential $\exp(-\alpha c^\nu)$, where c is polymer concentration, α is a scaling prefactor, and ν is a scaling exponent.

Correlations of the scaling parameters with polymer molecular weight, concentration, and size are examined, and compared with predictions based on the form's hydrodynamic and renormalization-group derivations. α increases markedly with polymer molecular weight, namely $\alpha \sim M^x$ for $x \approx 1$. ν is ≈ 0.5 for large polymers (M larger than 400 kDa or so), but increases toward 1.0 or so at smaller M . Scaling parameters for the diffusion of star polymers do not differ significantly from scaling parameters for the diffusion of linear chains of equal size.

I. INTRODUCTION

The objective of this review is to present the experimental phenomenology for polymer self-diffusion and for diffusion of tracer polymers through polymer solutions. We proceed by examining how the diffusion coefficient depends on polymer concentration c , polymer molecular weight M , solvent quality, and other variables. We examine how rapidly a probe polymer of molecular weight P diffuses through a matrix polymer of molecular weight M , perhaps as the concentrations of the matrix and probe polymers are varied. After establishing the phenomenological behavior, we compare the phenomenology with various classes of theoretical model.

This is not a review of the extremely extensive theoretical literature on polymer diffusion in solution. For such reviews, note works of Graessley¹, Tirrell², Pearson³, Skolnick⁴, Lodge⁵, and (more recently but less directly) McLeish⁶. Recent papers by Schweizer and collaborators^{7,8,9} include extensive references to the more recent literature. We will note classes of models, but not their underlying derivations. We also do not consider melt systems, or polymer mutual diffusion.

In comparing phenomenology with model predictions, it will remain critical to distinguish between properties that are consistent with a particular model, but do not actually prove it, and properties that require or refute the correctness of a particular model. For example, Skolnick¹⁰ has shown that the nominal signature of reptation $D_s \sim M^{-2}$ is found in computer models of polymers, in a model system in which the chains are very certainly not reptating. A finding $D_s \sim M^{-2}$ is thus consistent with many tube-type solution models, but does not prove their correctness. On the other hand, most tube-type models require that polymer chains move via constrained diffusion for shorter times. In these models, the shorter-time mean-square displacement of a single chain must scale more slowly than linearly with time. If the shorter-time mean-square displacement were instead linear in elapsed time, many constrained-diffusion models would be rejected by experiment.

Section II presents a theoretical background for the experimental papers reviewed here. Sections III and IV treat, respectively, data on (i) self-diffusion coefficients of polymers of solution and (ii) data on probe diffusion coefficients in polymer matrix solutions. Section V briefly remarks upon other papers on polymer self- and probe-diffusion that do not lend themselves to the analytic approach applied here. A systematic study of the phenomenological parameters obtained by our analysis appears in Section VI. Section VII summarizes conclusions. Tables of fitting parameters appear as Appendices.

II. THEORETICAL BACKGROUND

This Section presents a consistent nomenclature for polymer diffusion coefficients and describes methods whereby which such diffusion coefficients are measured. A short description is given of the literature on diffusion in multimacrocomponent solutions. The literature in question provides the fundamental basis for interpreting the experimental measurements. Finally, phenomenological classes of models for polymer dynamics are identified.

A. Nomenclature for Diffusion Coefficients

This section sets out a consistent nomenclature for the diffusion coefficients that we are reviewing. In a solution containing a solvent and one macromolecular species, two physically distinct diffusion coefficients usefully characterize macromolecule diffusion. One of these, the two-particle or *mutual* diffusion coefficient D_m , describes via Fick's law

$$\vec{J} = D_m \vec{\nabla} c \quad (1)$$

the relaxation of a concentration gradient. Here \vec{J} is the diffusion current and c is the local instantaneous macromolecule concentration. The other diffusion coefficient, the single-particle or *self* diffusion coefficient D_s , describes the diffusion of a single macromolecule through a

uniform solution of otherwise identical macromolecules. In a simple macromolecule solution, quasi-elastic light scattering spectroscopy (QELSS) measures the mutual diffusion coefficient of the macromolecules^{11,12}. Pulsed-field-gradient nuclear magnetic resonance (PFGNMR) measures the self-diffusion coefficient.

Solutions containing a solvent and two macromolecule species show a more complicated diffusive behavior. Theoretical treatments of this issue are described in the next section. In general, in two-macrocomponent solutions the temporal evolution of transient concentration fluctuations is described by two relaxation times, each describing the relaxation of a coupled mode involving the concentrations of both macromolecule species. An interesting special case arises if one macrocomponent, the *probe*, is adequately dilute, while the other macrocomponent, the *matrix*, may be either dilute or concentrated. In this special case, the diffusion of the probe species is governed by a single-particle diffusion coefficient, namely the *probe* diffusion coefficient D_p . In the special case that the matrix species and solvent are isorefractive, so that the index of refraction is independent of the relative amounts of matrix polymer and solvent, the matrix species scatters next to no light. If in this special case light scattering by a dilute probe species dominates scattering by the solution (which further requires that solvent scattering be sufficiently weak), the diffusion coefficient measured by QELSS is^{12,13} the probe diffusion coefficient D_p .

A variety of physical techniques have been used to measure probe diffusion through a polymer solution. In the fluorescence recovery after photobleaching (FRAP) technique, a small fluorescent label is attached to the probes. An intense pulse of light (the ‘pump’ laser beam) is then used to destroy (“bleach”) the fluorescent labels in some regions of the solution, the regions sometimes being defined via a holographic grating. Much weaker laser illumination (the ‘probe’ beam) is then used to monitor the recovery of the fluorescence intensity as unbleached fluorescent molecules diffuse back into the regions(s) in which the bleaching occurred.

An alternative to FRAP is Forced Rayleigh Scattering (FRS). In an FRS experiment, an intense laser pulse is used to generate a holographic brightness grating in solution. The grating selectively alters a photosensitive part of the probe molecule, thereby creating an index of refraction grating in the solution. A much weaker probe beam is then used to monitor the diffusive relaxation of the induced grating. Significant complications may arise if the photomodified and non-photomodified forms of the probe species differ significantly in their diffusive properties. If the probe species is dilute, with either FRAP or FRS the time dependence of the recovery profile is determined by the single-particle (probe-) diffusion coefficient of the probe molecules¹³.

A physically-distinct alternative to FRAP and FRS is fluorescence correlation spectroscopy (FCS), in which optical methods are used to measure fluctuations in the number of fluorescent molecules in a small volume of

space. In nondilute solution the diffusion coefficient measured by fluorescence correlation spectroscopy (FCS) varies from D_p to D_m as the fraction of macromolecules that bear fluorescent tags is varied from small to large¹³.

When is a probe species dilute? In general, the careful experimenter makes an adequate control study of the effect of varying the probe concentration c_p . D_p is the extrapolation of the measured probe diffusion coefficient to zero probe concentration. In some systems D_p is substantially independent of c_p , and no extrapolation is needed. In other systems (see below) D_p depends significantly on c_p , and extrapolation to $c_p \rightarrow 0$ must be performed. Several authors have measured the initial slope k_d of the dependence of D_p on probe concentration, and the effect of matrix concentration on k_d . It is also possible to study—most published work has used QELSS—the relaxation of concentration fluctuations in a ternary solvent:macromolecule:macromolecule system in which neither macrocomponent is dilute. As reviewed below, such studies give information on the diagonal—and cross-diffusion coefficients of the two species and on their thermodynamic interactions.

Strictly speaking, if FRAP or FRS is used to study the diffusion of a dilute labelled polymer through a matrix polymer solution, the labelled polymer differing from the matrix in that a fluorescent small-molecule label has been attached, the measured diffusion coefficient should be termed a probe diffusion coefficient, because the molecules being tracked are chemically distinguishable from the molecules not being tracked. However, for the purposes of this review, we distinguish between (i) the case in which the probe and matrix polymers are substantially distinct in molecular weight or chemical nature, and (ii) the case in which the probe and matrix polymers are very nearly the same except for the presence of the label. The phrase ‘probe diffusion coefficient’ is reserved for case (i), while measurements under case (ii) are here treated as determinations of the self diffusion coefficient.

The term *tracer* diffusion coefficient is synonymous with *single-particle* diffusion coefficient, and includes both the self and probe diffusion coefficients as special cases. The *interdiffusion* and *cooperative diffusion* coefficients characterize the relaxation times in a ternary system in which neither macrocomponent is dilute. In the following the latter two terms are almost never used.

B. General Theory of Diffusion in Multimacrocomponent Solutions

What is the basis for using spectroscopic methods such as QELSS, FRAP, FRS, or FCS to measure D_s or D_p ? In each case, there is a physical theory that links the correlation function determined spectroscopically to fluctuations in microscopic variables that describe the liquid. For example, for FCS the fluctuations in the fluorescent light intensity $I_f(t)$ arise from fluctuations in the number of fluorescent molecules in the scattering volume. The

time correlation function $C_f(\tau) = \langle I_f(t)I_f(t + \tau) \rangle$ of the fluorescent intensity follows faithfully the time correlation function $C_N(\tau) = \langle N(t)N(t + \tau) \rangle$ of the (fluctuating) number $N(t)$ of labelled molecules in the scattering volume, so to determine the time dependence of $C_f(\tau)$ one only needs to determine $C_N(t)$ and vice versa.

For QELSS, the spectrum is determined¹⁴ by the field correlation function $g^{(1)}(q, t)$ of the scattered light, which is in turn determined by the motion of the scattering molecules via

$$g^{(1)}(q, \tau) = \left\langle \sum_{i,j=1}^N \alpha_i \alpha_j \exp[i\mathbf{q} \cdot (\mathbf{r}_i(t + \tau) - \mathbf{r}_j(t))] \right\rangle, \quad (2)$$

where i and j label two of the N scatterers, $\mathbf{r}_i(t)$ is the position of scatterer i at time t , α_j is the scattering cross-section of particle j , and \mathbf{q} is the scattering vector. For the special case in which the scattering particles are dilute (non-scattering particles do not need to be dilute), correlations between the positions of two distinct scatterers at two times vanish. The correlation function for probe scattering then reduces to

$$g_P^{(1)}(q, \tau) = \left\langle \sum_{i=1}^N \alpha_i^2 \exp[i\mathbf{q} \cdot \Delta \mathbf{r}_i(\tau)] \right\rangle, \quad (3)$$

in which $\Delta \mathbf{r}_i(\tau) = \mathbf{r}_i(t + \tau) - \mathbf{r}_i(t)$.

There are three general approaches to calculating $g_P^{(1)}(q, \tau)$. First, scatterers can be treated as objects having hydrodynamic and direct, e.g., excluded volume, interactions, and the effect of the intermacromolecular interactions on $dg_P^{(1)}(q, \tau)/d\tau$ can be calculated. Second, it can be recognized that $\sum_i^N \exp[i\mathbf{q} \cdot (\mathbf{r}_i(t))]$ is the q^{th} spatial Fourier component of the scatterer concentration at time t , and semicontinuum hydrodynamic methods and the Onsager regression hypothesis can be used calculate the average temporal evolution of a fluctuation. Third, it can be proposed that the scatterers perform simple Brownian motion, with the probability distribution function for $\Delta \mathbf{r}_i(\tau)$ being applied to calculate $g_P^{(1)}(q, \tau)$.

Light scattering spectra of non-ideal single-component macromolecule solutions, including direct interactions and hydrodynamic interactions at the Oseen level, were initially calculated by Altenberger and Deutsch¹⁵. Calculations of light scattering spectra of non-dilute many-component macromolecule solutions soon followed^{11,12,16}. In the latter papers, diffusion coefficients were modeled on the lines of Kirkwood, et al.¹⁷, the diffusion coefficients being written as products of thermodynamic derivatives ($\partial\mu_i/\partial c_j$) obtained from the intermacromolecular forces, and phenomenological transport coefficients Ω_{ij} (here i and j label chemical species). If neither macromolecular species was dilute, the light scattering spectrum obtained by QELSS is predicted^{11,16} to contain two relaxation modes. Even if only one of the two macromolecule species scattered light, both modes are predicted to be visible, in general, in the light scattering spectrum¹².

A subsequent paper¹³ extended these findings to the special case explored e.g., by fluorescence correlation spectroscopy, in which some macromolecules are tagged so that their movements can be tracked. For the case that the tagged macromolecules are dilute, it was shown¹³ that fluorescence correlation spectroscopy and other equivalent techniques measure the self-diffusion coefficient of the tagged probe macromolecules diffusing through the unlabelled matrix macromolecules.

A Smoluchowski approach was used by Jones¹⁸ to examine interacting spherical polymers, including the special case that one of the polymer species is dilute and tagged so that its motions could be observed. In the special case, the measured diffusion coefficient was predicted by Jones to be determined only by the hydrodynamic interactions of the tracer polymers with their (predominantly matrix-polymer) neighbors. While Jones does not use the same nomenclature, the diffusion coefficient of the tracers calculated in ref. 18 may be recognized as the single-particle diffusion coefficient. The hydrodynamic approach culminates in analyses of Carter, et al.¹⁹ and Phillies²⁰ of mutual and tracer diffusion coefficients, including full hydrodynamic and direct interactions between interacting diffusing particles and reference frame issues.

Extensive studies of diffusion of interacting polymers using semicontinuum and related means were made by Akcasu, Benmouna, Cohen and others. In 1987, Benmouna, et al.²¹ calculated dynamic scattering from a solution containing two polymer species, including excluded volume terms with a Flory interaction parameter but ignoring hydrodynamic interactions between polymer chains. Hydrodynamic interactions were neglected in the sense that cross-species transport coefficients were assumed to vanish. The assumption that the hydrodynamic parts Ω_{ij} of the cross-diffusion tensor vanish cannot be true simultaneously in the solvent- and volume-fixed reference frames¹⁷. Polymer solutions can be very concentrated, so neglect of reference frame issues in entirely correct calculations may lead to complications in the physical interpretation of an assumption that hydrodynamics has been neglected.

Benmouna, et al.²¹ examined the special case of two species identical except for their optical scattering cross-sections, showing results consistent with those of Phillies^{12,13}, notably: If the matrix species scatters weakly, an interdiffusion mode describing single-chain motion is dominant at low probe concentrations. There is a thermodynamic regime relative to the spinodal where the diffusion equations describe phase separation. The Benmouna model was then extended to treat solutions of copolymers²², still with neglect of hydrodynamic interactions, and to treat homopolymer: copolymer mixtures²³.

In the same period, Foley and Cohen²⁴ analyzed concentration fluctuations in polymer: polymer: solvent mixtures, using an ornate Flory-Huggins form for the thermodynamic free energy of the mixture, again neglecting interchain hydrodynamic interactions. The case of a

solvent isorefractive with the matrix polymer, in the presence of a dilute scattering species, was treated. Foley and Cohen also examined systems in which both polymer species were nondilute, predicting that in this case the relaxation spectrum is characterized by three distinct relaxation times. In contrast, other calculations on similar models predict only two relaxation times.

Roby and Joanny²⁵ improved the model of Benmouna, et al.²¹ by incorporating interchain hydrodynamic interactions and by improving the model for direct chain-chain interactions. At elevated concentrations, the correctness of the reptation model was assumed. The effect of reptation dynamics on concentration fluctuations was estimated with the approximation that a solution is effectively a polymer melt in which mesoscopic polymer-solvent blobs play the role taken in polymer melts by monomer units. For simplicity, the model was restricted to systems containing equal amounts of two species having the same molecular weight. These restrictions are nontrivial to remove but exclude analysis of tagged-tracer experiments. A model calculation incorporating a similar picture, but without the restrictions, was reported by Hammouda²⁶.

An alternative analysis of a ternary solution of two polymers and a solvent was presented by Wang²⁷, who followed much of the earlier work on polymer solutions in assuming that the cross terms in the mobility matrix vanish. Wang systematically analysed a variety of general and special cases, showing a range of interesting parameters that can be determined from light scattering spectra if the accuracy of his model is assumed. In addition to the tracer case (one polymer:solvent pair isorefractive, visible polymer dilute), Wang analysed the special case “zero average contrast”, in which the polymer refractive increments are of opposite sign, so that concentration fluctuations, that change the total polymer concentration without changing the local polymer composition, scatter no light. Wang showed that the QELSS spectrum of a zero-average-contrast system is almost always bimodal, though it may happen that one of the modes is much weaker than the other.

Treatments of the field correlation function based on a Brownian motion description can be traced back to Berne and Pecora¹⁴, who treat the light scattering spectrum of a solution of dilute, *noninteracting* Brownian particles. The motion of such particles is described as a series of random, uncorrelated steps, in which case from the Central Limit Theorem the probability distribution for particle displacements is

$$G_s(\Delta\mathbf{R}, t) =$$

$$\left[\frac{2\pi}{3}\langle(\Delta\mathbf{R})^2\rangle\right]^{-3/2} \exp[-3(\Delta R)^2/2\langle(\Delta\mathbf{R})^2\rangle], \quad (4)$$

where the mean-square particle displacement is related to the diffusion coefficient by

$$\langle(\Delta\mathbf{R})^2\rangle = 6Dt. \quad (5)$$

Combining eqs 2 and 4,

$$g_P^{(1)}(q, \tau) \sim \int d\Delta\mathbf{r} \exp[i\mathbf{q} \cdot \Delta\mathbf{r}] \times \left[\frac{2\pi}{3}\langle(\Delta\mathbf{R})^2\rangle\right]^{-3/2} \exp[-3(\Delta R)^2/2\langle(\Delta\mathbf{R})^2\rangle], \quad (6)$$

which using eq 5 leads to

$$g_P^{(1)}(q, \tau) \sim \exp(-q^2 D\tau). \quad (7)$$

For Brownian particles in low-viscosity small-molecule solvents, the Stokes-Einstein equation

$$D = \frac{k_B T}{6\pi\eta R}, \quad (8)$$

in which k_B is Boltzmann’s constant, T is the absolute temperature, η is the solution viscosity, and R is the particle radius, generally predicts accurately the particle diffusion coefficient. For diffusion in polymer solutions, two *ad hoc* extensions of this form are encountered:

First, it might be the case that D is not predicted accurately by eq 8. In this case, one could formally define a microviscosity η_μ as

$$\eta_\mu = \frac{k_B T}{6\pi D R}, \quad (9)$$

and compares η_μ with the macroscopically-measured viscosities η of the solution and η_o of the solvent. The microviscosity is more commonly applied to describe diffusion of mesoscopic globular probe particles²⁸, rather than to treat the diffusion of random-coil polymers in solution.

Second, light scattering and other relaxation spectra are not always single exponentials. No matter what functional form $g_P^{(1)}(q, \tau)$ has, one may formally write

$$g_P^{(1)}(q, \tau) \sim \exp(-q^2 D(\tau)\tau) \quad (10)$$

as the *definition* of $D(\tau)$. In this equation, $D(\tau)$ formally appears to be a time-dependent diffusion coefficient, which equally formally defines a frequency-dependent diffusion coefficient such as

$$D(\omega) = \int_0^\infty d\tau \exp(-i\omega\tau)D(\tau), \quad (11)$$

and via several slightly different paths a frequency-dependent microviscosity

$$\eta_\mu(\omega) = \frac{k_B T}{6\pi D(\omega)R}. \quad (12)$$

The real and imaginary parts of $\eta_\mu(\omega)$ can be brought into correspondence with the storage and loss moduli $G'(\omega)$ and $G''(\omega)$.

The second extension has serious physical difficulties. In particular, comparing eqs 5, 7, and 10, and noting from

reflection symmetry that terms odd in q vanish, one finds that the extension assumes that

$$\langle \exp[-q^2(\Delta\mathbf{r})^2] \rangle = \exp[-q^2 \langle (\Delta\mathbf{r})^2 \rangle]. \quad (13)$$

Equation 13 would be correct if sequential random changes in $\sum_{j=1}^N \exp[i\mathbf{q} \cdot \mathbf{r}_j]$ were described by a Gaussian random process, because in that case (and only in that case) the average on the lhs of eq 13 would be entirely described by the mean-square average displacement via the expression $\langle (\Delta\mathbf{r})^2 \rangle$ seen on the rhs of this equation. Brownian motion, in which particle displacements are described by the Langevin equation, is an example of a dynamics that generates a Gaussian random process for which eq 13 is correct. For extensive details, see ref 14.

Omitted from, but critical to, the above discussion are the consequences of Doob's First Theorem²⁹. Doob treated the joint expectation value—what we would now call the correlation function—of random variables including those following Langevin dynamics. If eq 13 is correct, it is an *inescapable* consequence of Doob's Theorem that the relaxation spectrum is a *single* exponential. Conversely, if the spectrum is not a single exponential, then from Doob's theorem

$$g^{(1)}(\mathbf{q}, \tau) \neq \exp[-q^2 \langle (\Delta\mathbf{r})^2 \rangle]. \quad (14)$$

Berne and Pecora's text¹⁴ is sometimes incorrectly cited as asserting that eq 13 is uniformly correct for light-scattering spectra. The analysis in Berne and Pecora¹⁴, which correctly obtains eq 13, refers only to a special-case system. In the system that these authors correctly analyzed, particle displacements are governed by the simple Langevin equation, and particle displacements in successive moments are uncorrelated. That is, this analysis refers to systems in which particle motion is observed only over times *much longer* than any viscoelastic relaxation times.

If particle motion were observed over times shorter than the viscoelastic relaxation times, which in a concentrated polymer solution might be 1 second or more: Particle displacements in successive moments would be correlated. Equation 13 would not be correct. $\log[g^{(1)}(\mathbf{q}, \tau)]/q^2$ would not be proportional to the mean-square particle displacement during τ . The path from eq 2 to eq 12 might be an interesting heuristic, but would not be consistent with the properties of particles executing Brownian motion. Of course, with respect to polymer dynamics the interest in eqs 10–13 has been exactly the study of particle motions at short times, during which viscoelastic effects are apparent in $D(\tau)$, but these are precisely the circumstances under which eq 13 is incorrect.

In addition to the above, there are analyses of melt systems such as the very interesting work of Akcasu and collaborators^{30,31}. Melt systems are not considered here.

C. Phenomenological Forms for

Comparison with Experiment

The approach here is to compare experimental measurements of D_s and D_p with the functional forms and c , P , and M dependences predicted by various treatments of polymer dynamics. There are a very large number of proposed models. Most models fall into two major phenomenological classes, distinguished by the functional forms taken to describe $D_s(c)$. This section sketches predictions of classes of model, not including their underlying physical rationales, in preparation for the comparison.

(1) In *scaling-law* models³², the relationship between D_s , D_p , and polymer properties is described by scaling laws such as

$$D_s = D_1 M^\gamma c^{-x}, \quad (15)$$

where here γ and x are scaling exponents, and D_1 is a scaling prefactor, namely the nominal diffusion coefficient at unit molecular weight and concentration. In some cases, scaling laws are proposed to be true only over some range of their variables, or only to be true asymptotically in some limit. On moving away from the limit, corrections to scaling then arise. For melts, some models derive a scaling law for $D_s(M)$ from model dynamics, and then predict numerical values for γ . (In melts, D_s has no concentration dependence because c is constant.) For polymer solutions, more typically a scaling-law form is postulated. The theoretical objective is then to calculate the exponents γ and x .

Many scaling-type models propose a transition in solution behavior between a lower-concentration dilute regime and a higher-concentration semidilute regime. Scaling arguments do not usually supply numerical coefficients, so there is no guarantee that an interesting transition actually occurs at unit value of a predicted transition concentration c_t rather than at, say, $2c_t$. Correspondingly, the observation that a transition is found at $2c_t$ rather than c_t is generally in no sense a disproof of a scaling model, because in most cases scaling models do not supply numerical prefactors adequate to make a disproof. (Some level of rationality must be preserved. If a physical model leads to c_t as the transition concentration, and the nominally corresponding transition is only observed for 30–150 c_t , and then only in some systems, one is entitled to question if the observed transition corresponds to the transition implied by the model.)

Two transition concentrations are often identified in the literature. The first transition concentration is the overlap concentration c^* , formally defined as the concentration $c^* = N/V$ at which $4\pi R_g^3 N / (3V) = 1$. Here N is the number of macromolecules in a solution having volume V and R_g is the macromolecule radius of gyration. In many cases, c^* is obtained from the intrinsic viscosity via $c^* = n/[\eta]$ for some n in the range 1–4. The second transition concentration is the entanglement concentration c_e . In some papers, the entanglement concentration is obtained from a log-log plot of viscosity

against concentration by extrapolating an assumed low-concentration linear behavior and an assumed higher-concentration power-law behavior (c^x for, e.g., $x = 4$) to an intermediate concentration at which the two forms predict the same viscosity; this intermediate concentration is taken to be c_e . In other papers, the entanglement concentration is inferred from the behavior of the viscoelastic moduli; in particular, an onset of viscous recovery in the melt or solution is taken to mark c_e .

(2) In *exponential* models^{33,34}, the concentration dependence of D_s becomes an exponential or stretched exponential in concentration

$$D_s = D_o \exp(-\alpha c^\nu). \quad (16)$$

Here D_o is the diffusion coefficient in the limit of infinite dilution of the polymer, α is a scaling prefactor, and ν is a scaling exponent; $\nu = 1$ for simple exponentials. Under the circumstance that the probe and matrix molecular weights P and M differ, an elaborated form of the stretched exponential is

$$D_p = D_o P^{-a} \exp(-\alpha c^\nu P^\gamma M^\delta), \quad (17)$$

where γ , a , and δ are additional scaling exponents, D_o now represents the diffusion coefficient in the limit of zero matrix concentration of a hypothetical probe polymer having unit molecular weight, and P^{-a} describes the dependence, on probe molecular weight, of the diffusion coefficient of a dilute probe molecule. On setting $a = \gamma = 0$ and freeing D_o , eq. 17 becomes a parameterization of the matrix molecular weight dependence of D_p for a fixed probe molecular weight.

In the derivations^{33,34,35,36} of the stretched-exponential models, functional forms and numerical values for exponents and pre-factors were both obtained, subject to various approximations. The latter two derivations assume that chain motion is adequately approximated by whole-body translation and rotation, which may be appropriate if $P \approx M$, but which is not obviously appropriate if P and M are substantially unequal, since in this case whole-body motion of one chain and local modes of the other chain occur over the same distance scale.

Some exponential models^{37,38} also include a transition concentration, namely a transition between a lower-concentration regime in which some transport coefficients show stretched-exponential concentration dependences and a higher-concentration regime in which the same transport coefficients show power-law concentration dependences. The transition concentration, which experimentally is sharply defined^{37,38}, is here denoted c^+ . The lower-concentration regime is the *solutionlike* regime; the higher-concentration regime is the *meltlike* regime. Such transitions are seen in some but not all viscosity data³⁷, generally but not always³⁹ at very high concentrations $c[\eta] > 35$. A solutionlike-meltlike transition is very rarely apparent in measurements of D_s or D_p .

There has been interest in derivations of concentration and other dependences of transport coefficients from

renormalization group approaches. Power-law and exponential forms can⁴⁰ both follow from a renormalization-group approach, depending on the location of the supporting fixed point. The stretched-exponential form is³⁶ an invariant of the Altenberger-Dahler⁴⁰ Positive-Function Renormalization Group.

Our analysis will examine whether either of these functions describe experiment. While a power law and a stretched exponential both can represent a range of measurements, on a log-log plot a power law is always seen as a straight line, while a stretched exponential is always seen as smooth curve of nonzero curvature. Neither form can fit well data that is described well by the other form, except in the sense that in real measurements with experimental scatter a data set that is described well by either function is tangentially approximated over a narrow region by the other function.

It would also be possible to divide theories of polymer dynamics into classes based on assumptions as to the nature of the dominant forces in solution. Assertions as to the dominant forces are independent of assertions as to the functional form used to describe $D_s(c)$. The major forces common to all polymer solutions are the excluded-volume force that prevents polymer chains from interpenetrating each other, and the hydrodynamic force that creates correlations in the displacements of nearby chains. In some models, excluded-volume forces (topological constraints) are assumed to dominate, hydrodynamic interactions serving primarily to dress the monomer diffusion coefficient. In other models, hydrodynamic interactions between nearby chains are assumed to dominate, while chain-crossing constraints provide at most secondary corrections.

In addition to the generic forces, chains have chemically-specific interactions including in various cases van der Waals, hydrogen bonding, and electrostatic forces. These interactions substantially modulate the properties of particular polymers. However, diffusion coefficients and viscoelastic parameters of most neutral polymers show highly-characteristic “polymeric” behaviors, almost independent of the chemical identity of the polymer, implying that general polymer properties do not arise from chemically-specific interactions.

In the following, eqs. 15–17 will be systematically compared with the literature on D_s and D_p . The following largely treats diffusion by neutral polymers in good and theta solvents. There is rather little data on self-diffusion of random coil polyelectrolytes. The measurements reviewed here determine diffusion coefficients, not the physical nature of intermolecular forces, so our emphasis is on identifying the class of model, not the type of force, that is significant for solutions.

Comparisons were made via non-linear least-squares fits. The quantity minimized by the fitting algorithm was the mean-square difference between the data and the fitting function, expressed as a fraction of the value of the fitting function. This quantity is the appropriate choice for minimization if the error in the measurement

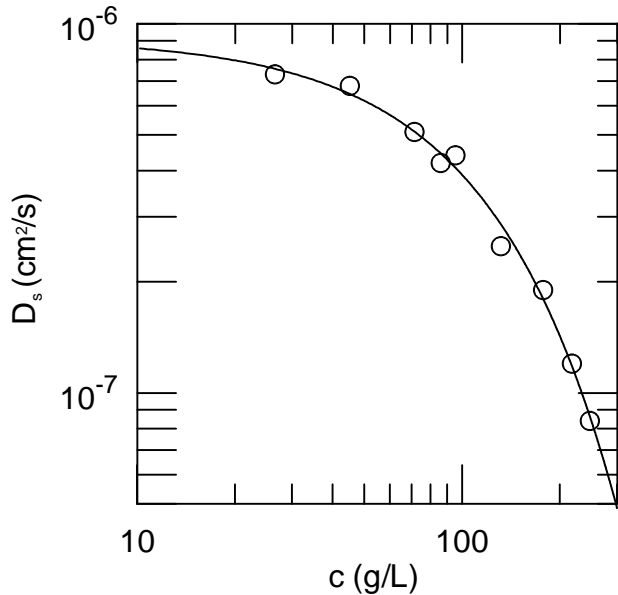


FIG. 1: D_s of 64.2 kDa dextran in water, as obtained with PFGNMR by Brown, et al.⁴¹, and a stretched-exponential fit.

is some constant fraction of the value of the quantity being measured, e.g., if regardless of the value of D_s , D_s was measured to within 1%. In some cases, one or more potentially free parameters were held constant (“frozen”) during the fitting process. For each fit, the corresponding Table reports the final fitting error.

III. SELF-DIFFUSION

This Section presents measurements of the true self-diffusion coefficient, which describes the motion of a labelled chain through a solution of otherwise identical chains. Measurements were primarily made with pulsed-field gradient nuclear magnetic resonance (PFGNMR) and forced Rayleigh scattering (FRS). Results are presented alphabetically by first author, showing for each paper the data and fits to stretched-exponential forms. Fitting parameters appear in Table I. A more detailed analysis of the fitting coefficients appears in Section VI. Whenever possible, polymer concentrations have been converted to grams/liter.

Brown, et al.⁴¹ report self-diffusion and sedimentation coefficients for dextran ($M_n = 44$ kDa, $M_w = 64.2$ kDa) in water, using PFGNMR to determine D_s . They report D_s and s as functions of c for concentrations as large as 250 g/L. Figure 1 shows their data and the corresponding stretched-exponential fit. The self-diffusion data are described accurately by the stretched-exponential form.

Brown and the same collaborators⁴² used PFGNMR to measure D_s of narrow (M_w/M_n of 1.02-1.20) polyethylene oxides in water. Polymer molecular weights were in

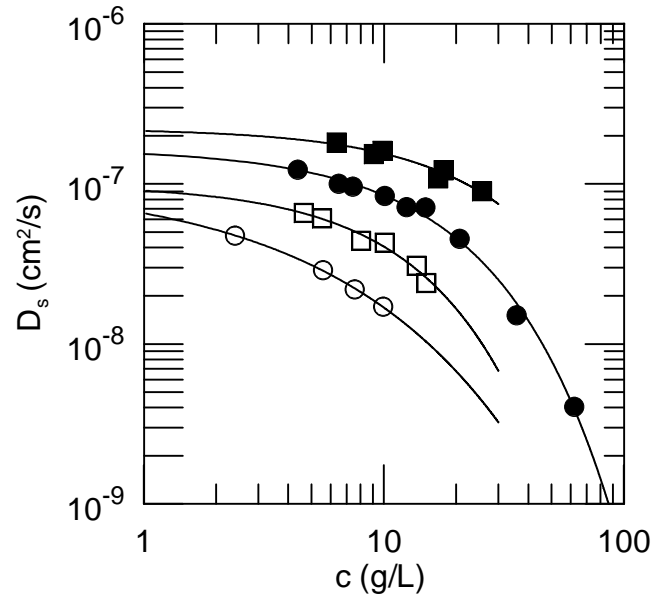


FIG. 2: Self-diffusion coefficients of (top to bottom) 73, 148, 278, and 661 kDa polyethylene oxides in water, using data of Brown, et al.⁴², and exponential fits.

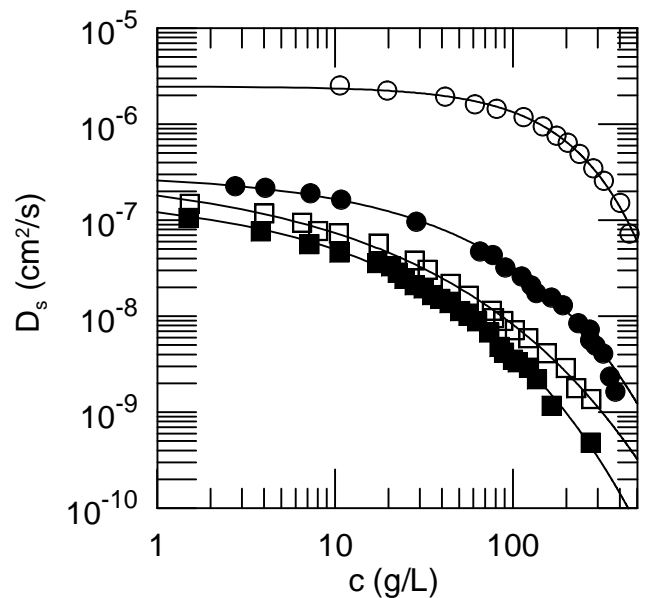


FIG. 3: D_s of [top to bottom] 2, 110, 233, and 350 kDa polystyrenes in CCl_4 as obtained with PFGNMR by Callaghan and Pinder^{43,44,45}, and fits to stretched exponentials.

the range 73-661 kDa; polymer concentrations ranged up to 70 g/l. The same paper reports measurements on these systems of the mutual diffusion coefficient (from QELSS) and the sedimentation coefficient. Figure 2 shows the measurements of D_s . Because measurements were only reported over a limited concentration range, the data

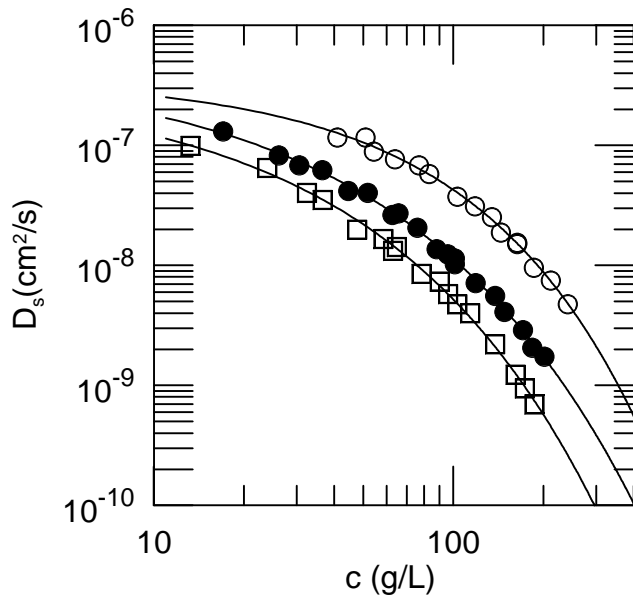


FIG. 4: D_s of [top to bottom] 110, 233, and 350 kDa polystyrenes in C_6D_6 as obtained with PFGNMR by Callaghan and Pinder^{43,44,45}, and fits to stretched exponentials.

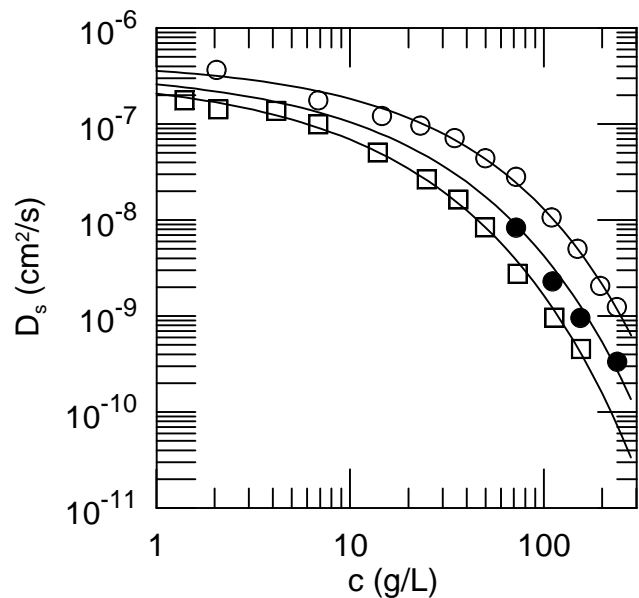


FIG. 5: D_s of [top to bottom] 262, 657, and 861 kDa polystyrenes in cyclopentane near the theta temperature, as obtained with FRS by Deschamps and Leger⁴⁶, and fits to stretched exponentials.

were fit both to a pure ($\nu = 1$) and to a stretched exponential in c . There is excellent agreement between D_s and a pure exponential in c , and almost no improvement in the quality of the fit attendant to allowing ν to be a floating parameter in the fit.

Callaghan and Pinder^{43,44,45} used PFGNMR to study

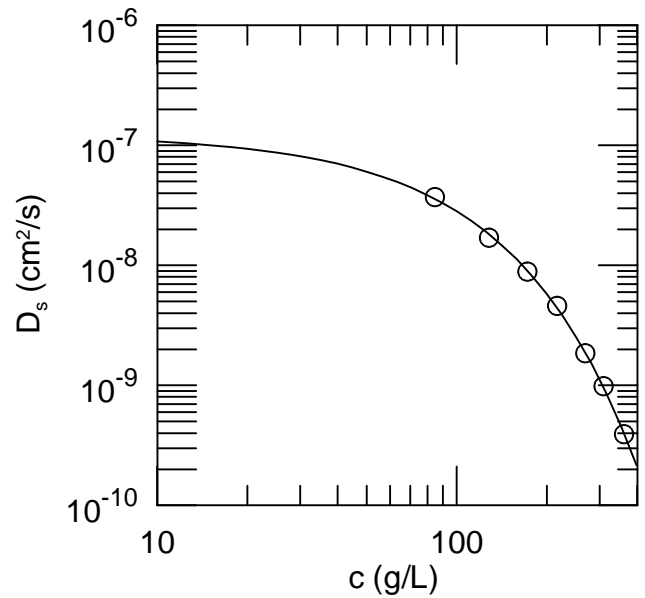


FIG. 6: D_s of 125 kDa polystyrene in toluene as obtained with PFGNMR by Fleischer⁴⁷, and a fit to a stretched exponential.

D_s of 2, 110, 233, and 350 kDa polystyrenes with M_w/M_n in the range 1.06-1.10. Polymer concentrations were as large as several hundred g/L. The solvents were CCl_4 and hexadeuterobenzene. In CCl_4 concentrations well into the dilute regime were observed; in C_6D_6 the measurements of D_s were not extended to low concentration. The data and corresponding stretched-exponential fits appear in figs. 3 and 4. For each polymer:solvent pair, a stretched exponential with constant parameters describes $D_s(c)$ well all the way from the lowest to the largest concentrations studied. The prefactor α tends to increase with increasing polymer M , while D_o and the exponent ν generally decrease with increasing polymer M .

Deschamps, et al.⁴⁶ used FRS to study self-diffusion of polystyrenes in cyclopentane in the vicinity of the theta point. The polymer molecular weights were 262, 657, and 861 kDa; polymer concentrations ranged from 1 to 240 g/L. The polymer polydispersity was in the range $M_w/M_n \approx 1.1 - 1.3$. Figure 5 shows their data and fits to stretched exponentials. For the 657 kDa polymer, D_s was only reported over a narrow, elevated concentration range. For the 657 kDa polymer, the stretched-exponential fit was therefore made by interpolating D_o and ν from their values for the 262 and 861 kDa polymers, leaving α as the only free parameter. For all three polymer molecular weights, the stretched-exponential forms are in good agreement with experiment. The stretched-exponential form for $D_s(c)$ remains valid after a change from good to near-theta solvent conditions.

As an aside, the data of Deschamps, et al.⁴⁶ illustrate well the principle that an experimental test of a par-

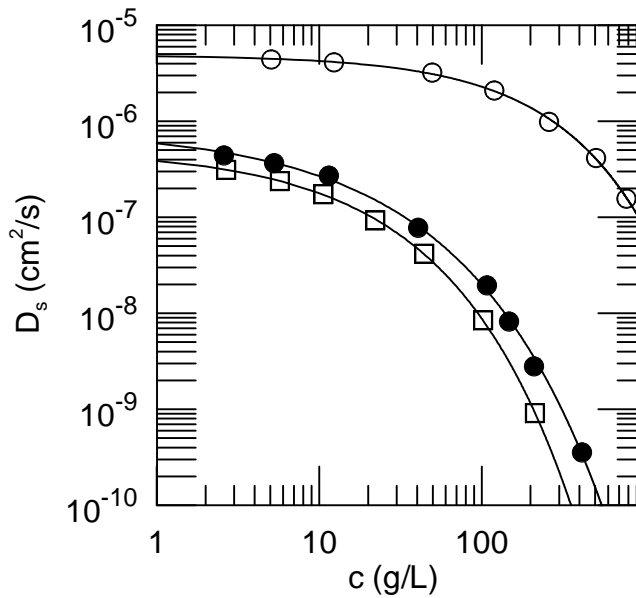


FIG. 7: D_s of [top to bottom] 15, 530, and 730 kDa polydimethylsiloxane in toluene, as obtained with PFGNMR and reported by Giebel, et al.⁵² based in part on work of Skirda, et al.⁵³, and fits to stretched exponentials.

ticular theoretical model is sometimes not optimal as a test for a different theoretical model. Deschamps and Leger's objective was to search for deGennes-type scaling behavior³² of polymer self-diffusion in a theta solvent. Scaling behavior is only expected in the semi-dilute concentration regime $c > c^*$. In Deschamps, et al.'s systems, the semi-dilute regime was expected to be found only for $c > 50 - 100$ g/L. In the context of their objective of studying scaling behavior, there was no strong reason for Deschamps, et al. to measure D_s at lower concentrations, so they rationally did not do so for the 657 kDa system. However, an accurate stretched-exponential fit requires measurements of D_s at small as well as large concentrations. Through no fault of the original authors, the range of concentrations studied for the 657 kDa polymer restrains the utility of the fits that can be made to some of their data.

Fleischer⁴⁷ used PFGNMR to observe self-diffusion of 125 kDa polystyrene, $M_w/M_n \approx 1.02$, in toluene for concentrations 80-320 g/L. These concentrations were estimated to cover $0.5c_e \leq c \leq 2c_e$, where c_e is the concentration above which entanglements were said to be present. c_e was estimated by applying a deGennes-type model to rheological data⁴⁸. Fleischer's measurement appear in Fig. 6. As seen in the Figure, the measured $D_s(c)$ is in good agreement with a stretched-exponential form.

Fleischer's PFGNMR measurements⁴⁷ of the incoherent dynamic structure factor $S_{inc}(q, t)$ of this system show only a single fast relaxation, even under conditions under which QELSS reveals that a slow mode dominates the QELSS spectrum. Fleischer's observation that

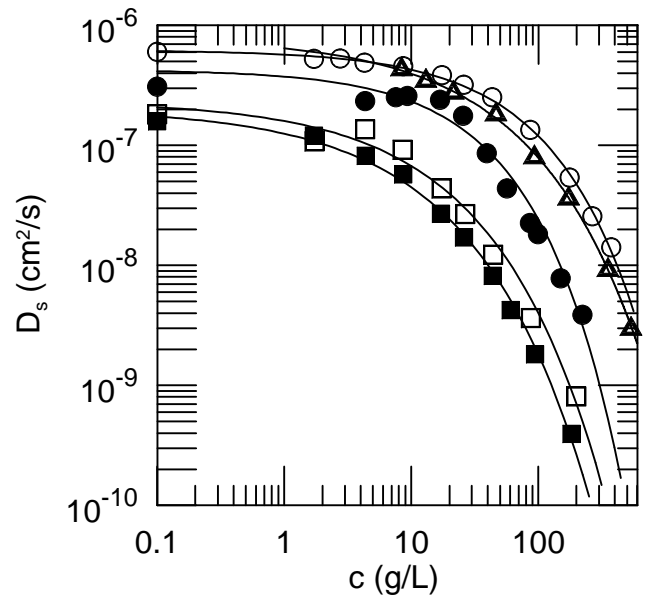


FIG. 8: D_s of [from top to bottom] 78, 123, 245, 599, and 745 kDa polystyrene in benzene, and fits to stretched exponentials (fit parameters, Table I, using data of Hervet, et al.⁵⁵ and Leger, et al.⁵⁶).

the QELSS slow mode cannot be seen in the PFGNMR data is immediately reminiscent of results of Zero and Ware⁴⁹ on fluorescence recovery after photobleaching in poly-L-lysine solutions at low salt concentration. In each set of results, the QELSS spectrum shows distinct slow and fast modes. The slow mode becomes dominant under conditions (higher polymer concentration, lower ionic strength) that enhance 'glassy' behavior. In each case, the appearance and then dominance of the slow mode, when 'glassy' behavior is enhanced, has no effect on the self-diffusion of individual chains. This behavior is hard to understand if the QELSS slow mode is interpreted as arising from long-lived chain clusters with a fixed list of members. The behavior is, however, understandable in terms of a slow mode arising from the appearance of long-lived dynamic structures within which individual chains only have short residence times. Such dynamic properties of D_s and D_m for interacting interpenetrating particles are also seen in Johnson et al.'s^{50,51} model glasses.

Giebel, et al.⁵² report D_s of 15, 530, and 730 kDa polydimethylsiloxane in toluene as obtained with PFGNMR, based in some part on data of Skirda, et al.⁵³. The original measurements cover the concentration range 2-900 g/L of polymer. Fitting parameters are in Table I. Figure 7 shows the actual data and their fits. For each polymer molecular weight, D_s is described well by a stretched exponential in concentration.

Hadgraft, et al.⁵⁴ used QELSS to measure the diffusion of polystyrenes in benzene as a function of molecular weight for $24.8 \leq M \leq 8870$ kDa at 25 C and very low polymer concentration. This data is of spe-

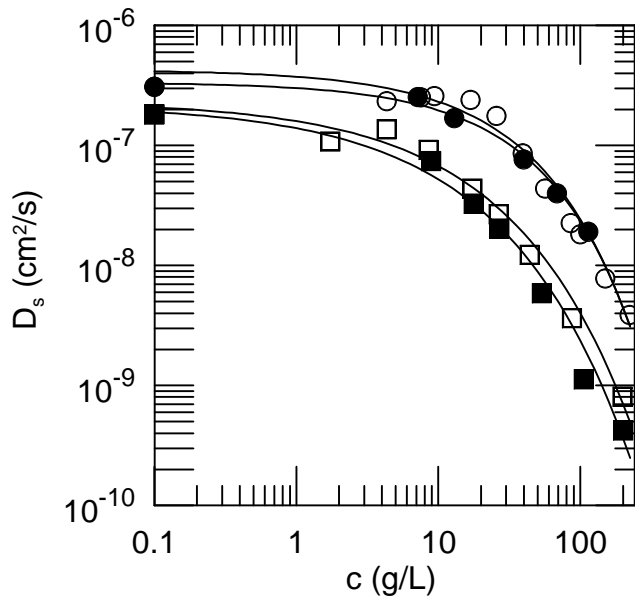


FIG. 9: D of 245 kDa polystyrene in 245 and 599 kDa polystyrene:benzene (open, filled circles, respectively), and 599 kDa polystyrene in 599 and 1800 kDa polystyrene:benzene (open, filled squares), using data of Leger, et al.⁵⁶ and parameters in Table I.

cific interest here in that it supplies values for D_s in the low-concentration region, as a supplement to data sets in which D_s was only obtained at relatively elevated concentrations. Omitting the largest- M point (and thereby reducing the RMS fractional error in the fit from 18% to 8.6%), their data follow $D_o = 4.54 \cdot 10^{-4} M^{-0.588}$.

Hervet, et al.⁵⁵ and Leger, et al.⁵⁶ studied D_s of polystyrene in benzene using FRS to measure the relaxation of photoexcitation patterns. Self-diffusion coefficients were obtained for polymers of molecular weight 78.3, 123, 245, 599, and 754 kDa, with $M_w/M_n \approx 1.06 - 1.12$, for concentrations up to 550 g/L. The same technique was used to obtain diffusion coefficients of labelled 245 kDa probe chains in a 599 kDa polystyrene matrix, and 599 kDa polystyrenes in a 1800 kDa polystyrene matrix. Matrix concentrations ranged from 5 to 400 g/L. To supplement these measurements, many of which were made at elevated polymer concentrations, we used the dilute-solution self-diffusion measurements of Hadgraft⁵⁴ to estimate D_s at very low c .

Figure 8 displays the self-diffusion data of Hervet, et al.⁵⁵ and Leger, et al.⁵⁶ and the fits to stretched exponentials. Except for the 245 (filled circles) and 598 (open squares) kDa polystyrenes, there is good agreement between the reported $D_s(c)$ and the fits. In the two anomalous systems, D_s at first increases with increasing c and then decreases at larger c . The initial increase in D_s with increasing c appears to be substantially larger than the random error in the measurements as inferred from random scatter in the data. The non-monotonic dependence

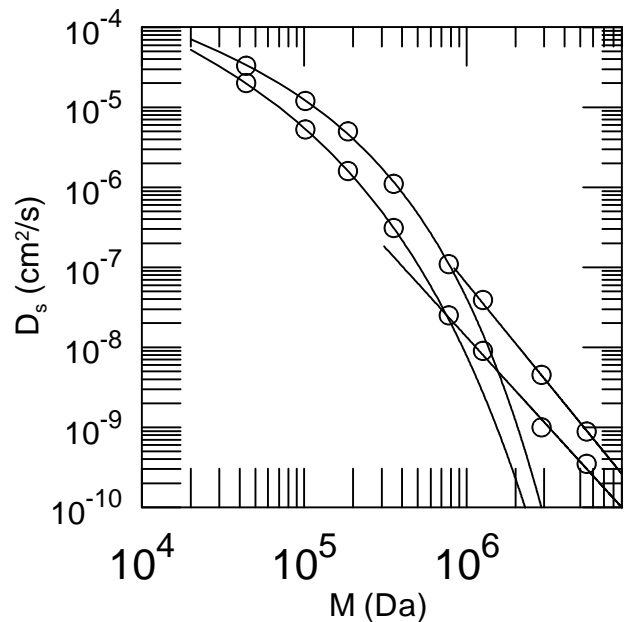


FIG. 10: D_s of 130 and 180 g/L polystyrene in dibutylphthalate as a function of molecular weight, showing the lower-molecular-weight stretched-exponential and the higher-molecular-weight power-law molecular-weight dependences of D_s , using data of Nemoto, et al.⁵⁷, Table II.

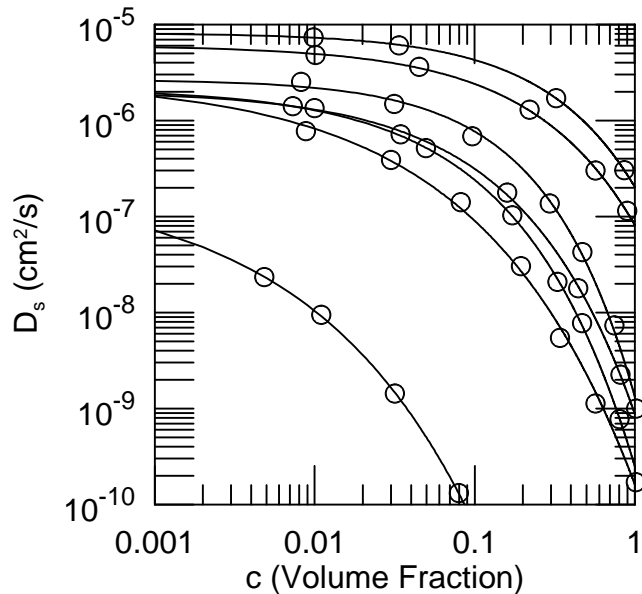


FIG. 11: D_s of poly(ethylene oxide), [from top to bottom, at $\phi \approx 0.1$] namely 2kDa in CHCl_3 and in dioxane, 20 kDa in benzene and in dioxane, 40 kDa in chloroform and in dioxane, and 3600 kDa in dioxane, after Skirda, et al.⁵⁹ Fig. 1a. Lines are fits to stretched exponentials in volume fraction.

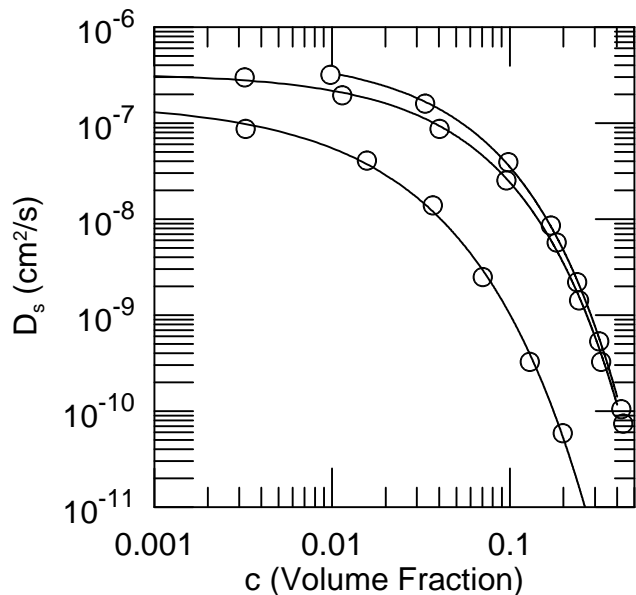


FIG. 12: D_s of polystyrene, namely [from top to bottom] 240kDa in benzene and 1300 kDa in benzene and carbon tetrachloride, respectively, after Skirda, et al.⁵⁹ Fig. 1b. Lines are fits to stretched exponentials in the volume fraction ϕ .

of D_s on c is unique to this specific set of measurements. The lack of agreement between the stretched exponential form and the measured D_s is therefore ascribed to some unique feature of this data, and not to a general property of polymers in good solvents.

Figure 9 presents $D_p(c)$ for the two probe-matrix systems and compares with $D_s(c)$ of polystyrenes of similar molecular weights. For both probe-matrix systems, $D_p(c)$ is described well by a stretched exponential, with no indication of the non-monotonic concentration dependence seen for $D_s(c)$ of the 245 and 598 kDa chains. The 245 kDa polystyrene diffuses approximately equally rapidly through 245 and 599 kDa matrices. The 599kDa polystyrene diffuses markedly more slowly through the 1800 kDa matrix than through the 599 kDa matrix.

Nemoto, et al.⁵⁷ used FRS to measure the self-diffusion coefficient of polystyrene as a function of polymer molecular weight at fixed concentration. The solvent was dibutylphthalate. Polymer molecular weights covered a range $43.9 \leq M_w \leq 5480$ kDa with polymer concentrations of 130 and 180 g/L. The polymers were quite monodisperse, with $1.01 \leq M_w/M_n \leq 1.09$, except for the 5480 kDa material, for which $M_w/M_n \approx 1.15$.

Nemoto, et al.'s results⁵⁷ appear in Fig. 10. A stretched-exponential molecular weight dependence of D_s is not observed at all M . At the two concentrations studied by Nemoto, et al., the molecular weight dependence of D_s has a transition near $M \approx 800$ kDa. At lower molecular weights, a stretched exponential in M describes $D_s(M)$ extremely well. At larger molecular weights, one finds a power-law dependence $D_s \sim M^{-\gamma}$

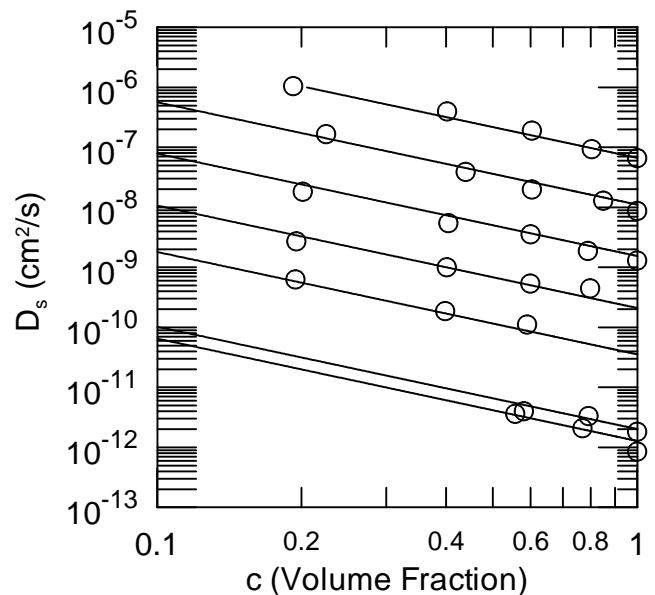


FIG. 13: D_s of hydrogenated polybutadienes in alkanes, with polymer molecular weights [from top to bottom] 4.9, 10.3, 23.3, 53.2, 111, 364, and 440 kDa, and the fitted scaling form $D_s = 55.0\phi^{-1.7}M^{-2.42}$, showing that three parameters and the scaling form suffice to describe $D_s(c, M)$ over a wide range of both parameters. Measurements are from Tao, et al.⁶⁰⁺.

with $\gamma \approx 2.49$ at 130 g/L and $\gamma \approx 2.22$ at 180 g/L.

Nemoto, et al.⁵⁸ used FRS and a cone and plate viscometer to determine D_s and the steady-state shear viscosity η of concentrated solutions (40 and 50 wt%) of 44 and 355 kDa polystyrene in dibutylphthalate. In terms of the transient lattice models, the solutions of the 44kDa polymer are expected to be unentangled, while the solutions of the 355 kDa polymer are expected to be entangled. They found that D_s/T and the fluidity η^{-1} have virtually the same dependence on temperature, at either concentration, both for the 44 kDa polystyrene and for the 355 kDa polystyrene.

Skirda, et al.⁵⁹ used PFGNMR to study the self-diffusion of polyethylene oxides ($M = 2, 20, 40,$ and 3000 kDa) and polystyrenes ($M_n = 240$ and 1300 kDa) in chloroform, benzene, dioxane, and carbon tetrachloride over a full range of polymer volume fractions ϕ . M_w/M_n was ≈ 1.1 for the polyethylene oxides (except the 3000 kDa polymer, for which $M_w/M_n \approx 2$) and ≈ 1.2 for the polystyrenes. Figures 11 and 12 show results for PEO and polystyrene, respectively, and the matching stretched-exponential fits, using parameters from Table I. For each polymer:solvent combination, a stretched-exponential form fits the data well.

Tao, et al.⁶⁰ measured D_s (using PFGNMR and forward recoil spectroscopy) and η (from the dynamic shear moduli) of hydrogenated polybutadienes in alkane solvents. Polymer volume fractions ϕ extended from 0.2 up to the melt while polymer molecular weights cover two orders of magnitude, from 4.8 to 440kDa, with M_w/M_n

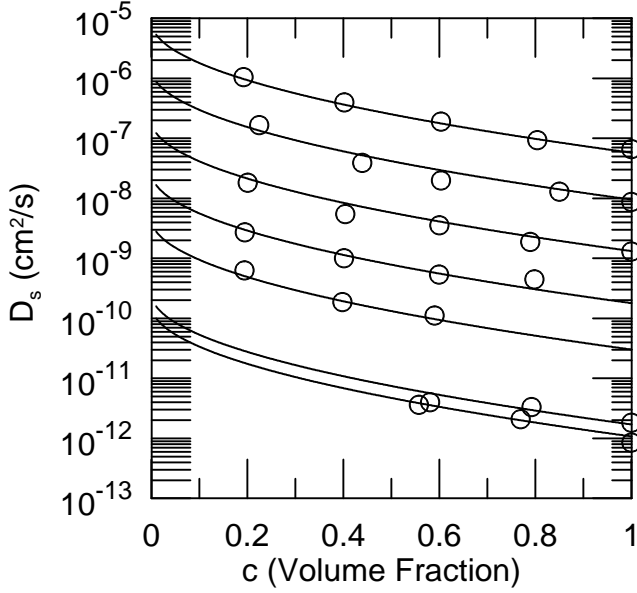


FIG. 14: Same as Fig. 13, except lines now show the fitted form $D_s = 5.54 \cdot 10^3 M^{-2.42} \exp(-5.026c^{0.5} M^{0.00019})$. RMS fractional errors in the fits shown in Figs. 13 and 14 are equal; a stretched exponential in c and M thus suffices to describe this data.

of 1.01-1.03 or less. Tao, et al. fit their self-diffusion data to a scaling description $D_s \sim \phi^a M^b$. When they⁶⁰ forced $a = -1.8$, a one-parameter fit found that the averaged $D_s \phi^{1.8}$ is $\sim M^{-2.41}$.

Figures 13 and 14 show Tao, et al.'s data as fit to power-law and stretched-exponential forms, respectively. In Fig. 13, all points were fit simultaneously to a scaling equation, finding $D_s \sim c^{-1.71} M^{2.42}$, with a fractional root-mean square fitting error of 20.2%. These exponents differ slightly from those of Tao, et al.⁶⁰: Tao, et al. did sequential 2-parameter fits first to determine a and then to determine b , while we did a single three-parameter fit to all points. Figure 14 shows a fit of all data points to the stretched-exponential form $D_{oo} M^{-z} \exp(-\alpha c^\nu M^\gamma)$. The factor M^{-z} appears here because we are combining data on polymers with multiple molecular weights, and the extrapolations $c \rightarrow 0$ of measurements at different molecular weight should extrapolate to a different D_o at each M . Formally, D_{oo} is the extrapolated zero-concentration diffusion coefficient of a highly hypothetical polymer having a molecular weight of unity. On forcing $\nu = 0.5$, we obtain $\gamma = 1.9 \cdot 10^{-4}$ and $z = 2.42$ with an RMS fractional error of 20.2%. Treating ν as a free parameter finds $\nu \approx 0.24$, with virtually the same value of z , $\gamma \approx 0$, and only a slightly improvement (to 19.6%) in the fit error. With either value for ν , the molecular-weight dependence of D_s is almost entirely determined by the prefix M^{-z} . The exponential itself has only a negligible dependence on M .

In Tao, et al.⁶⁰'s systems, scaling-law and stretched-exponential forms for D_s thus provide equally good de-

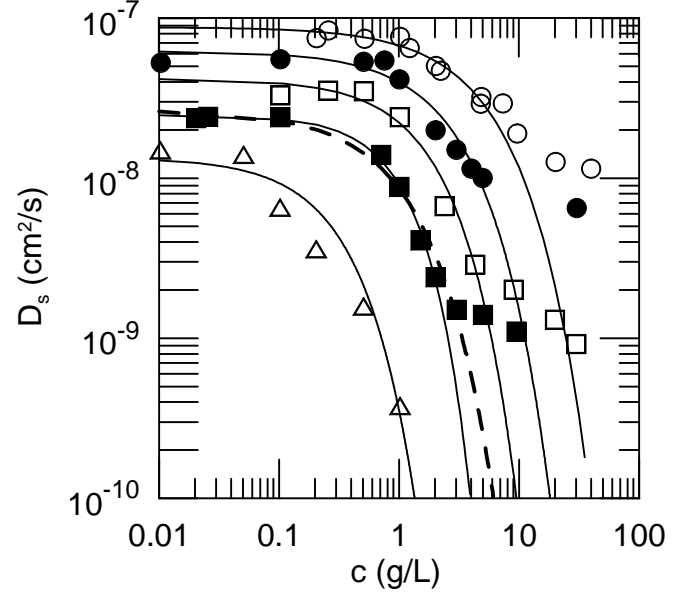


FIG. 15: D_s of xanthan, molecular weights [from top to bottom] 0.45, 0.99, 1.9, 3.8, and 9.4 MDa, in water, and fits of the lower-concentration data to stretched exponential forms. For the 3.8MDa polymer, solid and dashed lines represent fits to the first 7 and 8 data points, respectively. Measurements are from Tinland, et al.⁶¹ Fig. 3.

scriptions of the concentration dependence of D_s . The scaling and stretched-exponential forms also agree as to the molecular weight dependence of D_s at fixed c , namely $D_s \sim M^{-2.4}$. Tao, et al.⁶⁰ concluded that a scaling-law description of their data is correct. The analysis here corroborates this statement, but shows that it is incomplete, in that stretched-exponential forms describe equally accurately the measured $D_s(c, M)$.

Qualitatively, the larger part of Tao, et al.'s viscosity measurements⁶⁰ might have been expected to be in the larger-concentration meltlike ($\eta \sim c^x$) rather than the smaller-concentration solutionlike ($\eta \sim \exp(\alpha c^\nu)$) regime. The transition in the concentration dependence of η between these two functional forms is not transparently evident in $D_s(c)$, whose concentration dependence is consistent with a stretched exponential in c for concentrations up to the true melt. However, contrary to those other systems reviewed in this article, from which molecular-weight dependences can be extracted, here the molecular weight exponent γ of $\exp(-\alpha c^\nu M^\gamma)$ is very nearly zero, so in Tao, et al.'s systems the concentration dependence of D_s is very nearly the same at all M .

Tinland, et al.⁶¹ report on self-diffusion of xanthans of molecular weight 0.45-9.4 MDa, with M_w/M_n in the range 1.2-1.4, at concentrations 0.01-40 g/L. Xanthan forms wormlike chains. The experimental data of Tinland, et al. obtained with FRAP thus differs from D_s of almost all other polymers, in that $d \ln(D_s)/d \ln(c)$

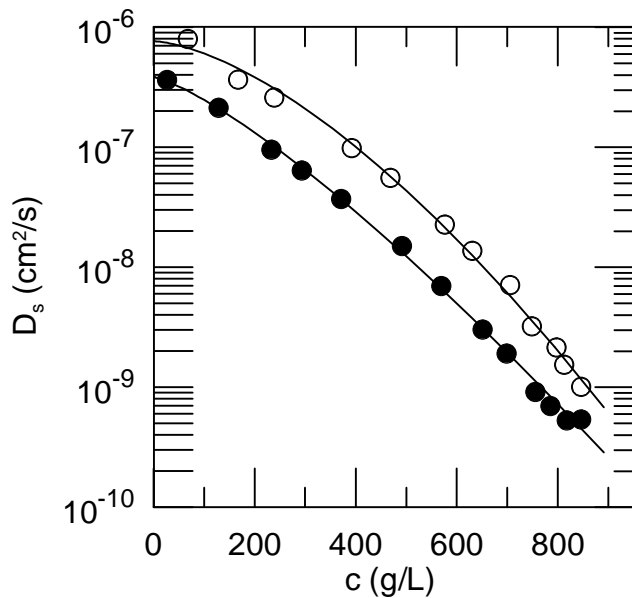


FIG. 16: D_s of $f = 2$ (open circles) and $f = 8$ (closed circles) polyisoprenes in C_6F_5Cl , both with $M_{span} = 5kDa$, and fits to stretched exponentials in c . Data from von Meerwall et al.⁶², Fig. 1.

does not decrease monotonically with increasing c . This phenomenon, which was noted by the original authors, is plausibly related to the appearance⁶¹ of a lyotropic liquid-crystalline phase in this material at elevated c . None of the polymer dynamics models discussed above would be expected to remain valid while the system underwent a phase transition, so the behavior observed by Tinland, et al. does not contradict any model for polymer dynamics. Figure 15 shows Tinland, et al.'s⁶¹ measurements and fits of the lower-concentration data at each molecular weight to a stretched-exponential form. As seen from Table I, the somewhat large RMS fractional errors show that agreement between the measured data and the functional forms is not outstanding. The fit depends marginally on the number of data points included in the analysis. For the 3800 kDa polymer, we indicate (solid, dashed lines) the fits to the first 7 or 8 data points.

For all but the largest- M polymer, there is a concentration c^{**} at which $D_s(c)$ deviates from its low-concentration decline. In Tinland, et al.'s language⁶¹, c^{**} is the concentration of the higher-concentration boundary of the semidilute regime. From Fig. 15, c^{**} appears to decrease with increasing polymer molecular weight.

von Meerwall, et al.⁶² used PFGNMR to measure D_s of linear and star polyisoprenes over a near-complete range of concentrations (polymer weight fraction $0.01 \leq x \leq 1$). The arm number f ranged from 2 to 18. Molecular weights of single arms were 5 and 18 kDa. Figure 16 compares von Meerwall, et al.'s⁶² data on $f = 2$ and $f = 8$ polyisoprene stars having 5kDa arms. Figure 17 shows D_s for $f = 2, 3, 8,$ and 18 star polyisoprenes

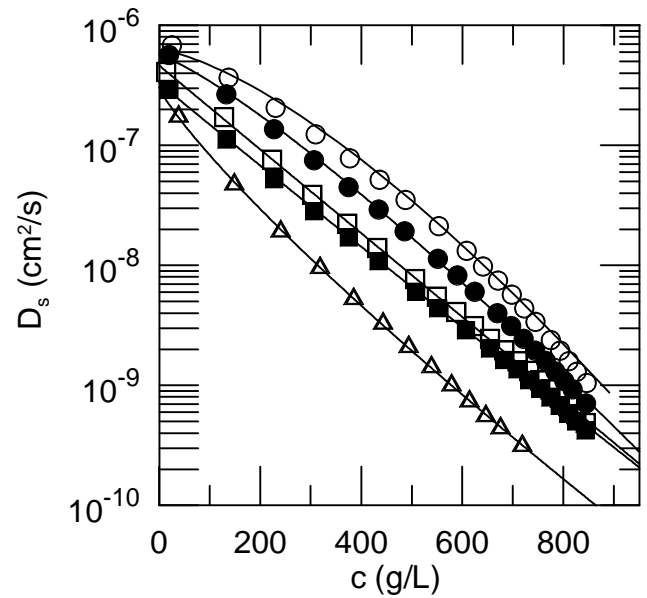


FIG. 17: D_s from von Meerwall, et al.⁶² on [from top to bottom] $f = 2, 3, 8, 18$ polyisoprenes with $M_{span} = 5kDa$ and $f = 8$ polyisoprene with $M_{span} = 14kDa$ in CCl_4 , and fits to stretched exponentials in c .

in CCl_4 . In the original paper, data were reported as smooth curves, not as measured points. To create Fig. 17, the smooth curves were sampled; fits were made to the sampled points. From Fig. 17, at all concentrations increasing the arm count at fixed span molecular weight reduces D_s : Increasing four-fold the number of arms reduces D_s by a factor of 2 to 3. At $f = 8$, an increase in span molecular weight reduces D_s .

In both figures, the solid lines are fits to stretched exponentials. Without exception, $D_s(c)$ for each f and M is described well by a stretched exponential in c . From the fit parameters in Table I, for fixed M_{span} and increasing f one finds that D_o and ν fall while α increases, a two-fold decrease in D_o via increasing f being accompanied by a 20-fold increase in α . For the smallest molecular weights (10-16 kDa) studied, $\nu > 1$ is observed.

von Meerwall, et al.⁶³ used PFGNMR to study linear and 3-armed star polybutadienes and polystyrenes in CCl_4 . They report low-concentration data on all systems, and extensive concentration dependence measurements on some star polymers. Polymer molecular weights ranged from 2.3 to 281 kDa with polydispersities M_w/M_n of 1.03-1.07. As seen in Figs. 18 and 19, for most systems the observed concentration range afforded a one-order-of-magnitude variation in D_s .

Figure 20 gives Ref. 63's measurements on the 6.5, 8.3, 29, and 76 kDa 3-armed stars, which were made over a far wider concentration range that afforded a 2.5-order-of-magnitude variation in D_s . Fits of these data to stretched-exponential forms describe well $D_s(c)$. As initially noted by von Meerwall, et al.⁶³, 'the slopes [in Fig.

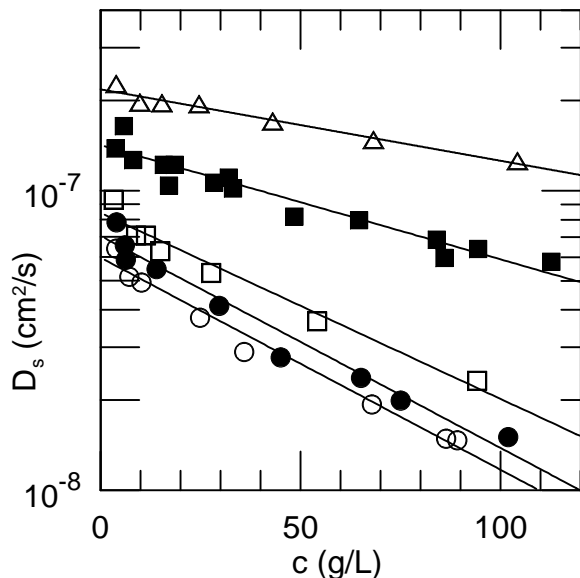


FIG. 18: D_s of [from top to bottom] 2.3 kDa linear, and 6.5, 16.1, 21, and 26 kDa three-armed polybutadienes in CCl_4 , and fits to stretched exponentials, using data of von Meerwall, et al.⁶³, Fig. 2.

20] change continuously' ... deGennes' prediction of a concentration scaling regime $D_s \sim c^{-1.75}$ ($c^* < c < c^{**}$) is not borne out by our data ... at any molecular weight'.

von Meerwall, et al.⁶⁴ used PFGNMR to measure self-diffusion of 10, 37.4, 179, 498, and 1050 kDa polystyrene in tetrahydrofuran at concentrations 6-700 g/L. The same technique was also used to measure D_s of tetrahydrofuran and hexafluorobenzene in the same polymer solutions. Von Meerwall, et al. did not report D_s for their polymers in dilute solution. D_s for these systems in the dilute limit is therefore inferred here from the molecular weight dependence of D_s observed by Hadgraft, et al.⁵⁴ for polystyrene in benzene, together with the viscosities of tetrahydrofuran and benzene. von Meerwall, et al.'s measurements, and stretched-exponential fits appear in Fig. 21, using parameters given in Table I.

Wesson, et al.⁶⁵ used FRS to measure self-diffusion of polystyrenes in tetrahydrofuran and benzene. The polystyrenes had M of 32, 46, 105, 130, and 360 kDa, and were observed for concentrations in the range 40-500 g/L. Wesson, et al.'s measurements were here supplemented by extreme low-concentration points calculated from results of Hadgraft, et al.⁵⁴. These points were included in the fits as having been taken at 0 g/L. Experimental results and the corresponding stretched-exponential fits appear in Fig. 22. Because D_s here covers four orders of magnitude, on the scale of the figure the fits look very good. In fact, RMS fractional errors are in the range 15-21%, making these among the poorer fits in this section to a stretched exponential.

Xuexin, et al.⁶⁶ used PFGNR to measure D_s of lin-

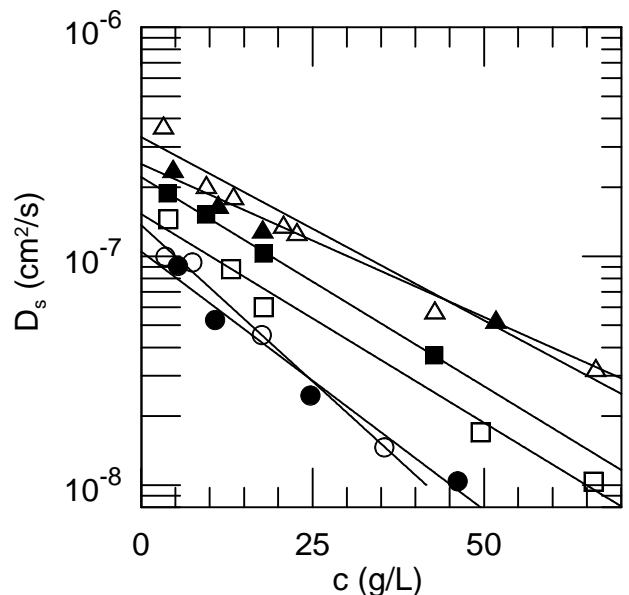


FIG. 19: D_s of [from top to bottom] 75, 76, 90, 161, 227, and 281 kDa polybutadienes in CCl_4 , the 75 and 90 kDa polymers being linear and the others being three-armed stars, and fits to pure exponentials, using data of von Meerwall, et al.⁶³, Fig. 3.

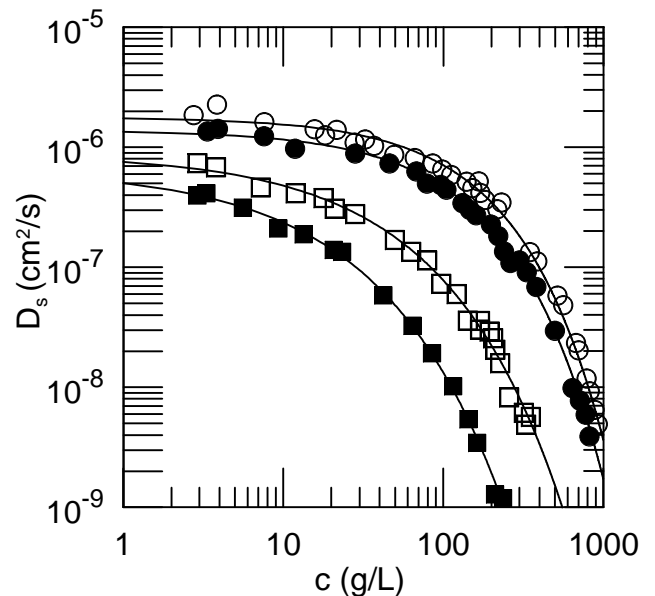


FIG. 20: D_s of [from top to bottom] 6.5, 8.7, 29, and 76 kDa three-armed polybutadienes in CCl_4 , and fits to stretched exponentials, using data of von Meerwall, et al.⁶³, Fig. 4.

ear and 18-armed star polyisoprenes in CCl_4 over a wide range of c and a 100-fold range of M . Their results (with concentrations replotted in g/L) appear as Figs. 23, 24, and 25. In every case the concentration dependence of D_s is described well by the stretched exponential form, with fitting parameters given in Table I.

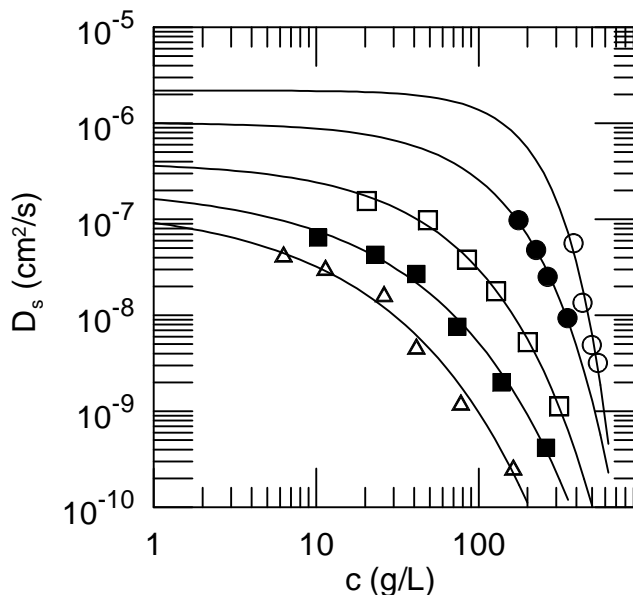


FIG. 21: D_s of 10, 37, 198, 498, and 1050 kDa linear polystyrenes in tetrahydrofuran, and fits to stretched exponentials in c . Data after von Meerwall et al.⁶⁴, with supplemental low-concentration data based on Hadgraft, et al.⁵⁴.

Figure 23 shows $D_s(c)$ for four low-molecular-weight (61, 92, 193, 216 kDa) 18-arm polyisoprenes. With increasing M and fixed f , D_o and ν decrease, while α increases, the increase in α being modestly more rapid with increasing M than is the decrease in D_o . These trends are continued in Fig. 24, which shows data from ref. 66 for larger- M (344, 800, 6300 kDa) stars. The displayed data on 302 kDa linear polyisoprene are fit by very nearly the same D_o , α and ν as is the data on a much larger (800 kDa) 18-arm star polyisoprene. Finally, Fig. 25 shows Xuexin, et al.'s data on $D_s(c)$ for three linear polyisoprenes, molecular weights of 70.8, 251, and 302 kDa, albeit over a narrower range of c than in Figure 23.

Nine of the above papers, namely Brown and Stilbs⁴², Callaghan and Pinder⁴⁵, Deschamps and Leger⁴⁶, Giebel, et al.⁵², Leger, et al.⁵⁶, von Meerwall, et al.⁶³, Wesson, et al.⁶⁵, and Xuexin, et al.⁶⁶ report self-diffusion coefficients at a series of concentrations and polymer molecular weights for a series of homologous polymers. A simultaneous fit of each of these sets of measurements to a joint function of c and M is then practicable. Here fits were made to eq. 17, using the convention that the molecular weight of the sole polymer species is P . The fits forced $\delta = 0$ to eliminate a notional dependence of D_s on the molecular weight M of a non-existent second polymer. Results of the fits appear in Table IV and Figs. 26-28.

In a majority of cases, the fits were quite good, with RMS fractional errors in the range 6-18%. Fits to the measurements of Leger, et al.⁵⁶ and Wesson, et al.⁶⁵ were less satisfactory; these are discussed separately below. Xuexin, et al.⁶⁶ cover an extremely broad range of M in

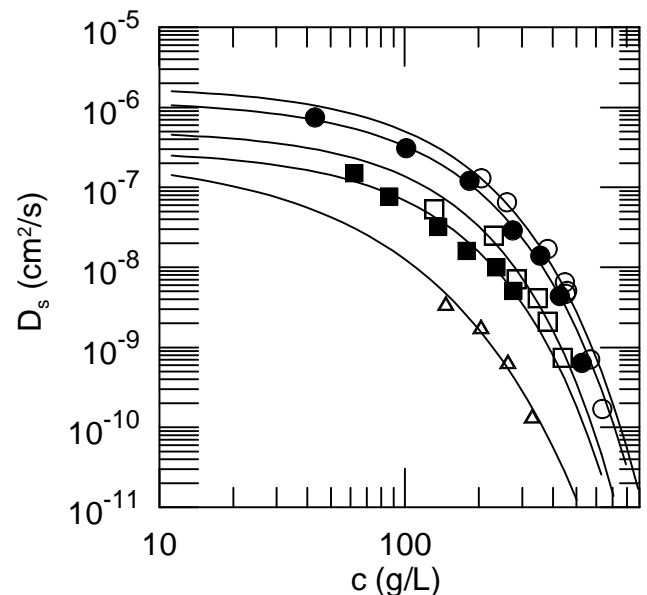


FIG. 22: D_s of [from top to bottom] 32, 46, 105, 130, and 360 kDa polystyrene in tetrahydrofuran, and associated stretched exponential fits. Data are from Wesson, et al.⁶⁵, Table II and associated Figures, as supplemented by the low-concentration measurements of Hadgraft, et al.⁵⁴.

their study of 18-armed stars. Over this range, ν from fits to data sets covering chains with a single molecular weight changes substantially, so a fit of all data over a full range of M to eq. 17, with ν a fixed constant, does not work well for very small or very large molecular weights. On limiting the fit to intermediate values for P , good agreement between the data and the fitted forms are encountered. Solid curves in Fig. 27 were calculated using the parameters to the fit to data in the intermediate- P range.

Omitting momentarily the fits to results of Leger, et al.⁵⁶ and Wesson, et al.⁶⁵: The exponent a for the molecular weight dependence of the bare diffusion coefficient is consistently -0.5. Except for Brown, et al.'s work on polyethylene oxide: water, the concentration exponent ν is in the range 0.5-0.75; Brown, et al.'s data⁴² imply $\nu \approx 0.93$. The molecular weight exponent γ is in the range 0.32-0.46, again with the exception of fits to data of Brown, et al.⁴², for which $\gamma \approx 0.6$. Inspection of the figures indicates that a joint stretched exponential in c and M fits each data set well, with no systematic deviations for particular values of c or M .

The two data sets that are fit less well by eq. 17 appear in Figure 28. The merged fit to Leger, et al.⁵⁶'s data on polystyrene:CCl₄ is poor. However, Leger, et al.'s data shows features – notably a non-monotonic dependence of D_s on c – that appears in data on no other polymer system, including other experiments that determined the concentration dependence of D_s of the same polymer. We infer that the poor fit of eq. 17 to Leger, et al.'s data

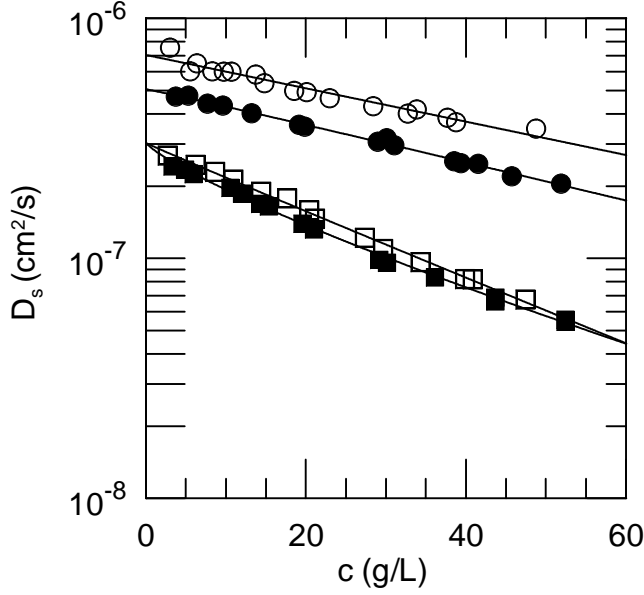


FIG. 23: D_s of [from top to bottom] 61, 92, 193, and 216 kDa 18-arm star polyisoprenes in CCl_4 , and fits to stretched exponentials, using data of Xuexin, et al.⁶⁶, Fig. 3.

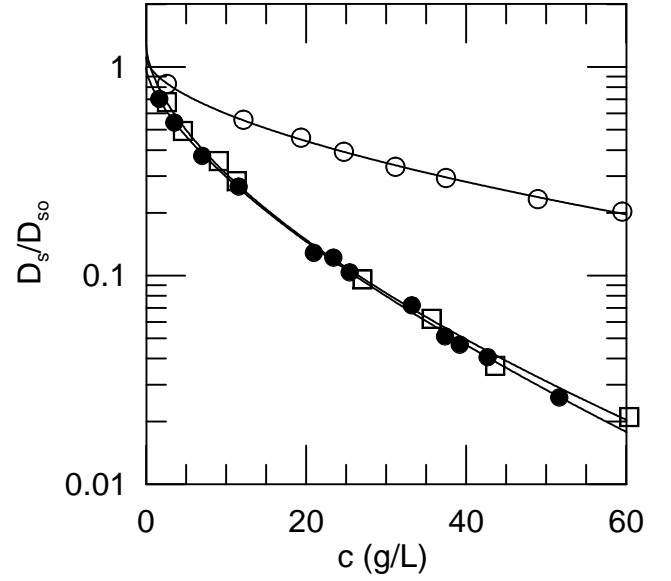


FIG. 25: D_s of [from top to bottom] 70.8, 251, and 302 kDa linear polyisoprenes in CCl_4 , and fits to stretched exponentials, using data of Xuexin, et al.⁶⁶, Fig. 4.

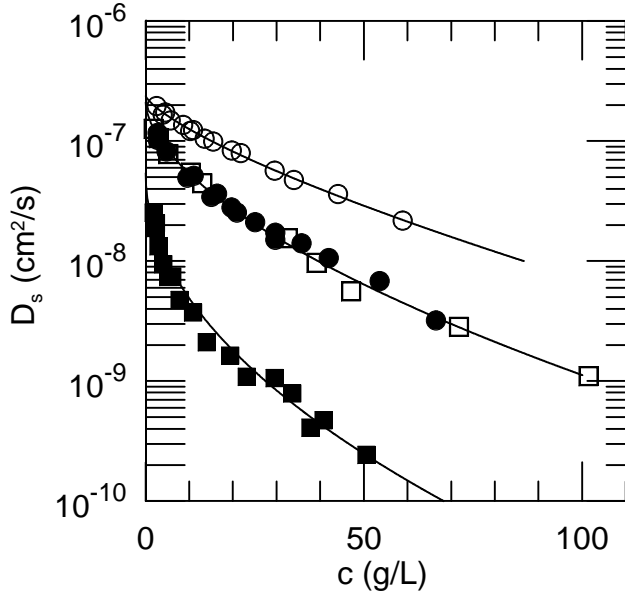


FIG. 24: D_s of 302 kDa linear polyisoprene (filled circles) and [from top to bottom] 340, 800, and 6300 kDa 18-armed star polyisoprenes (all in CCl_4) and fits to stretched exponentials, using data of Xuexin, et al.⁶⁶, Fig. 2.

arises from features unique to this polymer sample and set of measurements and not to a generic behavior of D_s for polystyrene solutions.

The merged fit to Wesson, et al.'s⁶⁵ measurements is also poor. However, this set of data is limited to elevated concentrations in which $D_s/D_{s0} < 1$, generally substan-

tially without matching low-concentration measurements on the regime in which $D_s \approx D_{s0}$. By inspection of Fig. 28b, the merged fit works reasonably well at small and large polymer molecular weight, but is least satisfactory at intermediate molecular weights. In particular, the 105 and 130 kDa polymers have nearly the same P but at elevated concentrations substantially different self-diffusion coefficients.

IV. DIFFUSION OF PROBE CHAINS THROUGH MATRIX POLYMER SOLUTIONS

This Section reviews measurements on the diffusion of polymeric probe molecules through solutions of a different polymer. These experiments involve intrinsically ternary solutions in which the molecular weight P of the probe polymer and the molecular weight M of the matrix polymer are not the same. In some cases, the probe and matrix polymers in the solution have a common monomer, and differ only in their molecular weights. In other cases, the probe and matrix polymers are chemically distinct. Studies are again presented alphabetically by first author, together with fits of the data sets to stretched exponentials in concentration and chain molecular weights. Fitting parameters appear in Tables II and III.

Brown and Rymden⁶⁷ used quasielastic light scattering to study the diffusion of linear polystyrenes and coated silica spheres through polymethylmethacrylate in toluene. Toluene and PMMA are almost exactly index-matched, so scattering from these systems was dominated

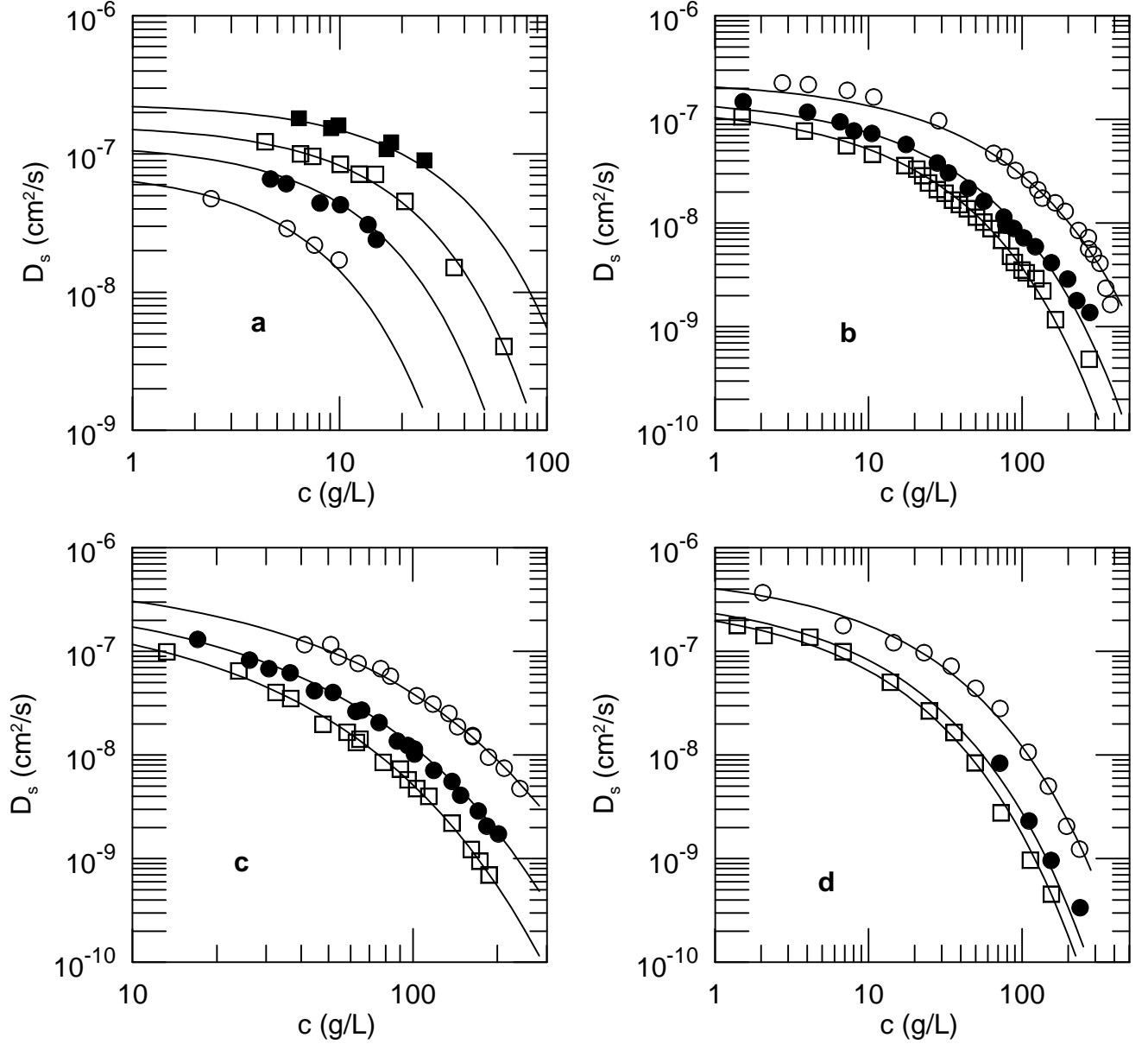


FIG. 26: D_s as measured by (a) Brown, et al.⁴² (cf. Fig. 2), (b) Callaghan, et al.⁴⁴ (cf. Fig. 3), (c) Callaghan, et al.⁴⁴ (cf. Fig. 4), and (d) Deschamps, et al.⁴⁶ (cf. Fig. 5), and fits to eq. 17, leading to the parameters in Table III.

by scattering from the dilute probe chains. The matrix PMMA's had molecular weights in the range 110 kDa–1.43 MDa. Probe polystyrenes had molecular weights of 2.95, 8, and 15 MDa, with M_w/M_n of 1.06, 1.08, and 1.30, respectively. In the original paper, data were reported after normalization by an unspecified diffusion coefficient obtained in the absence of the matrix polymer.

Reference 67 reported how D_p depends on matrix concentration and molecular weight. Figure 29a shows D_p/D_{p0} for the 8MDa polystyrene diffusing through each of six matrix polymethylmethacrylates. Each solid line represents a fit to a stretched exponential in matrix polymer concentration, using parameters in Table II. For

$D_p/D_{p0} < 10^{-3}$ or so, a condition attained only with the two largest matrix polymers, the measured D_p deviates markedly downward from a stretched exponential, so that fits to all data on these two systems show fractional RMS errors much worse (32–45% rather than 5–8%) than fits to the same probe polymer with the smaller matrix polymers. On excluding the final few points from the two fits, curves with far lower RMS fractional errors were generated. These are the curves shown in the Figure. It is difficult to determine from these measurements whether there is a systematic change from stretched-exponential to some other concentration dependence at very small D_p/D_{p0} , or whether the apparent deviations arise from

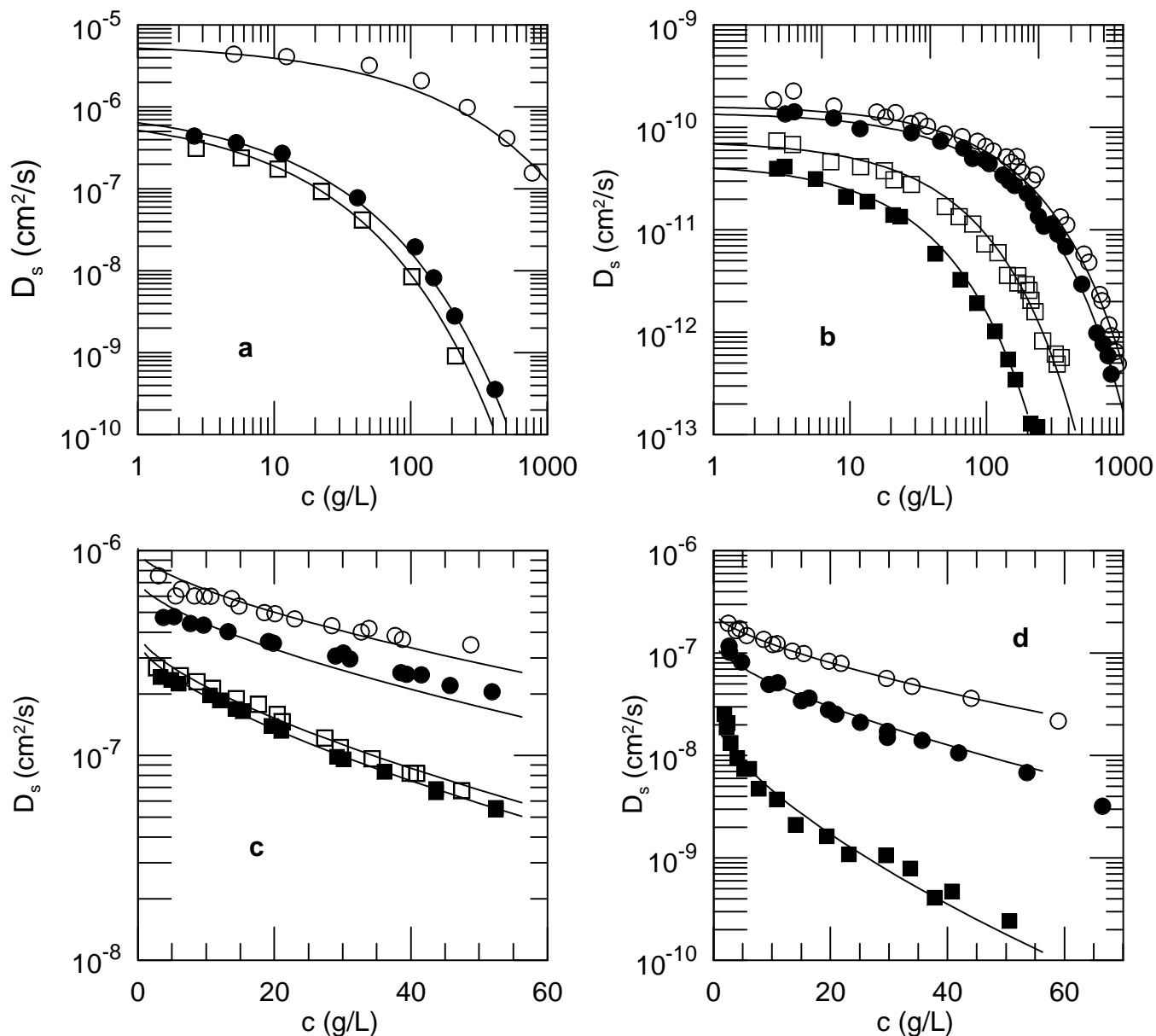


FIG. 27: D_s as measured by (a) Giebel, et al.⁵², (b) von Meerwall, et al.⁶³ and (c), (d) Xuexin, et al.⁶⁶, and fits to eq. 17, leading to the parameters in Table III. Other details as in Figs. 7, 20, 23, and 24, respectively.

experimental challenges at very small D_p .

Figure 29b shows the same data, now fit simultaneously to eqn. 17, the joint stretched exponential in c and M . Fitting parameters appear in Table IV. Except for the lowest- M matrix polymer, the fits are almost as good as the individual fits shown in Figure 29a. For the lowest- M 101 kDa matrix polymer, the fitted form predicts too strong a dependence of D_p upon c .

Brown and Rymden⁶⁷ also examined how D_p depends on probe molecular weight. Figure 30 shows D_p of the 3, 8, and 15 MDa probe polystyrenes, all diffusing through the 445kDa PMMA. Fits are to stretched exponentials in c , leading to parameters given in Table II. The ma-

trix chains are all much larger than the probe chains. As noted by the original authors⁶⁷, the three curves come very close to superposing except perhaps at the very highest matrix concentrations examined.

Brown and Stilbs⁶⁸ used PFGNMR to measure the probe diffusion coefficient of polyethylene oxide in aqueous solutions of dextran. Polyethylene oxides had molecular weights of 73, 278, and 1200 kDa with M_w/M_n of 1.02-1.12; dextrans had molecular weights of 19, 110, and 510 kDa. The 1200 kDa PEO represented the lower limit at which D_p could be determined with then-available technology; the authors limited their detailed analysis to the two lower-molecular-weight probes.

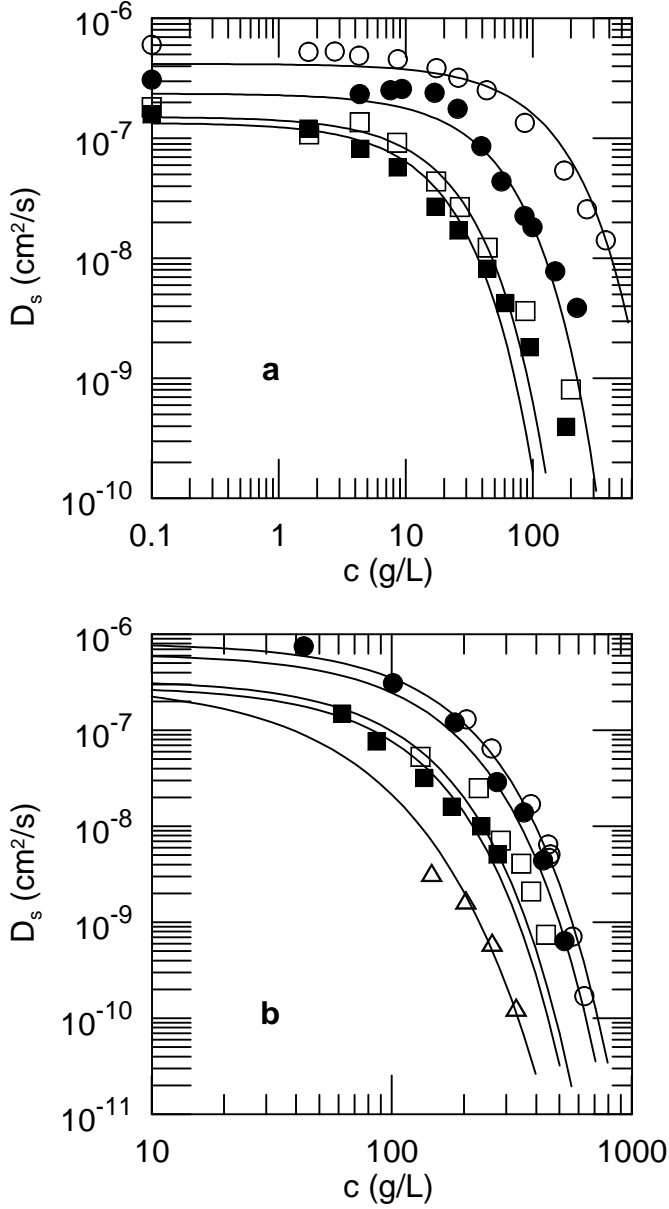


FIG. 28: Joint fits to all data of (a) Leger, et al.⁵⁶ and (b) Wesson, et al.⁶⁵, showing the poor quality of fits of eq. 17 to these data sets. Fit parameters are in Table III; all other plot properties are the same as Figs. 8 and 22, respectively.

Figures 31a and 31b show D_p of the 73 and 278 kDa polyethylene oxides, normalized by the measured D_{o0} of the same probes in the absence of the matrix polymers. All measurements were simultaneously fit to $D_{p0}/D_{o0} \exp(-\alpha c^\nu P^\gamma M^\delta)$, yielding the smooth curves shown in the Figures and the parameters listed in Table IV. Agreement between the data and the fitted curves was very good for the 73 kDa probe. For the 278 kDa probe in the 19 kDa matrix, the fitting function significantly underpredicts D_p . From the fitting parameters, D_p/D_{o0} has a very weak dependence on the

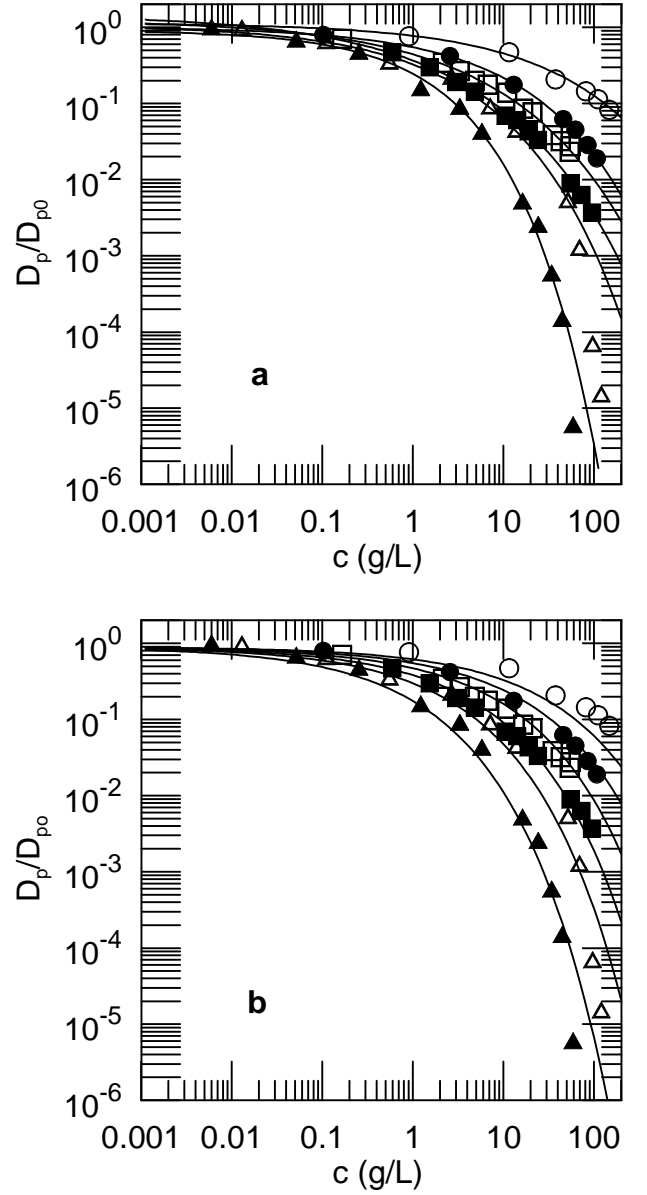


FIG. 29: D_p/D_{p0} of 8 MDa polystyrene diffusing through [top to bottom] 101, 163, 268, 445, 697, and 1426 kDa poly-methylmethacrylate in toluene⁶⁷, and (a) separate fits of the data for each matrix polymer to a stretched exponential in c , and (b) simultaneous fit of all data to a single stretched exponential in c and M .

probe molecular weight (other than that hidden in D_{o0}), but has a marked dependence on the matrix molecular weight. The same data were also fit, individually for each probe:matrix pair, to a stretched and a pure exponential in c . Without exception, for each probe:matrix pair $D_s(c)$ follows accurately the exponential form, RMS fractional errors being in the range 1-4%. Because D_p varied over a limited range, the parameters reported in Table II reflect fits to the pure exponential.

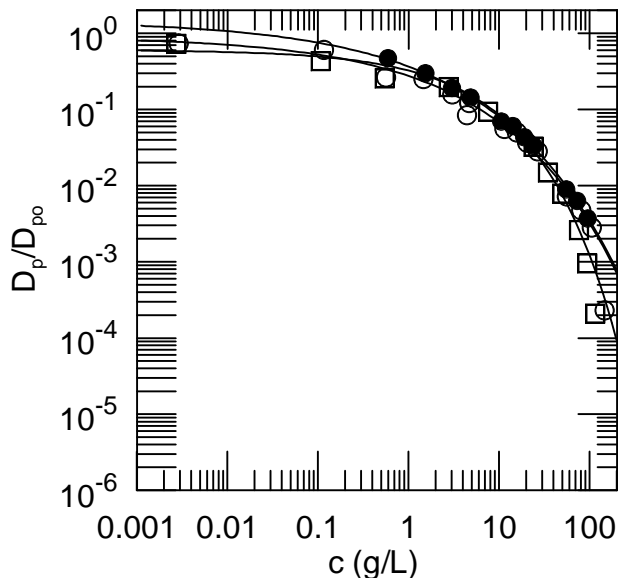


FIG. 30: D_p/D_{p0} against c for 3 (open circles), 8 (closed circles), and 15 (squares) MDA polystyrenes diffusing through 445 kDa polymethylmethacrylate in toluene, using data of Brown and Rymden⁶⁷, and fits to stretched exponentials in matrix concentration.

Daivis, et al.⁶⁹ used quasielastic light scattering spectroscopy to measure diffusion of relatively dilute 864 kDa dextran in not-necessarily-dilute solutions of 20.4 kDa dextran. Polymer polydispersities were in the range 1.24-1.3. The concentration of the lower-molecular-weight dextran ranged up to 166 g/L. Analysis of the bimodal QELSS spectra of these systems shows that the slower mode corresponds to probe diffusion by the 864 kDa dextrans. As seen in Figure 32, the data fit reasonably well to a simple exponential concentration dependence, using parameters found in Table II.

In a separate paper, Daivis, et al.⁷⁰ used QELSS and PFGNMR to measure the diffusion of a 110 kDa polystyrene, $M_w/M_n = 1.06$, through solutions of 110 kDa polyvinylmethylether, $M_w/M_n \approx 1.3$, in the PVME's isorefractive solvent toluene. Good agreement was found between the QELSS measurements of D_p and the earlier measurements of D_p by Martin⁷¹ on the same system.

Figure 33 shows Daivis, et al.'s data⁷⁰ as obtained using both physical methods. In the figure, lines represent separate fits of each data set to a stretched exponential in matrix polymer concentration, with fitting parameters given in Table II. Stretched exponentials in c describe well each data set. The QELSS data is significantly less scattered than the PFGNMR data, so the parameters from the former's fit are probably to be preferred.

De Smedt, et al.⁷² used FRAP to measure the diffusion of 71, 148, and 487 kDa dextrans ($M_w/M_n < 1.35$), labeled with fluorescein isothiocyanate, through solutions of hyaluronic acid ($M_n = 390$ kDa; $M_w = 680$ kDa).

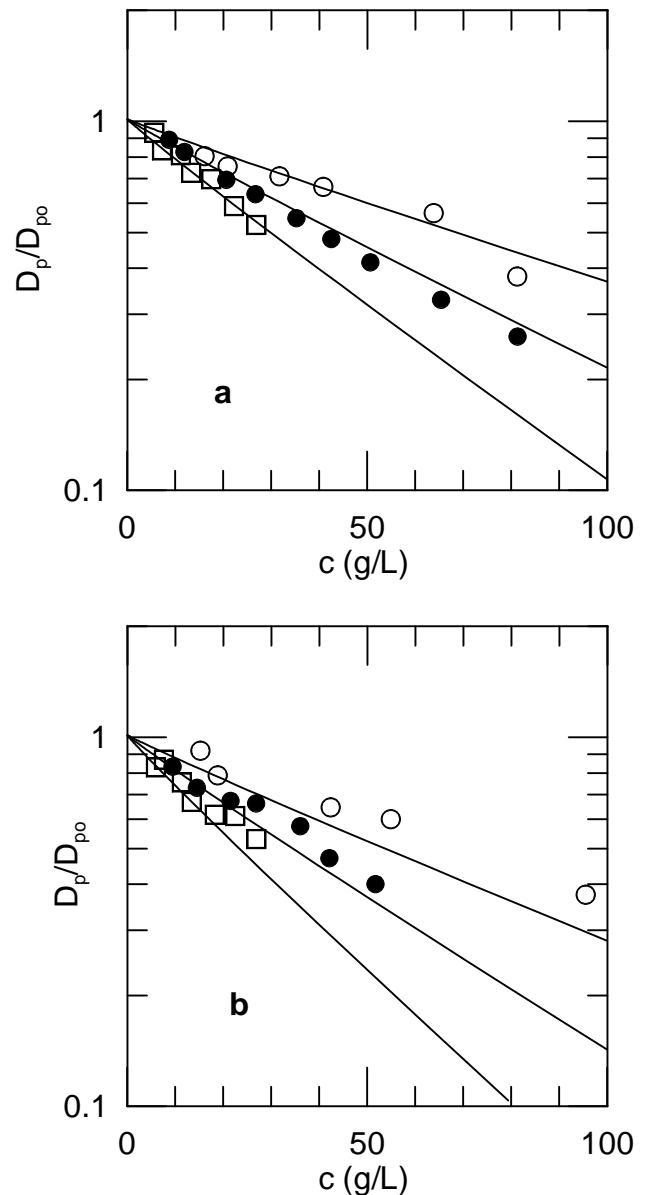


FIG. 31: D_p/D_{p0} of (a) 73 kDa polyethylene oxide and (b) 278 kDa polyethylene oxide in [top to bottom] 19, 110, and 510 kDa dextrans in aqueous solution, and simultaneous fit of all measurements to a stretched exponential in c , M , and P , using data of Brown and Stilbs⁶⁸.

Hyaluronic acid concentrations ranged from the dilute up to 18 g/L. D_p of the dextrans varied roughly five-fold over this concentration range. De Smedt, et al.'s data⁷² appear in Fig. 34, together with stretched-exponential fits using the parameters in Table II. As seen in the Figure and initially reported by the original authors, the data fits well to stretched exponential forms.

Hadgraft, et al.⁵⁴ used QELSS to study the diffusion of polystyrene probe polymers, molecular weights 25, 162, 410, 1110, and 4600 kDa through solutions of

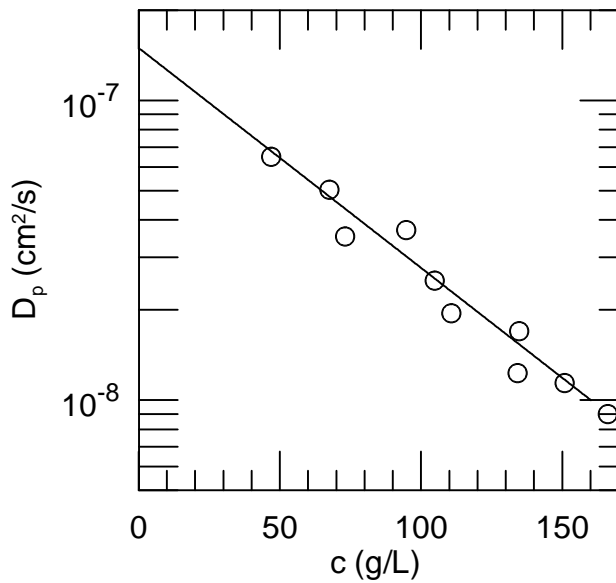


FIG. 32: D_p of 864 kDa dextran in solutions of 20 kDa dextrans and fits to stretched exponentials, using data of Daivis, et al.⁶⁹.

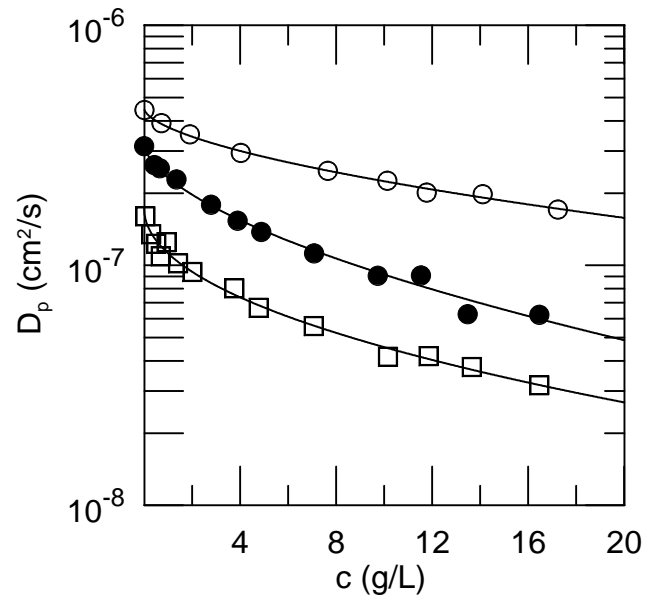


FIG. 34: D_p of [from top to bottom] 71, 148, and 487 kDa dextrans in M_w 680 kDa hyaluronic acid, and fits to stretched exponentials, using data of De Smedt, et al.⁷².

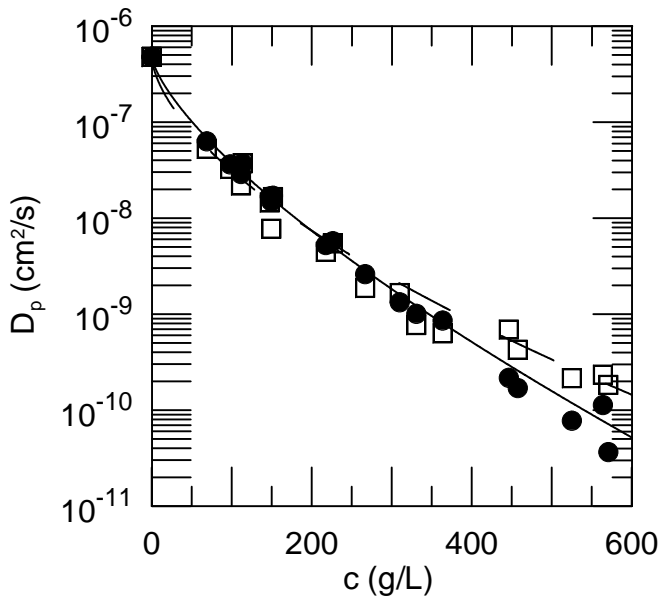


FIG. 33: D_p of 110 kDa polystyrene through 110 kDa polyvinylmethylether:toluene, based on QELSS (circles) and PFGNMR (squares) measurements of Daivis, et al.⁷⁰, together with fits (solid, dashed lines, respectively) to stretched exponentials in the matrix concentration.

105 kDa polymethylmethacrylate in its isorefractive solvent benzene at PMMA concentrations up to 100 g/L. Polystyrene and PMMA are not compatible, implying that the radius of the polystyrene chains may have depended very strongly on the matrix polymer concentration. As seen in Fig. 35, D_p of the 25 kDa polystyrene was

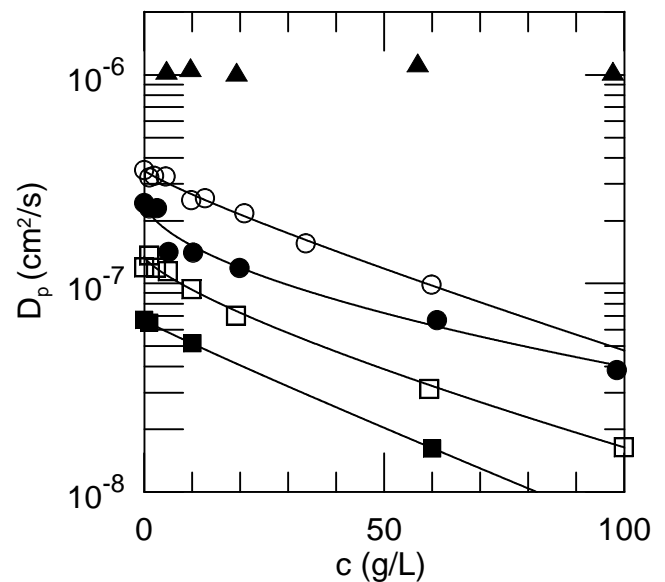


FIG. 35: D_p of [from top to bottom] 25, 162, 410, 1110, and 4600 kDa polystyrenes in 1.05 MDa polymethylmethacrylate: CCl_4 as a function of polymethylmethacrylate concentration, and fits to stretched exponentials, using data of Hadgraft, et al.⁵⁴.

substantially independent of PMMA concentration. The data on the 410 kDa polymer is significantly more scattered than is data on the other polystyrenes. The range of variation of D_p is sufficiently small (roughly a factor of three) that the fits to these data are less reliable than are the fits to data on some other systems. Nonetheless,

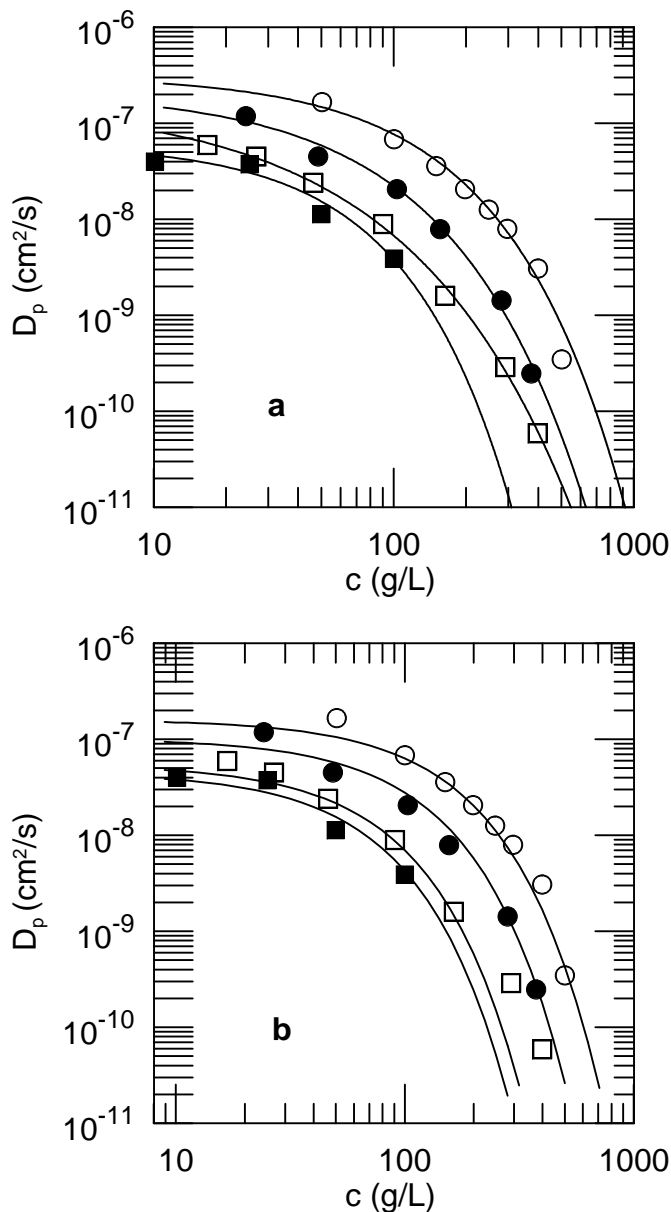


FIG. 36: D_p of [from top to bottom] 50, 179, 1050, and 1800 kDa polystyrenes in ortho-fluorotoluene solutions of 60 kDa polyvinylmethylether against matrix polymer concentration, using data of Hanley, et al.⁷³ and (a) separate fits at each P and (b) simultaneous fits at all P , with fitting parameters from Tables II and III, respectively.

D_p of the higher-molecular-weight polystyrenes shows a stretched-exponential dependence on PMMA concentration, with parameters seen in Table II.

Hanley, et al.⁷³ used light scattering spectroscopy to examine the diffusion of polystyrenes through the matrix polymer polyvinylmethylether in its isorefractive solvent ortho-fluorotoluene. The polystyrenes had molecular weights of 50, 179, 1050, and 1800 kDa. The polyvinylmethylether had $M_w \approx 60$ kDa with $M_w/M_n \approx 3$. Han-

ley, et al.'s data⁷³ are given in Fig. 36a, together with fits of separate stretched-exponentials in c to each data set, yielding parameters shown in Table II. The entire data set was also fit simultaneously to the joint stretched exponential of eq. 17, yielding parameters seen in Table III, and fitted curves seen in Fig. 36b. The lack of measurements at very low matrix concentration substantially broadens the range of fitting parameters that yield reasonable descriptions of this data. The fit to the joint stretched exponential is substantially less satisfactory than the individual fits at each P to separate stretched exponentials (RMS fractional errors of 34% rather than 9-24%). The inadequacy of eq. 17 relates primarily to the 1050 kDa probe chains, for which D_p was determined only over a limited range. As seen in Table III, excluding data on the 1050 kDa probes from the simultaneous fit leads to a marked reduction in the RMS fractional fit error (to 24%), modest changes in α and ν , but only small changes in the other fitting parameters.

Kent, et al.⁷⁴ applied static and quasielastic light scattering to measure radii of gyration and diffusion coefficients of 233 and 930 kDa polystyrenes in 7, 66, 70, 840, and 1300 kDa polymethylmethacrylates in ethyl benzoate (for static light scattering) and toluene (for quasielastic light scattering). With one exception (66 kDa PMMA), M_w/M_n was always ≤ 1.10 . Different probe:matrix combinations were used for static and quasielastic light scattering. D of the polystyrene was measured as a function of polystyrene concentration, and linearly extrapolated to the dilute-in-polystyrene limit, thereby obtaining both the probe diffusion coefficient D_p of the polystyrene and the initial linear dependence of D_p on polystyrene concentration.

Figure 37 shows Kent, et al.'s⁷⁴ measurements of the radius of gyration of 930 kDa polystyrene in solutions of 7, 70, or 1300 kDa PMMA as a function of PMMA concentration, together with fits of R_g to a stretched exponential

$$R_g = R_{g0} \exp(-\alpha c^\nu) \quad (18)$$

in matrix concentration c . The fits are good throughout, using parameters in Table V. Unlike the scaling-law prediction $R_g \sim c^{-0.25}$, the stretched exponential form shows acceptable behavior down to zero matrix concentration.

Kent, et al.⁷⁴ also measured D_p of 233 kDa polystyrene in solutions of 66 and 840 kDa PMMA, and 930 kDa polystyrene through 840 kDa PMMA. Their experimental data is shown in Fig. 38a, together with fits to exponentials using parameters given in Table II. Within experimental error, the simple exponential fits with $\nu = 1$ forced are as good as the stretched-exponential fits to the data: the former are in the figure. Experimentally, the scaling prefactor α depends strongly on matrix molecular weight (a 12-fold change in M leads to a two-fold change in α) but at most weakly on probe molecular weight. Figure 38b shows a fit of the same data to a joint stretched exponential in c , P , and M , based on parameters in Table

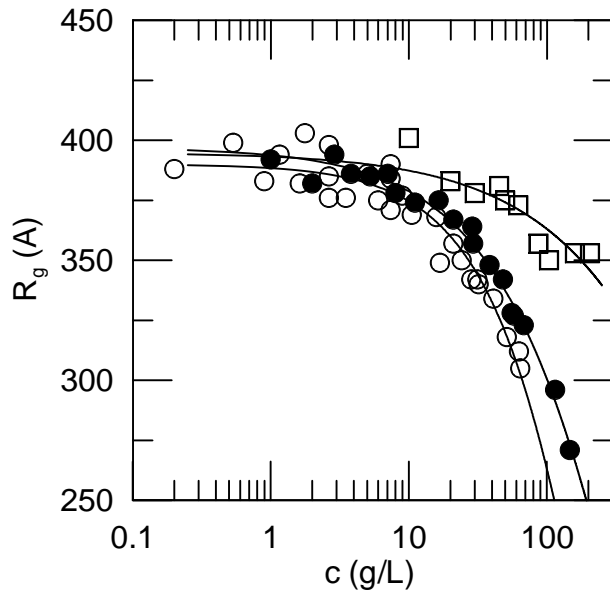


FIG. 37: R_g of 930 kDa polystyrene in [from top to bottom] 7, 70, and 1300 kDa polymethylmethacrylate: ethylbenzoate as a function of polymethylmethacrylate concentration, and fits to stretched exponentials, using data of Kent, et al.⁷⁴.

III. The joint fit clearly works well for all three polymer pairs.

Kim, et al.⁷⁵ measured the diffusion of dye-labeled polystyrenes through matrix solutions of unlabeled polystyrenes in toluene. The objective was to test the prediction of some scaling models that D_p becomes independent of matrix molecular weight if $M/P \geq 1$. The probe polystyrenes had molecular weights from 10 to 1800 kDa; matrix chains had molecular weights from 51 to 8400 kDa. Ref. 75 also reported the dependence of D_p on the matrix molecular weight for several probes (51, 390, 900 kDa) at multiple matrix concentrations for matrix molecular weights in the range 35–8400 kDa. Polymer polydispersities were largely < 1.06 , with a maximum of 1.17. Kim, et al.⁷⁵ also report limited data using methyl red as a low-molecular weight probe. As seen in Fig. 39a, the authors found that D_p becomes substantially independent of M only if $M/P > 3$.

With respect to the models discussed in Section II, the published derivations of the stretched-exponential form refer to polymer chains whose motions are adequately approximated by whole-chain translation and rotation. These approximations are only likely to be adequate if the probe and matrix chains are of similar size, because otherwise the whole-chain motions of probe or matrix would effectively sample some of the internal modes of the other chain species, whether matrix or probe. At fixed c , from the hydrodynamic model D_p would have a stretched-exponential dependence on M if $M/P \approx 1$, but might well not have a stretched-exponential matrix molecular weight dependence if $M/P \gg 1$ or $M/P \ll 1$.

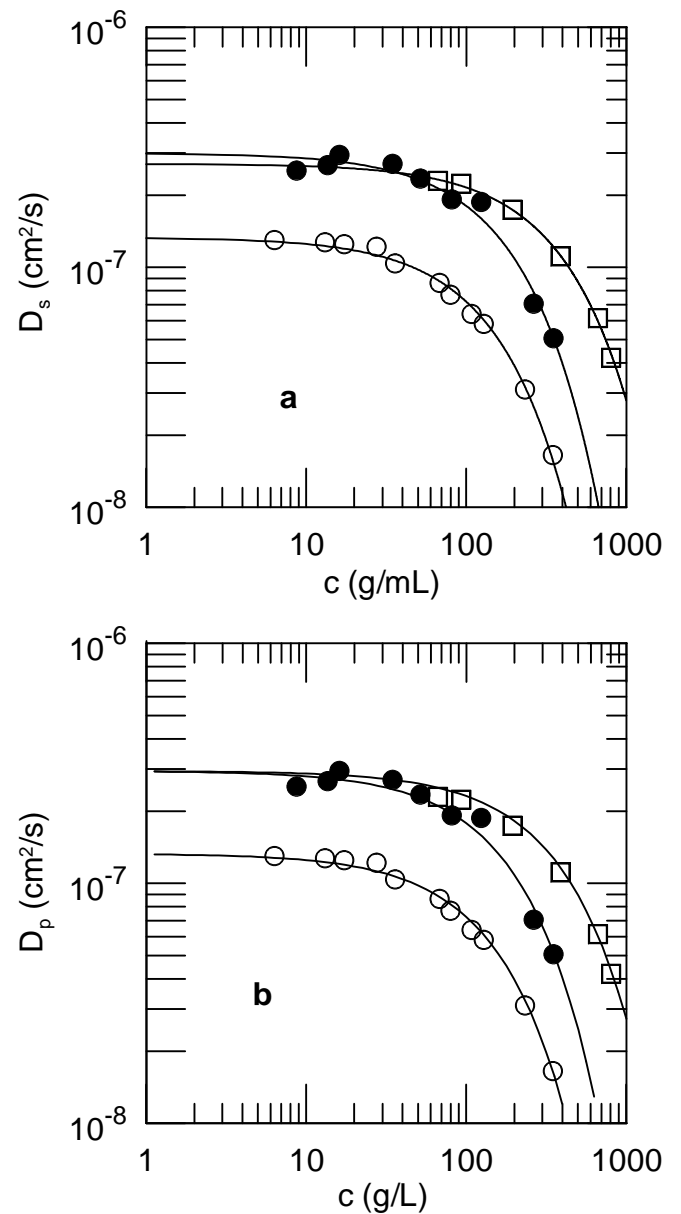
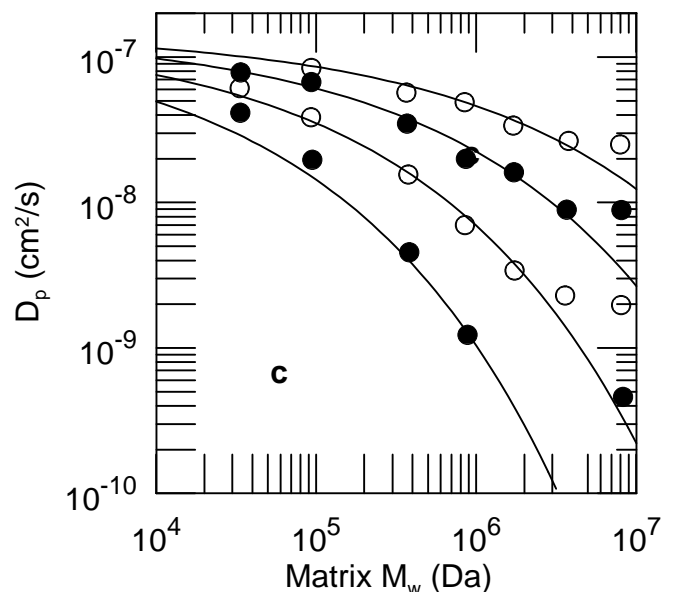
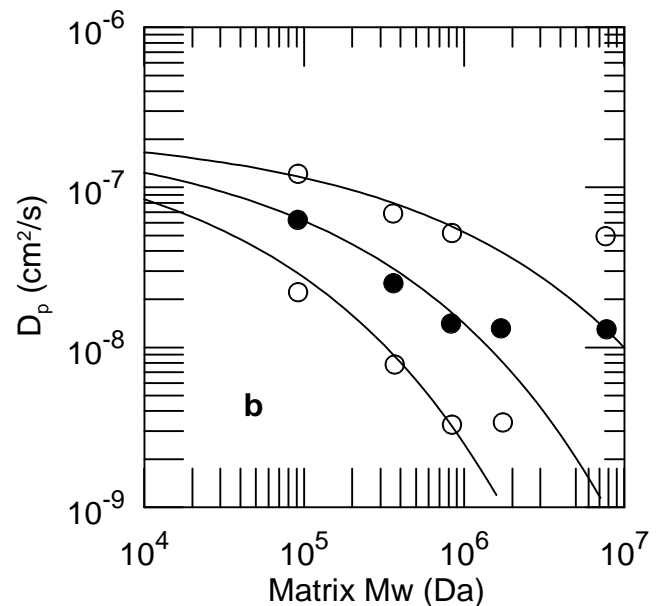
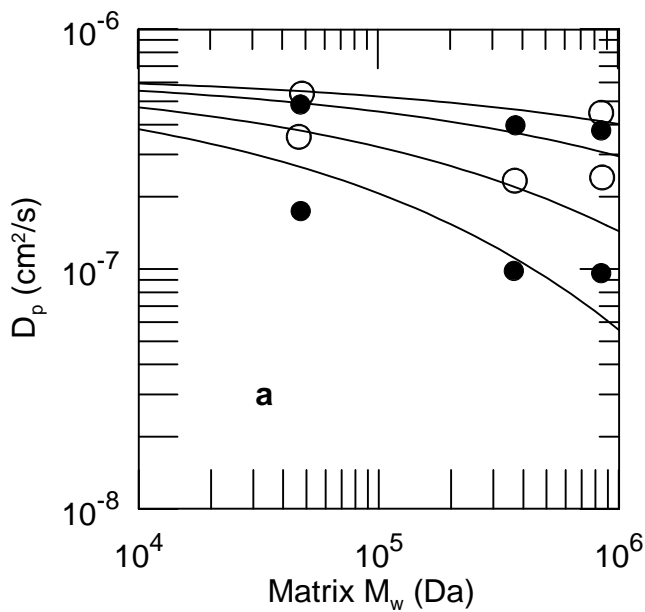


FIG. 38: D_p of polystyrene through polymethylmethacrylate:toluene with molecular weight combinations $P : M$ [from top to bottom] 233:66, 233:840, and 930:840 kDa as functions of polymethylmethacrylate concentration, using data of Kent, et al.⁷⁴, and (a) a separate fit to a stretched exponential for each combination and (b) a single fit to a joint stretched exponential in c , P , and M .

Kim, et al.'s⁷⁵ results thus are not necessarily inconsistent with exponential-type models of polymer dynamics.

Kim, et al.'s data⁷⁵ for the domain $M/P < 3$, as seen in Figs. 39, were fit to the form $D_o P^{-a} \exp(-ac^\nu P^\gamma M^\delta)$, yielding parameters in Table III. As seen in Fig. 39, D_p is indeed described well by the joint stretched exponential over a wide range of c , P , and M , except in the regime $M/P > 3$ in which the form is not necessarily expected



to apply.

Kim, et al. also studied the concentration dependence of D_s and D_p at large M/P . Figure 40 shows Kim, et al.'s⁷⁵ determination of self-diffusion of 900 kDa polystyrene in toluene, and our stretched-exponential fit to the data, yielding the parameters in Table I. Figure 41 shows measurements of probe diffusion, using as probes methyl red and 10, 35, 100, 390, 900, and 1800 kDa polystyrenes, all through matrix polystyrenes. The molecular weight of the matrix polystyrene ranges from 51 to 8400 kDa, varying from data point to data point, with $M/P > 3$ and generally $M/P > 6$. This ratio of M/P was chosen by Kim, et al. based on their interpretation of their data that showed D_p to be independent of M for $M/P > 3$. As seen in Figs. 40 and 41, stretched-exponential functional forms using parameters in Table II describe the matrix-polymer concentration dependences of $D_s(c)$ and $D_p(c)$ well over a wide range of polymer concentrations and probe molecular weights, even though the ranges of P and M are very wide. The stretched exponential in c continues to describe well the concentration dependence of D_p in the large M/P range which eq. 17 does not represent well the P and M dependences of D_s .

Lodge and collaborators have reported an extensive series of studies of probe diffusion in polymer solutions, using quasielastic light scattering to measure D_p of a dilute probe polymer, generally polystyrene, through the isorefractive matrix polymer:solvent pair polyvinylmethylether: ortho-fluorotoluene. Variables studied include the probe and matrix molecular weights, the matrix concentration, and the topology (linear and star) of the probe polymers.

An early letter⁷⁶ of Lodge reports D_p of 179 kDa and 1.05 MDa polystyrenes through a 50kDa polyvinylmethylether. The data, and corresponding stretched-

FIG. 39: D_s of polystyrene in matrix polystyrene:toluene solutions as functions of matrix molecular weight at various matrix concentrations, based on data of Kim, et al.⁷⁵, Fig. 3. Probe molecular weights were (a) 51 kDa, (b) 390 kDa, and (c) 900 kDa. Matrix concentrations [top to bottom] were (a) 10, 20, 50, and 100 g/L; (b) 20, 50, and 100 g/L; and (c) 10, 20, 40, and 80 g/L. A single stretched exponential $D_o P^{-a} \exp(-\alpha c^r P^b M^\gamma)$ with constant parameters was fit (solid lines) to all data in the figures having $M/P < 3$.

exponential fits, appear in Fig. 42. Fit parameters are in Table II. A stretched exponential in concentration describes well both data sets.

Lodge and Wheeler⁷⁷ compared the diffusion of linear and 3-armed star polystyrenes through a high molecular weight polyvinylmethylether. Polystyrene molecular weights were 422 and 1050 kDa for the linear chains

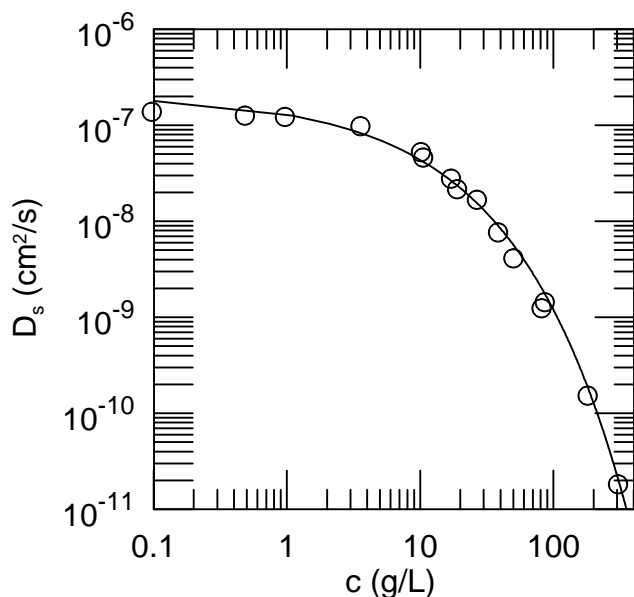


FIG. 40: D_s of 900 kDa in toluene, based on data of Kim, et al.⁷⁵, Fig. 1, and a fit to a stretched exponential.

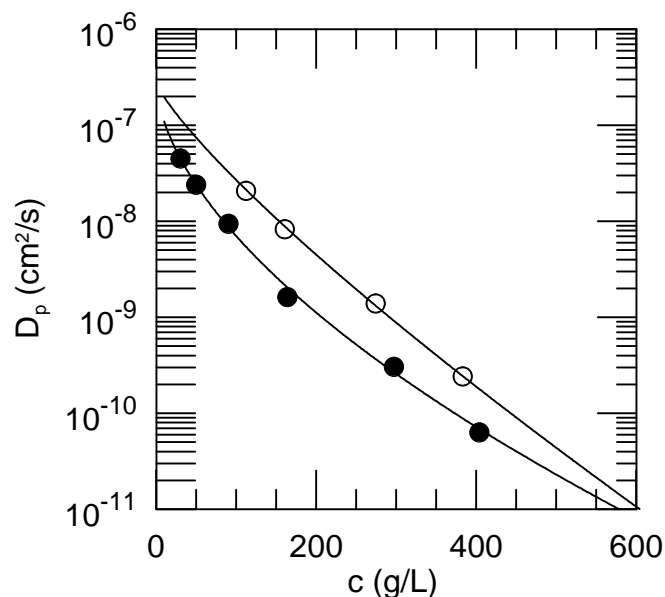


FIG. 42: D_p of 179 kDa and 1.05 MDa polystyrene through 50 kDa polyvinylmethylether in ortho-fluorotoluene, based on data of Lodge⁷⁶, and fits to stretched exponentials in c .

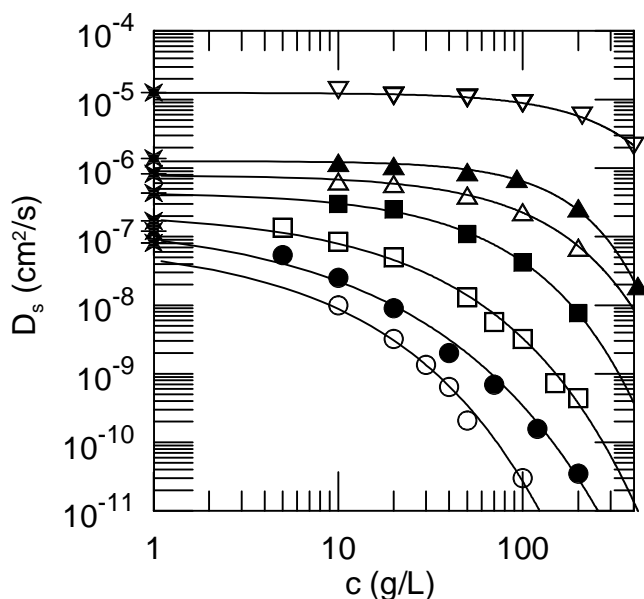


FIG. 41: Probe diffusion of (top to bottom) methyl red, and 10, 35, 100, 390, 900, and 1800 kDa D_s polystyrenes through high-molecular-weight ($M/P > 3$) polystyrenes in toluene, based on data of Kim, et al.⁷⁵, Table II, and fits to stretched exponentials. The left axis shows zero-matrix-concentration data.

and 379 and 1190 kDa for the stars; the polystyrenes were identified as being 'relatively monodisperse'. The PVME had an M_w of 1.3 MDa, with an estimated $M_w/M_N \approx 1.3$. D_p was obtained over $1 \leq c \leq 100$ g/L in PVME concentration.

Figure 43a shows Lodge and Wheeler's

measurements⁷⁷, together with fits of data on each probe polymer to a stretched exponential in c . D_p varies over nearly four orders of magnitude. Over the full range, agreement of the data with the functional form is very good, with RMS fractional errors of 2.6-10% and parameters as seen in Table II. Figure 43b shows the same data, with the linear chains and star polymers separately fit to a stretched exponential in c and P . As seen in Table III, the fractional errors in these fits are very nearly as good as the fits to individual probe species. The P^{-a} scaling of the zero-concentration diffusion coefficient and the P^γ scaling of the scaling prefactor α account for the dependence of D_p of linear and star polymers on probe molecular weight.

Lodge and Markland⁷⁸ used light scattering spectroscopy to measure the single-particle diffusion coefficients of tracer 12-armed star polystyrenes through solutions of 140 kDa polyvinylmethylether, $M_w/M_n \approx 1.6$, in the isorefractive solvent ortho-fluorotoluene. The polystyrenes had M_w of 55, 467, 1110, and 1690 kDa, with $M_w/M_n \leq 1.10$. Lodge and Markland estimate for the matrix that $c^* \approx 20$ g/L and $c_e \approx 100$ g/L. Figure 44 shows Lodge and Markland's data. In the two graphs, the solid lines represent, respectively, fits to individual stretched exponentials in c and to fits to a joint stretched exponential in c and P . Fitting parameters appear in Tables II and III. Parameters in Table II differ modestly from Table II of Ref. 78. The sets of fits are excellent, with RMS fractional individual fits here are excellent, with errors of 2-4%; the RMS fractional error for the joint fit was 12%. The most notable deviation for the joint exponential is for the smallest probe at large

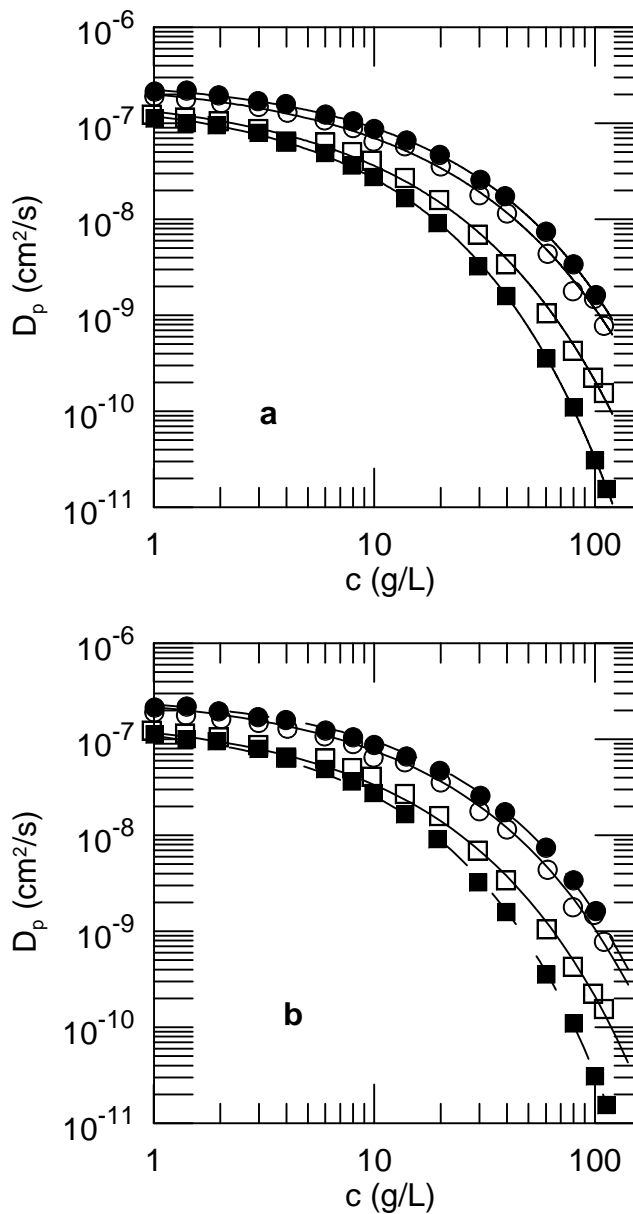


FIG. 43: D_p of polystyrenes [from top to bottom: 379 kDa $f = 3$ star, 422 kDa linear chain, 1050 kDa linear chain, and 1190 kDa $f = 3$ star] through 1300 kDa polyvinylmethylether in ortho-fluorotoluene, based on data of Lodge⁷⁷ and fits of a stretched exponential to (a) data on each probe separately and (b) all data on linear chains (solid lines) and separately all data on 3-armed star polymers (dashed lines).

concentration, where the fitting function underestimates D_p .

Lodge, Markland, and Wheeler⁷⁹ used light scattering spectroscopy to measure the diffusion of 3-armed and 12-armed star polystyrenes through solutions of polyvinylmethylether in its isorefractive solvent ortho-fluorotoluene. The 3-armed stars had M_w of 379 and 1190 kDa; the 12-armed stars had M_w of 55, 467, 1110, and

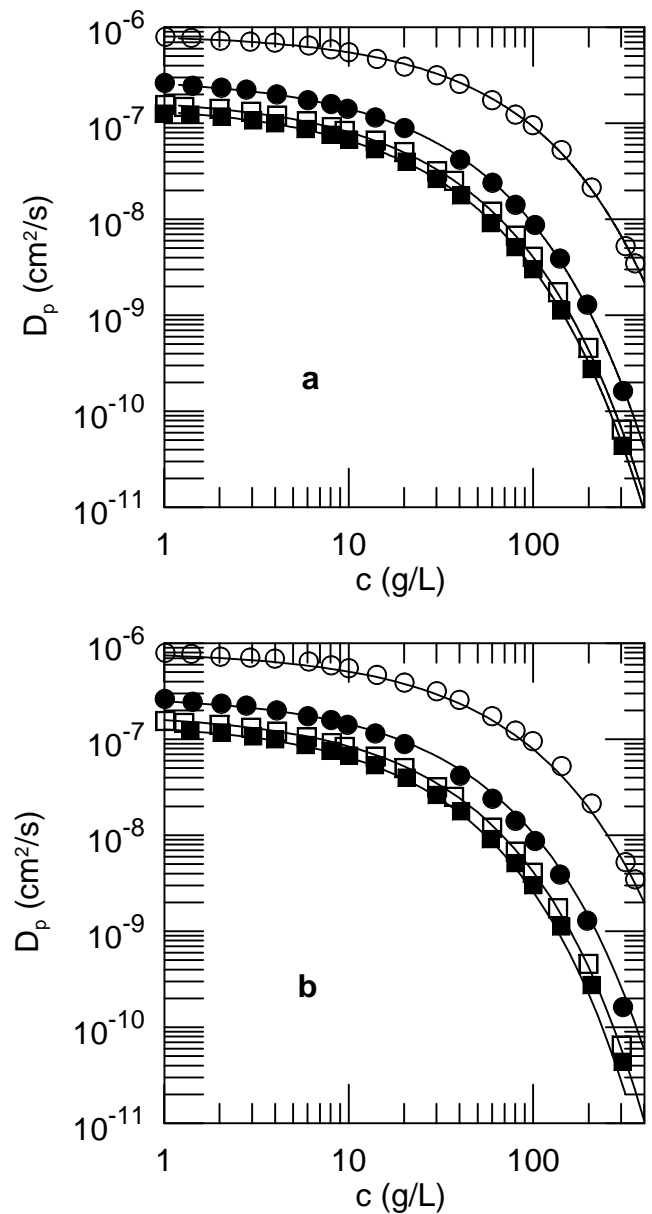


FIG. 44: D_p of 12-arm star polystyrenes (from top to bottom, M_w of 55, 467, 1110, and 1690 kDa) diffusing through solutions of 140 kDa polyvinylmethylether:ortho-fluorotoluene based on data of Lodge, et al.⁷⁸, their Table 1. Solid lines are fits of (a) a separate stretched-exponential for each probe, with parameters in II and (b) fits of a single stretched exponential in c and P to all data with parameters in Table III.

1690 kDa. Polyvinylmethyl ethers used as matrices had M_w of 140, 630, and 1300 kDa. Polystyrenes all had $M_w/M_n < 1.1$; the matrix polymers had $M_w/M_n \approx 1.6$. Light scattering measurements were also made of the radii of gyration of linear, 3-arm and 12-arm stars with molecular weights above 1MDa in the presence of 250 kDa polyvinylmethylether at concentrations as large as 50 g/L. Lodge, et al.⁷⁹ reported that they modified their

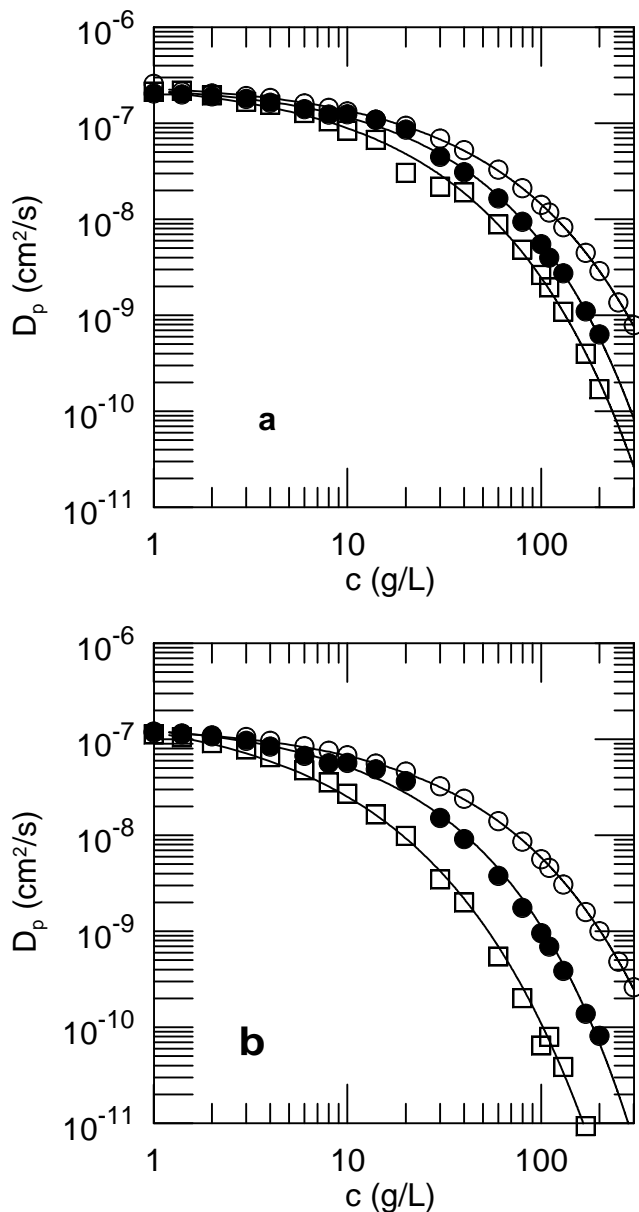


FIG. 45: D_p of (a) 379 kDa and (b) 1.19 MDa 3-arm star polystyrenes in (from top to bottom, 140, 379, and 1300 kDa) polyvinylmethylethers in ortho-fluorotoluene, based on data of Lodge, et al.⁷⁹. Solid lines are stretched-exponential fits with parameters in Table II.

reported D_p to take account of the concentration dependence of a local friction factor, using a process described by Wheeler and Lodge⁹² (see below). This modification factor was removed from Lodge, et al.'s⁷⁹ data, before making the analysis here, in order that this data be made more strictly comparable with the remainder of the literature.

Figures 45 and 46 show Lodge, et al.'s⁷⁹ measurements of D_p for 3-armed and 12-armed stars. As is apparent from the figures, for every $M : P$ combination a stretched

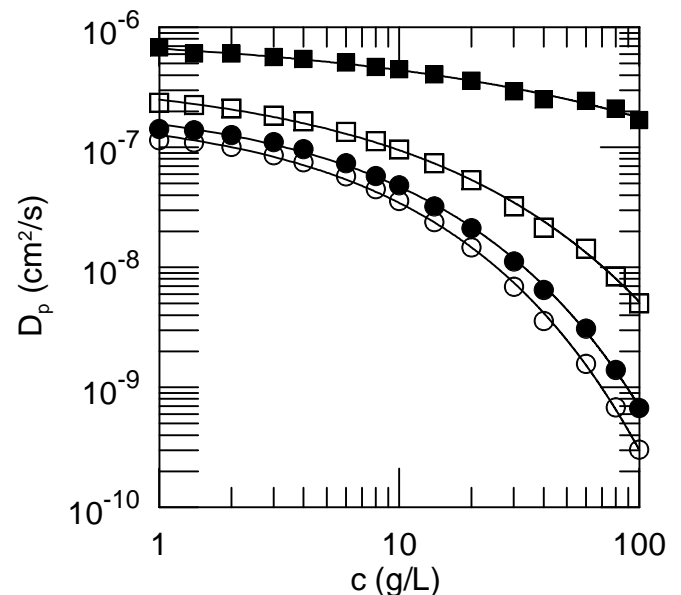


FIG. 46: D_p of 12-arm star polystyrenes (from top to bottom, M_w of 55, 467, 1110, and 1690 kDa) diffusing through solutions of 1300 kDa polyvinylmethylether:ortho-fluorotoluene based on data of Lodge, et al.⁷⁹. Solid lines are stretched-exponential fits with parameters in Table II.

exponential gives an excellent description of the the concentration dependence of D_p , with RMS fractional errors in the range 4-18% (cf. Table II).

The entirety of Lodge and collaborators' data^{78,79} on 12-armed and 3-armed stars were also fit (separately for each arm number) to equation 17, the joint stretched exponential in c , P , and M . Fitting parameters appear in III. Figure 47 shows the fit of D_p for the 3-armed stars to the joint stretched exponential. As in the few other cases in which there are substantial differences between the fitted curve and measurements, the stretched-exponential form overestimates the concentration dependence of D_p .

Figure 48 shows the outcomes of the joint fit to D_p of the 12-armed stars. Except for the smallest (55kDa) star in the 1.3MDa matrix polymer, eq. 17 describes very well the entire dependence of D_p on all three variables. The fit for $f = 12$ is markedly more outstanding than is the fit to the $f = 3$ stars, particularly with the 379 kDa pVME as the matrix polymer. The displayed curves represent fits to all data points except for the 55kDa probe in the 1.3 MDa matrix polymer for $c \geq 10$ g/L. Including these 55kDa probe points in the fit raises the fractional RMS error from 14.6 to 19.5%, changes the three scaling exponents by 0.01 each, and otherwise has almost no effect on the fitted curves.

Figures 47 and 48 show that eq. 17 and a single set of fitting parameters account well for the dependence of D_p on c , P , and M for star polymers of given arm number in linear matrices. All three independent variables ranged over extensive domains: more than two orders of magni-

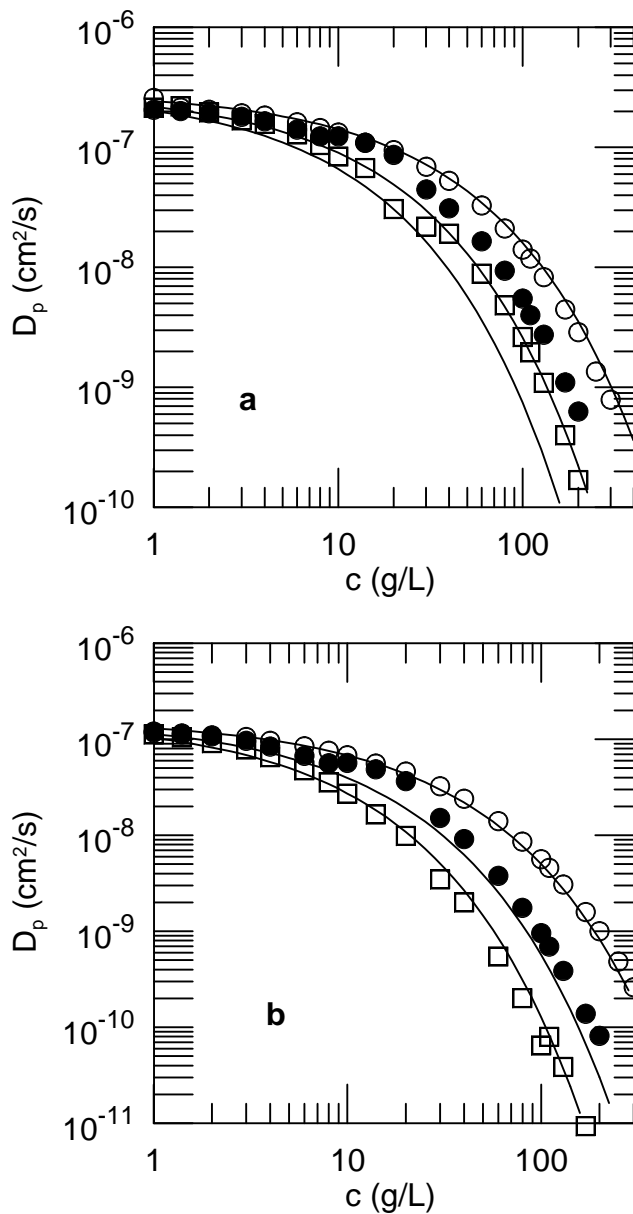


FIG. 47: D_p of (a) 379 and (b) 1190 kDa 3-arm star polystyrenes in (from top to bottom, 140, 630, and 1300 kDa) polyvinylmethylether:ortho-fluorotoluene as jointly fit to eq. 17.

tude in c , a factor of 30 in P , and an order of magnitude in M . The only failure in the fit occurred for the smallest probe in the largest matrix polymer ($P/M \approx 25$) at elevated matrix concentrations.

Martin^{71,80} examined polystyrenes diffusing through polyvinylmethylether (as the matrix polymer) in toluene, with which the matrix is isorefractive. Polystyrenes had molecular weights of 50, 100, 420, and 900 kDa with $M_w/M_n \leq 1.1$. The polyvinylmethylether had from intrinsic viscosity measurements a molecular weight ca. 110 kDa and a 'fairly polydisperse' molecular weight distri-

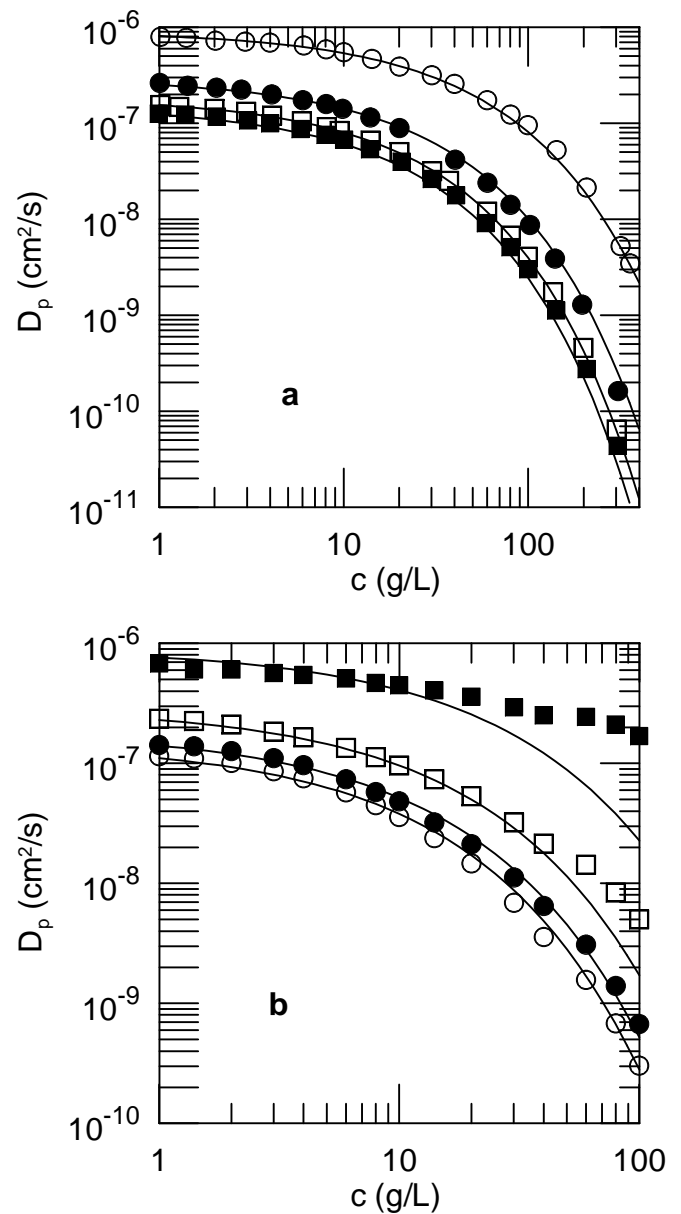


FIG. 48: D_p of 12-arm star polystyrenes (from top to bottom, M_w of 55, 467, 1110, and 1690 kDa) in (a) 140 kDa and (b) 1.3 MDa polyvinylmethylether:ortho-fluorotoluene⁷⁹, and the fit to the joint stretched exponential in c , P , and M .

bution. Diffusion coefficients of the probe polymers were obtained with QELSS; Martin^{71,80} also determined the viscosities of the polymer solutions.

Figure 49 shows D_p for each of the four probe polymers, as functions of matrix concentration. In Fig. 49a, D_p for each probe polymer was separately fit to a stretched exponential in c , yielding the parameters given in Table II and the four solid lines seen in the Figure. Stretched exponential forms do an excellent job of describing $D_p(c)$. In Fig. 49b, all data on the four probes was fit simultaneously to a single stretched exponential

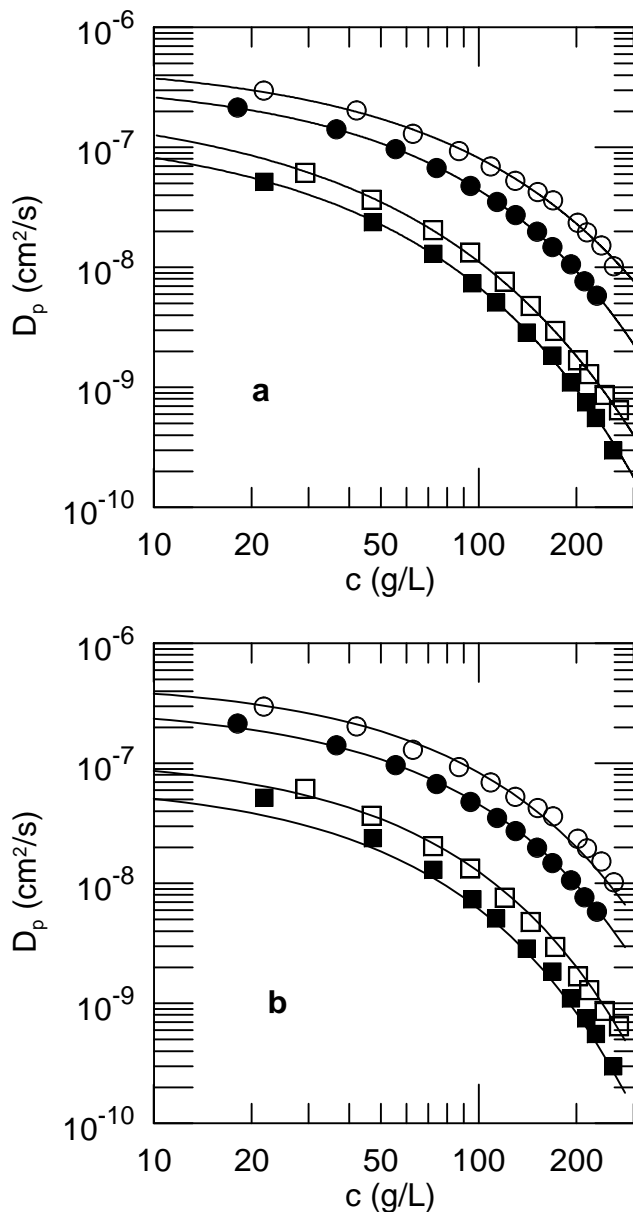


FIG. 49: Probe diffusion of (top to bottom) 50, 100, 420, and 900 kDa polystyrenes through 110 kDa polyvinylmethyl ether in toluene, based on data in Martin^{71,80}. Solid lines are (a) fits of data for each probe and (b) fits of data for all probes to stretched exponential forms.

in c and probe molecular weight P , obtaining fitting parameters given in Table III. Martin only reports results for one M , making it impossible to evaluate the M -dependence of D_p from his results. Plots of this stretched exponential, as functions of c at fixed P , give the solid lines of Fig. 49b. Agreement between the fitting function and experiment is good in the second Figure, though less good than in the first.

Martin⁷¹ also measured the viscosity of his matrix polymer solutions. At lower polymer concentrations, es-

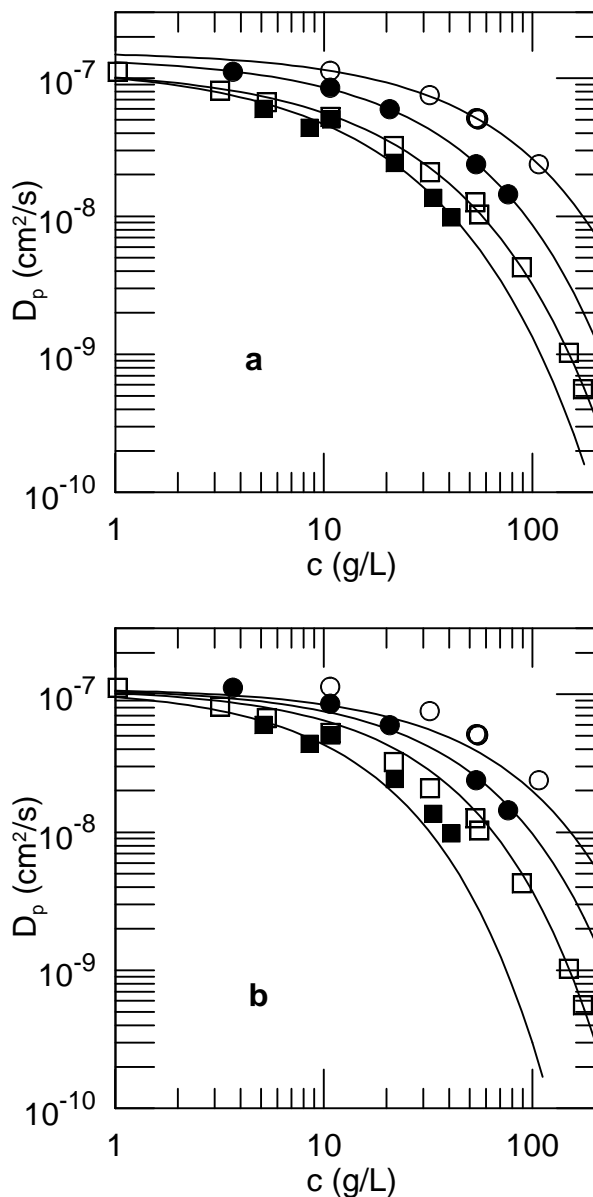


FIG. 50: D_p of 342 kDa polymethylmethacrylate in polystyrene: thiophenol (data of Nemoto, et al.⁸²) against polystyrene c concentration for polystyrene M of [top to bottom] 44, 186, 775, and 8420 kDa, and fits (a) for each M to a separate stretched exponential in c , and (b) to $D_o P^{-a} \exp(-\alpha c^\nu P^\delta M^\gamma)$ with D_o , α , and γ as fitting parameters.

pecially for the lower-molecular-weight probe polymers, Martin⁷¹ found that $D_p \eta$ is nearly constant. At elevated concentrations, especially for the larger probe chains, Stokes-Einstein behavior ceases to obtain: $D_p \eta$ increases with increasing c , so that at large c and P the polymer chains diffuse faster than might have been expected from the macroscopic solution viscosity.

In addition to the self-diffusion studies noted in the previous Section, Nemoto, et al.⁸² used ultracentrifuga-

tion and quasielastic light scattering to measure sedimentation and probe diffusion coefficients of dilute polymethylmethacrylates (as probe polymers) in isorefractive polystyrene: thiophenol solutions. Polystyrene molecular weights were 43.9, 186, 775, and 8420 kDa; the PMMA had a molecular weight of 342 kDa. The reported M_w/M_n were in the range 1.10-1.17.

Figure 50a shows Nemoto, et al.'s⁸² measurements of D_p of PMMA in solutions of each of the four polystyrenes. For each molecular weight of the matrix, $D_p(c)$ is described to good accuracy by a stretched exponential in matrix concentration. Fitting parameters are given in Table II. Figure 50b shows the same data with all measurements simultaneously fit to a stretched exponential in c and M , yielding parameters in Table III. Over nearly 200-fold variations in these variables, the single stretched exponential in c and M describes reasonably well the behavior of D_p , with a 20% RMS fractional error.

Nemoto, et al.⁸² report that D_p/D_o depends more strongly on c and P than does s/s_o . At large c , especially at large M , D_p/D_o was found to be significantly less than s/s_o . Nemoto, et al. concluded that at elevated matrix concentrations and polymer molecular weights the sedimentation and self-diffusion behaviors of PMMA in polystyrene solutions are quite distinct.

For two samples with the same D_p/D_o but very different matrix molecular weights (44, 8420 kDa), Nemoto, et al. also measured the shear viscosity η , finding that η differed 'by more than two orders of magnitude' between the two samples. Nemoto, et al. thus showed that D_p is not governed by the shear viscosity of the matrix solution. (The original paper did not specify which solution was the more viscous. Note that the comparison is being made at fixed D_p/D_o , *not* at fixed c , so the correspondence is not self-evident.)

Nemoto and collaborators^{83,84} also used forced Rayleigh scattering to study the diffusion of probe polystyrenes through polystyrene:dibutylphthalate solutions. A first study⁸³ focused on self-diffusion and tracer diffusion of labeled polystyrene through 40 wt% solutions of very long chains ($M/P > 5$) and very short chains ($M/P < 0.2$). Thirteen polystyrenes having $2.8 \leq M_w \leq 8420$ kDa and $M_w/M_n < 1.07$ (except for chains larger than 1MDa, for which M_w/M_n was in the range 1.09-1.17) were used in the studies.

Nemoto, et al.'s data⁸³ appears as Fig. 52. For D_s and for D_{tr} of short probe chains in solutions of long matrix molecules, a best-fit to the molecular weight dependence of D gives parameters seen in Table III, the P -dependence of the prefactor being forced rather than obtained from the fit. Because all data is at the same concentration, a concentration dependence was not obtained. Similarly, if we fit the data of Nemoto, et al.⁸³ on D_p of long probe chains in short matrix chains to $D_o P^{-a} \exp(-\alpha P^\gamma)$, we find that D_p gains its molecular weight dependence almost entirely through the factor P^{-a} . The data are fit well with $a = 0.52$, in which case

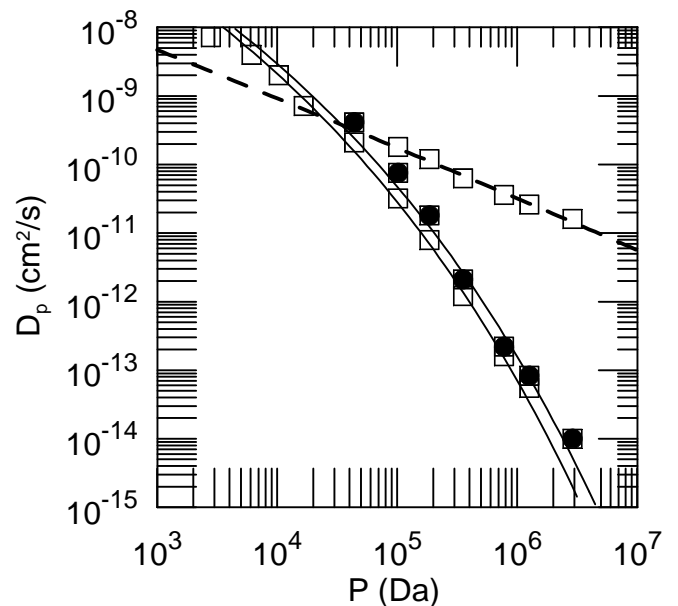


FIG. 51: D_s (filled points) and D_p (open points) from Nemoto, et al.⁸³, Tables 2 and 3. Dashed line marks systems with $M \ll P$; solid lines represent a joint fit to D_s and to systems with $M/P > 5$.

the best-fit gives $\gamma \approx 0.03$.

In a separate paper, Nemoto, et al.⁸⁴ used forced Rayleigh scattering to measure D_p of probe polystyrenes in dibutylphthalate solutions of high-molecular-weight matrix polymers at 13 and 18 % matrix concentration. The probe polystyrenes were in the molecular weight range $6.1 \leq M_w \leq 2890$ kDa, with polydispersities $M_w/M_n \leq 1.17$, and generally ≤ 1.09 . Table IV shows the fits to this data. RMS fractional errors were 12-13% for single concentrations, but ca. 30% for the fit to both concentrations. It should be stressed that D_p covers more than five orders of magnitude, so the errors are not large relative to the total range of D_p . We find a significant dependence of D_p on matrix as well as probe molecular weight. With only a few points for any particular P or M , it is difficult to present the data as a simple figure.

Numasawa, et al.⁸⁵ used QELSS to study the diffusion of tracer polystyrene chains through index-matched solutions of matrix polymethylmethacrylates in benzene. Polystyrene molecular weights were in the range 185-8420 kDa, with M_w/M_n in the range 1.04-1.17. Polymethylmethacrylates had molecular weights 850-4050 kDa, with $M_w/M_n \leq 1.08$, except for the 850 kDa polymer, for which M_w/M_n was 1.35. PMMA matrix concentrations were a half-dozen values in the range 0-36 g/L. The tracer polystyrenes were dilute in all solutions. In addition to measuring the probe diffusion coefficients, Numasawa, et al.⁸⁵ also report the zero-shear viscosity of the matrix polymers and (on the basis of static light scattering) determinations of the radii of gyration of the probe polymers as a function of matrix concentration.

Numasawa, et al's results⁸⁵ appears as Fig. 52. Figure 52a shows D_p of the 420 kDa and the 8.42 MDa polystyrene in solutions of two polymethylmethacrylates, as a function of matrix concentration. Figure 52b shows D_p of five polystyrenes in each of four polymethylmethacrylates, all at a matrix concentration near 37 g/L. One observes that D_p decreases monotonically with increasing probe molecular weight and with increasing matrix concentration and molecular weight.

All eight solid lines in both figures represent a simultaneous fit of a stretched exponential in c , P , and M to all of the data in both Figures and to one additional data point. Fit parameters appear in Table III. It is important to emphasize that the same fitting parameters were used to generate all eight curves in both Figures. From Fig. 52a, the stretched exponential captures well the c -dependence of D_p , and the variation of that dependence with P and M . From Figure 52b, at fixed c , the stretched exponential captures reasonably well the dependence of D_p on M at fixed P , but at fixed M and c does less well at capturing the dependence of D_p on P .

Nyden, et al.⁸⁶ used PFGNMR to determine probe diffusion of monodisperse ($M_w/M_n < 1.1$) polyethylene oxides (molecular weights 10-963 kDa) diffusing through aqueous solutions of 100kDa ethylhydroxyethylcellulose. The authors studied 1% and 6% solutions and a 1% chemically cross-linked gel. Figure 53 shows D_p/D_o of the polyethylene oxides in 1% of the matrix polymer as a function of their hydrodynamic radii. The solid line in the Figure represents a stretched exponential

$$D_p/D_{p0} = D_1 \exp(-\alpha R^\beta) \quad (19)$$

in probe hydrodynamic radius R , where α and δ are a scaling prefactor and exponent, D_{p0} is the diffusion coefficient of the probe polymer in pure solvent, and D_1 is the probe diffusion coefficient for a nominal $R = 0$ polymer chain. The best-fit parameters were $D_1 = 0.33$, $\alpha = 0.33$, and $\beta = 0.57$; the RMS fractional error in the fit was 7%. Nyden, et al.⁸⁶ note $R = KP^a$ with $a = 0.53$ for probes having molecular weight P , so equation 19 is equivalent to a stretched exponential in P^γ with $\gamma \approx 0.30$. This value of γ is consistent with values for γ found for other systems, as seen in Table III.

Nyden, et al.⁸⁶ also examined probe diffusion in 6% solutions of their matrix polymer. dD_p/dM does not change monotonically with increasing M . However, at the larger M at which the anomalous behavior occurs, the PFGNMR echo decays are no longer simple exponentials, implying that diffusive behavior has become more complex.

Pinder⁸⁷ reported from PFGNMR measurements the tracer diffusion coefficient of styrene and low-molecular-weight probe polystyrenes ($P \leq 2470$ Da) through solutions of deuterated polystyrenes ($10.7 \leq M \leq 430$ kDa) in theta (cyclohexane) and non-theta (CCl_4) solvents. D_p was measured as a function of matrix polymer concentration for matrix concentrations up to 300 g/L. The matrix polymer polydispersities were $M_w/M_n \leq 1.14$,

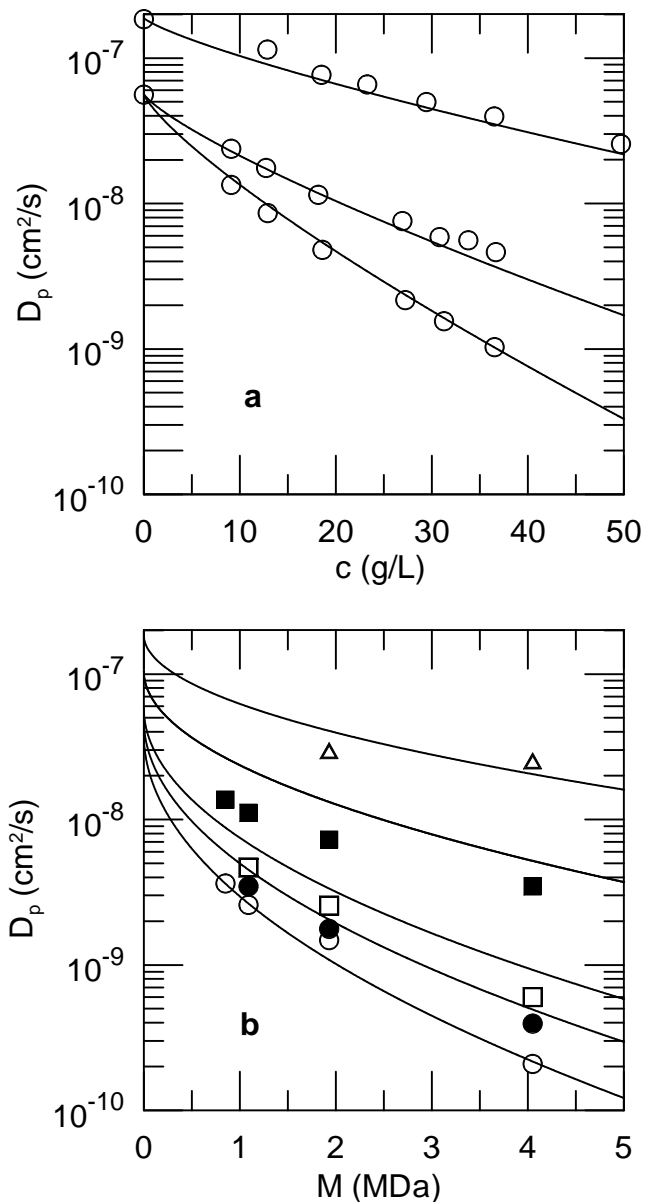


FIG. 52: D_p of polystyrenes in polymethylmethacrylate: benzene (a) as a function of matrix concentration, with $P:M$ of [top to bottom] 420 kDa:4.05 MDa, 8.42 MDa: 1.95 MDa, and 8.42 MDa: 4.05 MDa, and (b) as a function of molecular weight, for [top to bottom] 0.42, 1.26, 3.84, 5.48, and 8.42 MDa polystyrene probes in 36.7 g/L polymethylmethacrylate. The lines all show the same best-fit stretched exponential in c , P , and M .

with in most cases $M_w/M_n < 1.08$.

Figure 54a shows the tracer diffusion coefficient of styrene in polystyrene solutions. The matrix molecular weights were 68 and 200 kDa in the non-theta solvent and 68, 87, 200, and 430 kDa in the theta solvent. Within the scatter in the data—there are not a large number of data points for any particular matrix M — D_p does not appear to depend on M . $D_p(c)$ was fit both to pure and

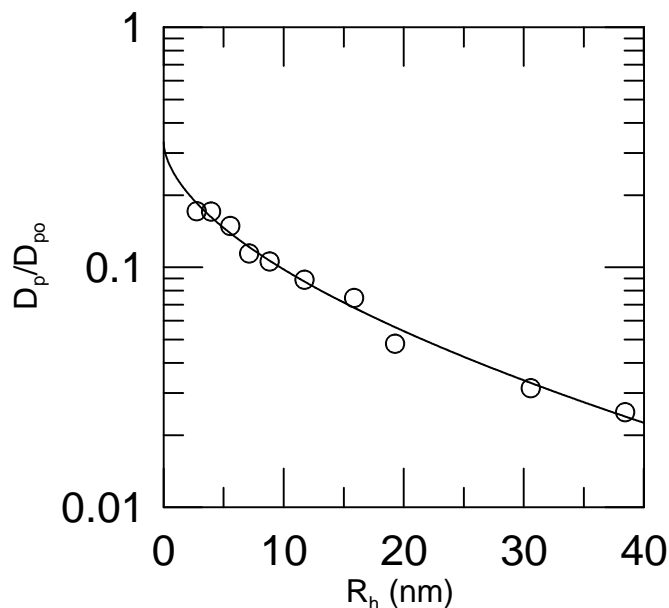


FIG. 53: D_p/D_{p0} from Nyden, et al.⁸⁶ for polyethylene oxides with a range of molecular weights diffusing in 1% solutions of 100kDa ethylhydroxyethylcellulose, plotted as a function of the hydrodynamic radii of the probes in pure water.

stretched exponentials in c . As seen in Table II, there appears to be very little improvement in the fit on allowing $\nu \neq 1$, so the Figure shows the fits to the pure exponentials in c .

Figure 54b shows the tracer diffusion coefficient of styrene and three low-molecular-weight polystyrenes ($P \leq 2470$ Da) through a range of high-molecular-weight polystyrenes ($10.7 \leq M \leq 430$ kDa). For each probe, matrix molecular weights were varied by factors of 3-5 with no apparent significant effect on D_p . In all cases, M/P was in the range 15-20 or larger. $D_p(c)$ for each probe was fit to a separate stretched exponential, giving excellent results reported in Table II. The merged results for all four probes were also fit jointly to a stretched exponential in c and P . The computed D_p for styrene monomer underestimates $D_p(c)$ by a nearly constant multiplicative factor. Because styrene is little larger than a solvent molecule, a second fit including only the polymer probes was made. Parameters for both fits are in Table IV. The Figure shows the second fit, to the three polymeric probes. The second fit has a modestly better RMS fractional error, and finds in the limit of zero matrix concentration that $D_p \sim P^{-0.52}$. If the styrene monomer is included in the fits, in the same $c \rightarrow 0$ limit $D_p \sim P^{-0.68}$ is obtained.

Smith, et al.⁸⁸ used fluorescence recovery after pattern photobleaching to measure the diffusion of labeled 33.6 kDa polypropylene oxide (PPO) chains through solutions of unlabeled 32kDa PPO chains dissolved in a melt of 1 kDa PPO chains. The probe and solvent were relatively monodisperse ($M_w/M_n = 1.1$) while the matrix polymer

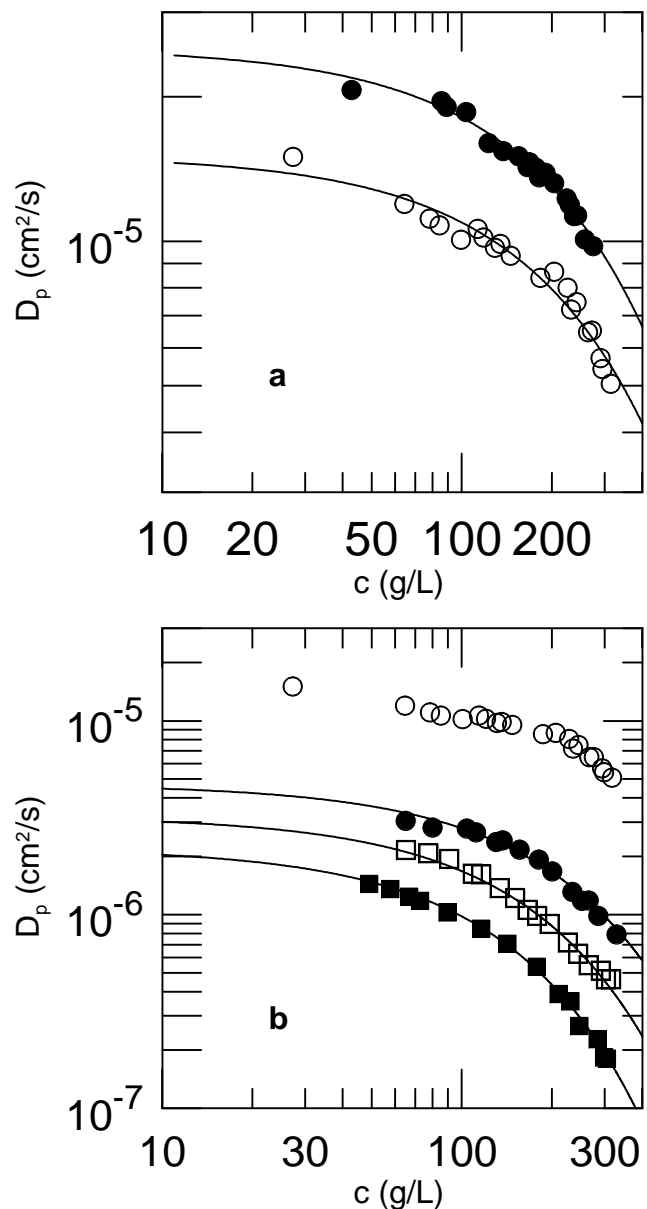


FIG. 54: D_p , using data of Pinder⁸⁷, of (a) styrene monomer through solutions of high-molecular-weight polystyrenes in cyclohexane (theta solvent, filled points) and CCl_4 (non-theta solvent, open points), and pure-exponential fits, and (b) [top to bottom] styrene monomer and 580, 1200, and 2470 Da polystyrene polymers in CCl_4 and a high-molecular weight polystyrene matrix polymer with (lines) fits of the polymeric probes data to $D_p = D_o P^{-a} \exp(-acP^\gamma)$.

was relatively polydisperse ($M_w/M_n = 1.6$). The matrix concentration was varied all the way from dilute solution up to the matrix melt. Smith, et al.'s data⁸⁸ are shown in Fig. 55. The solid line in the Figure is a stretched-exponential fit using parameters in Table II. A single stretched exponential with constant parameters describes the concentration dependence of D_p all the way from dilute solution up to the matrix melt.

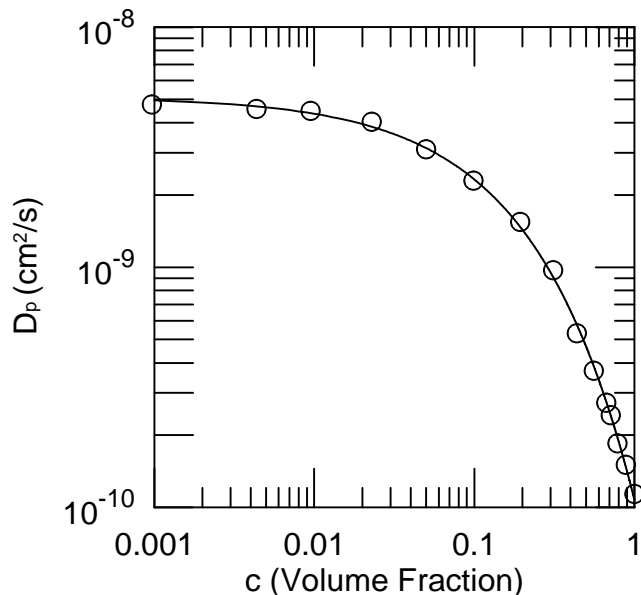


FIG. 55: D_p of 33.6 kDa labeled polypropylene oxide chains through solutions of 32 kDa PPO chains in a 1 kDa PPO melt, using results of Smith, et al.⁸⁸, Figure 1. The solid line represents a stretched-exponential fit.

Tead and Kramer⁸⁹ studied diffusion of 255 kDa deuterated polystyrene through solutions of large-molecular-weight (93, 255, and 20 000 kDa) polystyrenes dissolved in a low-molecular-weight (10 kDa) polystyrene melt. The matrix polymer volume fraction covered the full range $0 \leq \phi \leq 1$. The temperature was 150 C for the 93 and 255 kDa matrix polymers and 175 C for the 20 000 kDa matrix polymer. Probe diffusion coefficients were obtained using forward recoil spectroscopy to measure concentration profiles of the probe molecules as a function of time. As seen in Fig. 56, D_p is represented well by a stretched exponential in the matrix polymer concentration c , no matter whether the matrix molecular weight is less than, equal to, or far larger than the probe molecular weight. The agreement with the stretched-exponential form is good from low concentrations of a short (93 kDa) chain out to high concentrations (melt) of a very large (20 000 kDa) chain.

Tinland and Borsali⁹⁰ used fluorescence recovery after photobleaching and quasielastic light scattering to make independent measurements of the probe diffusion coefficient of 433 kDa dextran through solutions of 310 kDa polyvinylpyrrolidone in water. PVP concentrations ranged from 0 to 120 g/L. The polydispersity M_w/M_n is 1.5 for the matrix polymer but ca. 1.9-1.95 for the probe chains. Except perhaps at the very highest concentrations studied, values of D_p from the two techniques do not agree. In the following analysis, we use D_p as obtained from FRAP, since the values from this technique do not rely so heavily on detailed model assumptions of the relationship between the scattering spectrum and the

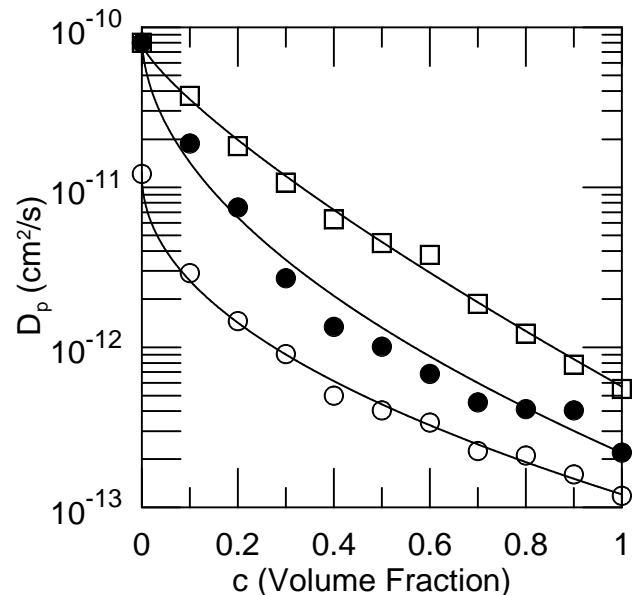


FIG. 56: D_p of 255 kDa deuteropolystyrene in solutions of [top to bottom] 93, 250, and 20 000 kDa polystyrene in molten 10 kDa polystyrene, at 150, 150, and 175 C, respectively, from Tead and Kramer⁸⁹ Figures 4 and 6. Solid lines are stretched-exponential fits using parameters given in Table II. For clarity, the 150 C data has been multiplied by a factor of 100.

underlying diffusion coefficients. Tinland and Borsali's data appear in Fig. 57, with data points from the original paper⁹⁰ and a smooth curve showing the stretched exponential in c generated from the fitting parameters in Table II. Agreement between the measurements and the functional form is good at all polymer concentrations.

Wheeler, et al.⁹¹ studied tracer diffusion of linear polystyrenes having molecular weights 65, 179, 422, and 1050 kDa (with $M_w/M_n \leq 1.1$) through a 1.3 MDa polyvinylmethylether matrix polymer, $M_w/M_n \approx 1.6$, in orthofluorotoluene. D_p was determined using quasielastic light scattering, which was possible because the polystyrenes were present at trace concentration while the matrix polymer and solvent are isorefractive. Matrix concentrations covered the range 1–100 g/L. For this matrix polymer, $1/[\eta] = 2.2$ g/L, so much but not all of the data is in the range $c > c^*$.

The data and corresponding stretched-exponential fits are in Figs. 58a and 58b, with fit parameters in Tables II and III, respectively. Figure 58a shows fits made separately for each probe polymer. As in the other systems discussed above, the concentration dependence of D_p for each probe is described extremely well by a stretched exponential in polymer concentration. Figure 58b shows the outcome of a simultaneous fit of a single stretched exponential in c and P to all data on all four probes. At the scale of the Figures, the curves in the two Figures for the 179 and 422 kDa probes are coincident, while the curves for the 1050 kDa probes are very close. However, for the smallest probe and large matrix concentrations the joint

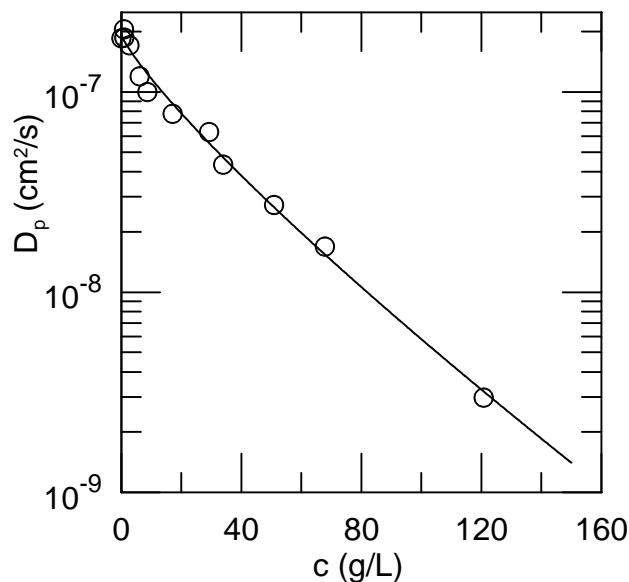


FIG. 57: D_p of 433 kDa dextran diffusing through aqueous solutions of 310 kDa polyvinylpyrrolidone, based on data of Tinland and Borsali⁹⁰, Table 2 and Figure 3. Solid line is a stretched-exponential fit from parameters in Table II.

stretched exponential substantially underestimates D_p .

Wheeler and Lodge⁹² used QELSS to measure the diffusion of linear polystyrenes through polyvinylmethylether:ortho-fluorotoluene. The polystyrenes had molecular weights of 65, 179, 422 and 1050 kDa, with polydispersities $M_w/M_n < 1.1$. The polyvinylmethylether samples had molecular weights of 140, 630, and 1300 kDa; concentrations of these matrix polymers ranged up to 300 g/L. Reference 92 represents a major extension of Ref. 91 in the range of matrix concentrations, number of matrix molecular weights, and number of concentrations studied. For the three matrix polymers, c^* was estimated at 11, 5.7, and 3.3 g/L, respectively (based on $c^* = 1.5/[\eta]$), while c_e was estimated at 50, 12, and 6 g/L, respectively. The matrix polymers had $M_w/M_n \approx 1.6$.

Wheeler and Lodge also used PFGNMR to measure D_{s0} of ortho-fluorotoluene diffusing through the 1300 kDa polyvinylmethylether at matrix concentrations up to 300 g/L. D_{s0} fell by 62% over this concentration range. To good approximation, $D_{s0}(c)$ of the ortho-fluorotoluene is fit by a simple exponential $D_{s0} = 2.15 \cdot 10^{-5} \exp(-2.98 \cdot 10^{-3} c)$. Wheeler and Lodge⁹² and also Lodge, et al.⁷⁹ used these data to modify D_p of their polystyrene polymer probes to remove the concentration dependence of a nominal local friction $\zeta = k_B T / D_{s0}$. This local friction modification was here removed from the probe diffusion data of Refs. 92 and 79 before analyzing them further.

Figures 59 show Wheeler, et al.'s⁹² data on their four probe polystyrenes in the 140 and 630 kDa polyvinylmethylethers. Solid lines represent fits to stretched ex-

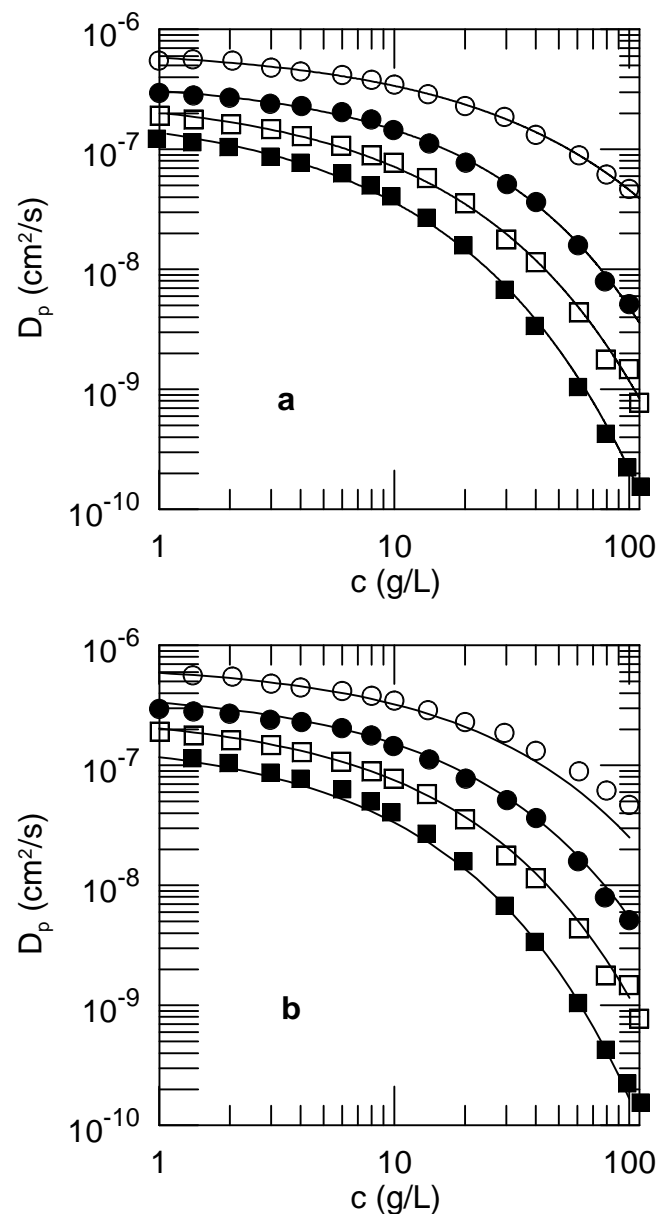


FIG. 58: D_p of polystyrenes (from top to bottom, M_w of 65, 179, 422, and 1050 kDa) diffusing through solutions of 1.3 MDa polyvinylmethylether:ortho-fluorotoluene based on data of Wheeler, et al.⁹¹, with solid lines showing fits to (a) separate stretched exponentials at each P , and (b) jointly to a stretched exponential in c and P .

ponentials in c for individual probe:matrix pairs. The fits are uniformly extremely good, with RMS fractional errors in the range 2-12% and fitting parameters as seen in Table II

We also fit all of Wheeler, et al.'s data^{91,92} to a joint stretched exponential in c , P , and M , as seen in Figs. 60. The solid lines are the best-fit $D_p(c)$, plotted for fixed P and M , all lines being computed from a single set of parameters given in Table III. In Fig. 60c, measurements

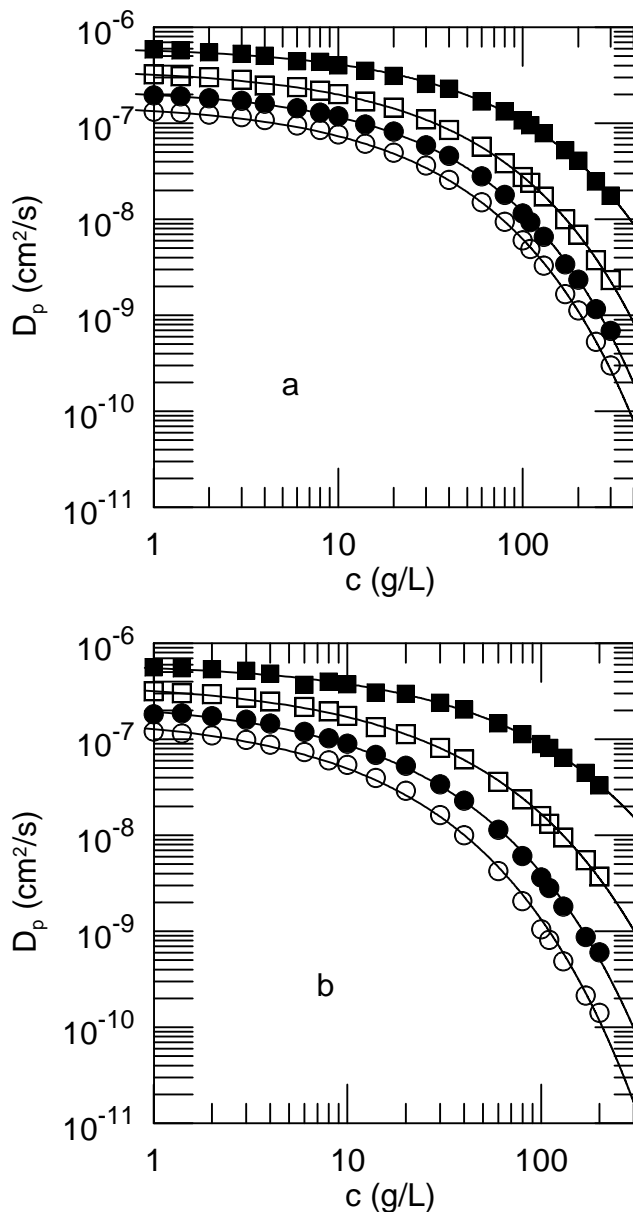


FIG. 59: D_p of polystyrenes (from top to bottom, M_w of 65, 179, 422, and 1050 kDa) diffusing through solutions of (a) 140 kDa and (b) 630 kDa polyvinylmethylether:orthofluorotoluene based on data of Wheeler, et al.⁹², and (lines) separate stretched-exponential fits for each $P : M$ combination.

from Ref. 92 were supplemented with the data of Ref. 91; the latter reference reported D_p for all probes in 1300 kDa polyvinylmethylether solutions having $c \leq 100$ g/L.

Over an order of magnitude in matrix molecular weight, a factor of 15 in probe molecular weight, and a factor of 300 in matrix concentration, the joint stretched exponential of eq 17 represents reasonably well the joint dependence of D_p on c , P , and M . The RMS fractional error in the fit is 25%. As noted above in the analysis for Ref. 91's data, for the smallest probe in the 630 and

1300 kDa matrix polymers (Fig. 60), the stretched exponential form noticeably underpredicts D_p . A similar issue arises for the 1050kDa probe in the 140 kDa matrix polymer (fig. 60a): at large c the predicted D_p is too small, because the predicted curve does not bend quite sharply enough between small and large c .

V. OTHER EXPERIMENTAL STUDIES

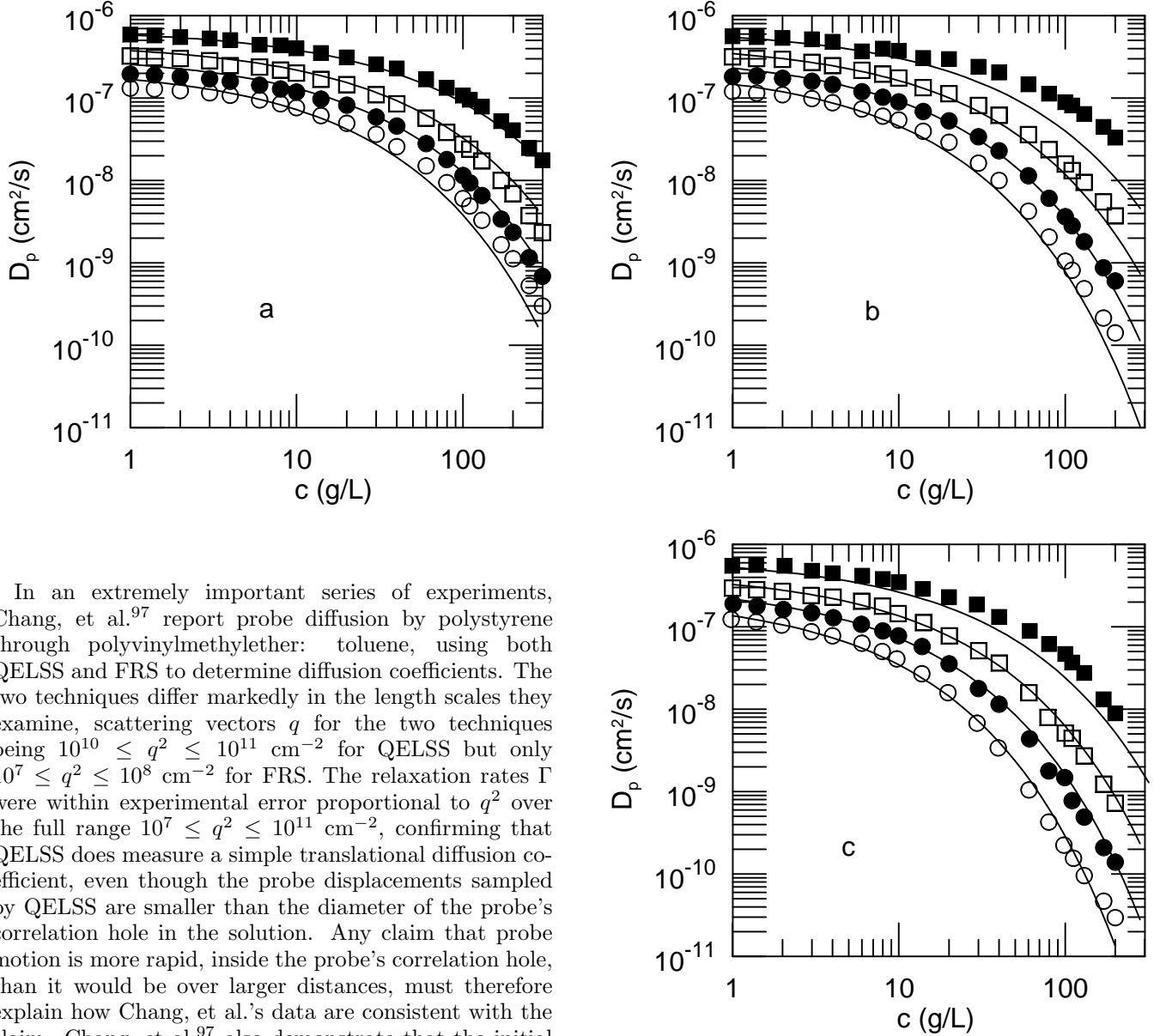
In addition to the work reviewed above, a variety of other studies of polymer tracer diffusion appear in the literature. These are papers whose experimental foci are not the same as those of the papers examined in the previous sections, and which are not amenable to analysis on the lines employed above. For example, a number of papers report scattering spectra of polymer: polymer: solvent mixtures in which neither polymeric species is dilute, and therefore in which the spectral relaxation times do not correspond to the self-diffusion coefficient.

Aven and Cohen⁹³ measured the diffusion of dilute polystyrenes through 15 vol% solutions of polydimethylsiloxane in tetrahydrofuran. The tracer diffusion coefficients of the polystyrenes, the molecular weight dependence, and the initial linear slope of the concentration dependences were obtained with light scattering spectroscopy.

Borsali, et al.⁹⁴ studied QELSS spectra of 970 kDa polystyrene: 950 kDa polymethylmethacrylate: toluene, PMMA and toluene forming an isorefractive pair. Semi-quantitative experimental tests were made of the theoretical work of Benmouna, et al.²¹. When neither polymer was dilute, the observed spectrum was biexponential. The mode amplitude ratio and relaxation times were within a factor of two of predictions of the Benmouna model²¹. The mutual diffusion coefficient of polystyrene in toluene and the cooperative diffusion coefficient of the mixture, both measured at the same total polymer concentration, are equal to within 6%, also in agreement with the theory.

Borsali, et al.⁹⁵ extended their work on this ternary system with measurements at several large (weight fraction > 0.8) polystyrene concentrations and a range of total polymer concentrations, finding two relaxational modes in QELSS spectra. The diffusion coefficient associated with the fast mode increased with increasing polymer concentration. The diffusion coefficient associated with the slow mode decreased markedly with increasing polymer concentration. Results were consistent with the Benmouna, et al.²¹ model.

Borsali, et al.⁹⁶ also studied mixtures of polystyrene and polydimethylsiloxane in tetrahydrofuran (which is isorefractive with polydimethylsiloxane) and in toluene, which is a zero average contrast solvent for these polymers and conditions. Measured spectral forms (one or two relaxations), relaxation times, and their concentration dependences were consistent with the Benmouna model²¹.



In an extremely important series of experiments, Chang, et al.⁹⁷ report probe diffusion by polystyrene through polyvinylmethylether: toluene, using both QELSS and FRS to determine diffusion coefficients. The two techniques differ markedly in the length scales they examine, scattering vectors q for the two techniques being $10^{10} \leq q^2 \leq 10^{11} \text{ cm}^{-2}$ for QELSS but only $10^7 \leq q^2 \leq 10^8 \text{ cm}^{-2}$ for FRS. The relaxation rates Γ were within experimental error proportional to q^2 over the full range $10^7 \leq q^2 \leq 10^{11} \text{ cm}^{-2}$, confirming that QELSS does measure a simple translational diffusion coefficient, even though the probe displacements sampled by QELSS are smaller than the diameter of the probe's correlation hole in the solution. Any claim that probe motion is more rapid, inside the probe's correlation hole, than it would be over larger distances, must therefore explain how Chang, et al.'s data are consistent with the claim. Chang, et al.⁹⁷ also demonstrate that the initial dependence of the measured diffusion coefficient on the probe concentration depends strongly on matrix concentration, the initial slope being substantially positive in the absence of matrix polymer and becoming significantly negative as polystyrene concentration is increased.

B. Chu, et al.^{101,102} report on the diffusion of polymethacrylate probes through a polystyrene matrix. The solvent was a mixture of toluene and α -chloronaphthalene. By adjusting the solvent composition and the temperature, it was possible to make a virtually exact match of the indices of refraction of the mixed solvent and the matrix, so that scattering arose only from the probe. By varying the solvent composition, the motions of the matrix could separately be examined. A weak fast mode and a dominant slow mode were apparent, even at low angles, for probe chains much larger than the matrix chains. The slow mode had a weaker concentration dependence than does the solvent viscosity.

FIG. 60: Merged data from Figs. 58 and 59, with (a) 140 kDa, (b) 630 kDa, and (c) 1300 kDa matrix polymers, probe symbols as in the previous figures, and (solid line) fit of all data to a single stretched exponential in c , P , and M . Parameters are in Table III.

S. Chu and collaborators⁹⁸ studied the motion of fluorescently labelled DNA molecules in non-dilute solution. They propose that they have confirmed the reptation model, based on their observations that (i) stretched DNA chains relax as though they were confined to tubes, (ii) D_s scales as M^{-2} for nondilute probe chains, and (iii) a scaling law $D_s \sim c^{-1.75}$ is consistent with their data.

However, referring to these points seriatim: (i) Even within the reptation model a stretched chain relaxes from stretching primarily via its higher-order modes, revealing

only tube confinement on a short time scale. (ii) The scaling result $D_s \sim M^{-2}$ is a common feature of many models, is in no sense a signature of reptation⁹⁹, and in any event is inconsistent with the modern¹⁰⁰ analysis of data on synthetic polymers, (iii) Ref. 98's measurements of $D_s(c)$ are too scattered to demonstrate $c^{-1.75}$ behavior. Furthermore, if these data had demonstrated concentration scaling, they would be inconsistent with essentially all other data in the literature on the concentration dependences of D_s and D_p of polymers in solution, as reviewed here, in that in almost all other systems D_s and D_p have stretched-exponential, not power-law, concentration dependences.

Finally, as was not emphasized in the original paper, the data of Chu and collaborators⁹⁸ conclusively reject the reptation model for their system. According to the reptation model, polymer chains only perform free diffusion after they escape from their tubes, which occurs at times longer than τ_d . At times $t < \tau_d$, polymer chains remain confined to their tubes and perform confined diffusion, so for $t < \tau_d$ a chain's mean-square displacements satisfy $\langle x^2 \rangle \sim t^x$ where x is 0.5 or less. Ref. 98 reports that their chains under their conditions remain within the hypothesized tube for a time $\tau_d \approx 1.2$ or $\tau_d > 2$ minutes, depending on which of several methods is used to estimate τ_d . However, ref. 98 measured directly $\langle x^2(t) \rangle$. Figure 2 of ref. 98 shows $\langle x^2(t) \rangle \sim t^1$ for times as short as $\tau_d/7$ or less. That is, ref. 98 found that their chains were performing free, Brownian, non-constrained diffusion even on time scales sufficiently short that under the reptation model the chains would have been confined to their tubes. This last finding is completely incompatible with the reptation model, which requires that chains perform constrained curvilinear diffusion along their tubes so long as they remain inside their tubes. The data of Chu and collaborators⁹⁸ thus indicates that a key aspect of the reptation picture, namely tube confinement, is incorrect, at least in Chu, et al.'s system.

Corrotto, et al.¹⁰³ performed static light scattering and QELSS measurements on bidisperse nondilute mixtures of polystyrene in toluene, extracting fast and slow mode relaxations.

Cosgrove and Griffiths¹⁰⁴ used PFGNMR to study the diffusion of protonated polystyrenes through solutions of deuterated polystyrenes, varying the matrix concentration, and the probe and matrix molecular weights. Data was obtained over limited ranges of D_p on the dependence of D_p on each of these variables. D_p generally declined with increasing matrix concentration and molecular weight, and also declined with increasing probe molecular weight, except for very large probes in relatively dilute solutions of small polymers, in which D_p was nearly independent of matrix molecular weight.

Cotts¹⁰⁵ report QELSS measurements on polystyrene: polyvinylmethylether: toluene, proposing that radii of gyration, hydrodynamic radii, scaling exponents, and modes of diffusive motion can be measured systematically for the dilute visible chains. This and other⁷⁶ early

work on polystyrene: polyvinylmethylether: toluene flowered into the systematic studies of Lodge, Wheeler, and collaborators^{77,78,79,91,92} on this system.

Daivis and Pinder¹⁰⁶ report QELSS studies of polystyrene: polyvinylmethylether mixtures dissolved in toluene or carbon tetrachloride. The first ternary mixture is nearly unique, in that the polymers are nearly compatible, toluene is a good solvent for both polymers, and toluene and PVME are isorefractive. The second ternary mixture differs from the first in that CCl_4 is only a marginal solvent for polystyrene. In CCl_4 , spectra become nonexponential. The diffusion coefficient in nondilute CCl_4 solutions is reduced by more than three-fold relative to diffusion by the same concentrations of the two polymers in toluene, but the probe radius of gyration is only very slightly reduced by increasing the matrix concentration.

Desbrieres and collaborators¹⁰⁷ applied QELSS to solutions of dextran and polyvinylpyrrolidone in water in solutions more concentrated than the overlap concentration. Two modes whose properties are consistent with Benmouna²¹-type models of diffusion in ternary polymer solutions were observed. The mixtures have a phase separation at elevated concentration. As polymer concentrations are increased towards the phase separation, a third slow mode whose various properties are consistent with the formation of aggregates was observed.

Giebel and co-workers^{108,109} studied QELSS spectra of polydimethylsiloxane and polymethylmethacrylate in several solvents as a function of the relative concentration of the two polymers. At the fixed total polymer concentration, the polymers were reasonably expected to be non-dilute. Comparison was made with theoretical results of Benmouna, et al.²¹, with particular attention to the "zero average contrast" condition. A strong variation of some spectral parameters with composition was described well by Benmouna²¹-type models and a small number of free parameters.

Jamil, et al.¹¹⁰ report QELSS measurements on the diffusion of random-coil polystyrene probes through solutions of the rigid-rod polymer poly-(γ -stearyl α ,L-glutamate) in its isorefractive solvent toluene. The polymers are incompatible, poor miscibility of rods with random coils being identified by Jamil, et al.¹¹⁰ as a significant experimental challenge. Experimentally, the light scattering spectrum in these systems is due entirely to the polystyrene probes.

Jamil, et al.¹¹⁰ found that the dominant slow mode of the QELSS spectra is strongly concentration-dependent. At lower matrix concentration the diffusion coefficient corresponding to the slow mode increases with increasing probe concentration. At elevated matrix concentration this diffusion coefficient instead decreases with increasing probe concentration. Extrapolating this diffusion coefficient to zero probe concentration gives the tracer-diffusion coefficient of the probe polymer through the rod matrix. Jamil et al. reported fitting their six values of D_s to a stretched-exponential form. They found

$\alpha \approx 0.4$ and $\nu \approx 1.3$. Jamil, et al.¹¹⁰ interpret the finding $\nu > 1$ as arising from end-to-end aggregation of the matrix polymer; the matrix polymer increases its hydrodynamic radius as its concentration is increased.

Konak, et al.¹¹¹ report QELSS spectra of mixtures of polystyrene and polymethylmethacrylate in toluene. Neither polymer was dilute. Comparison was made for a limited number of concentrations with theoretical models arising from work of Benmouna, et al.²¹. Treating spectra as bimodal, the ratio of relaxation times was predicted theoretically to better than 50%, but predictions of the mode amplitude ratio were often inexact by factors of 2 or 3.

Marmonier and Leger¹¹² report extensive measurements using FRS on tracer diffusion of labelled polystyrenes through polystyrene in a good solvent. Unfortunately, the reported data were modified by dividing them by an unreported *concentration-dependent* factor, namely the normalized concentration-dependent tracer diffusion coefficient of the free label in the same polymer solutions. It is therefore impossible to compare these measurements with other papers analyzed here.

Numasawa, et al.¹¹³ report scattering spectra of a series of dilute polystyrenes in polymethylmethacrylate (in its isorefractive solvent benzene). The major focus was the scattering-vector dependence of the linewidth Γ , especially at larger scattering vectors q . At larger q , Γ/q^2 of the self-diffusive mode increases with increasing q . Measurements were only made at a single non-dilute matrix concentration, preventing further analysis of this data along the lines of this review.

Russo, et al.¹¹⁴ report self-diffusion coefficients for poly(γ -benzyl- α ,L-glutamate) in pyridine. The rodlike polymer has an isotropic-cholesteric liquid crystal phase transition with increasing concentration. Russo, et al. found that D_s decreases with increasing polymer concentration until the phase transition is reached. At the phase transition, D_s increases abruptly; it then decreases again as the polymer concentration is further increased. $D_s(c)$ is qualitatively consistent with a stretched exponential form in the isotropic phase, but the number and spacing of points in the isotropic regime limits the accuracy of a quantitative fit to this very interesting data.

Scalettar, et al.¹¹⁵ used FRAP and FCS to study diffusion of phage λ DNA solutions. By comparing systems in which either few, or almost all, molecules were labelled, Scalettar, et al. were able to confirm the prediction of this author¹³ that if very few macromolecules are labelled, fluorescence correlation spectroscopy determines their tracer diffusion coefficient, but if almost all macromolecules are labelled, fluorescence correlation spectroscopy determines their mutual diffusion coefficient.

Sun and Wang^{116,117,118} report a series of studies of polystyrene/polymethylmethacrylate mixtures (in benzene, dioxane, and toluene, respectively) using QELSS as the major experimental technique. Both polymers were in general nondilute. Neither polymer is isorefrac-

tive with any of the solvents. The objective was to study the bimodal spectra that arise under these conditions and to show that the two relaxation times and the mode amplitude ratio can be used to infer diffusion and cross-diffusion coefficients of the two components. Experimental series varied both the total polymer concentration and the concentration ratio of the two components. The theoretical model predicts a biexponential spectrum; the experimental data was fit by a bimodal distribution of relaxation rates or by a sum of two Williams-Watts functions. The inferred self-diffusion coefficients of both species fall with increasing polymer concentration, but the concentration ranges that Sun and Wang studied are too narrow for further interpretation.

VI. ANALYSIS

The above sections have presented a detailed examination of nearly the entirety of the published literature on polymer self-diffusion and probe diffusion in polymer solutions. The dependences of D_s and D_p on polymer concentration, probe molecular weight, and matrix molecular weight have been determined. Some features of this literature are incidental consequences of the chemical identity of the polymer being studied. The objective of this Section is to extract systematic behaviors from the above particular results. Here we ask: If we rise above particular features determined by the identity of the polymer under examination, what are the ideal features common to self- and probe-diffusion of all polymers in solution?

In the following: First, the functional forms of the concentration and molecular weight dependences of the self- and probe diffusion coefficients are considered. Second, having found that D_s and D_p uniformly follow stretched exponentials in c , correlations of the stretched-exponential scaling parameters with other polymer properties are examined. Third, for papers in which diffusion coefficients were reported for a series of homologous polymers, we examine a joint function of matrix concentration and matrix and probe molecular weights and what it reveals about polymer diffusion. Fourth, we examine the few cases in which stretched-exponential behavior is not seen, or in which particular features of a given system clarify the systematic behavior of the phenomenological parameters used to describe D_s and D_p . Finally, other results implying a generalized phenomenology for aspects of diffusion behavior are examined.

First, in the above I have reviewed virtually the entirety of the published literature on self-diffusion and probe diffusion of random-coil polymers in solution. As seen from the Figures in the preceding sections, the concentration dependences of D_s and D_p are essentially always described well by stretched exponentials (eq. 16) in the matrix concentration c .

Correspondingly, scaling (power-law) behavior is clearly rejected by almost the entire published litera-

ture on polymer self- and probe-diffusion. On a log-log plot, a stretched exponential appears as a smooth curve of monotonically varying slope. In contrast, on a log-log plot, scaling (power-law) behavior would appear as a straight line. Almost without exception, log-log plots of real measurements of $D_s(c)$ give smooth curves, not straight lines. Power laws could be fit to reported data, but in almost every case the power law would only provide an accurate description of a tangent to the data over some narrow range of concentrations.

An observation that experimental data is described very well by a particular mathematical form does not prove that the form in question is physically significant. In principle it may be the case that several different mathematical forms describe, to within the actual experimental error, the same data. However, the observation that experimental data is uniformly *not* described by some mathematical form, to well beyond experimental error, is good evidence that models that predict the mathematical form are inadequate. Power laws appear on log-log plots as straight lines. As seen from the above 70+ figures, straight lines are almost never observed in plots of D_s or D_p against c or other physical variables. Correspondingly, the concentration dependence of D_s and D_p almost never shows scaling (power-law) behavior. Scaling models that predict or assume for polymer *solutions* that D_s and D_p follow power laws in c , P , and/or M are very definitely rejected by almost the entirety of the published literature on D_s and D_p .

Second, referring to eqs 16, there are systematic correlations between scaling parameters α and ν and the solution variables P and M . These correlations reflect the concentration and molecular weight dependences of D_s and D_p . In particular:

The scaling prefactor α depends strongly on M . Figure 61 shows the scaling prefactor α from measurements of the self-diffusion coefficient and fits to eq. 16, as plotted against polymer molecular M . The Figure, based on Table I, shows almost all data on linear and star polymers, with concentrations in g/L. Results from the one system⁶¹ with a large-concentration phase transition are omitted. M varies over nearly three orders of magnitude; α varies over almost four orders of magnitude. While there is substantial scatter, the figure is consistent a power-law correlation between α and M . The solid line in the Figure is a best fit to measurements on linear polymers. It shows $\alpha = 2.45 \cdot 10^{-4} M^{1.10}$ with M in kDa.

It is also possible to examine the correlation of α with the size of the polymer, as reflected, e.g., by the diffusion coefficient D_o . However, the variation in D_o from system to system arises in part from differences in the measurement temperature and solvent viscosity. To eliminate these effects, D_o was used to compute a nominal chain hydrodynamic radius

$$R = \frac{k_B T}{6\pi\eta D_o}. \quad (20)$$

Here k_B is Boltzmann's constant and T is the absolute

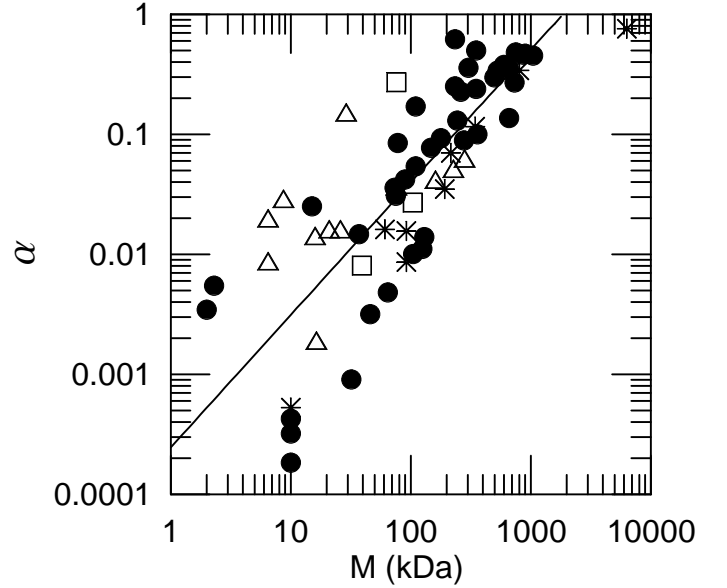


FIG. 61: Scaling pre-factor α for linear polymers (\circ) and 3-, 8-, and 18- armed star polymers (\triangle , \square , $*$) as listed Table I, plotted against polymer molecular weight M . Solid line is a power law $\alpha \sim M^{1.1}$.

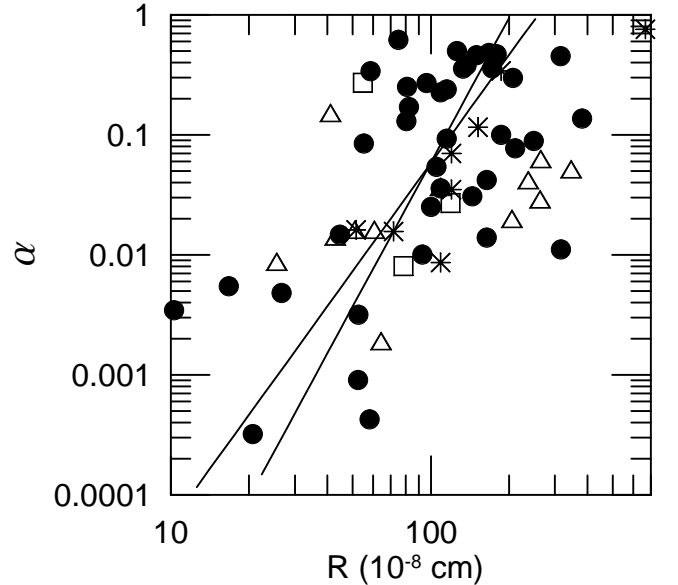


FIG. 62: Scaling pre-factor α for linear polymers, Table I, plotted against the bare hydrodynamic radius R , eq. 20. Solid lines represent power laws with exponents of 3 and 4.

temperature. The solvent viscosity η was taken from standard tables and interpolated as necessary to actual temperatures. In a few cases, reported experimental conditions do not permit an accurate conversion from D_o to R ; these cases are not considered further.

Figure 62 plots α as a function of R . In Fig. 62, the

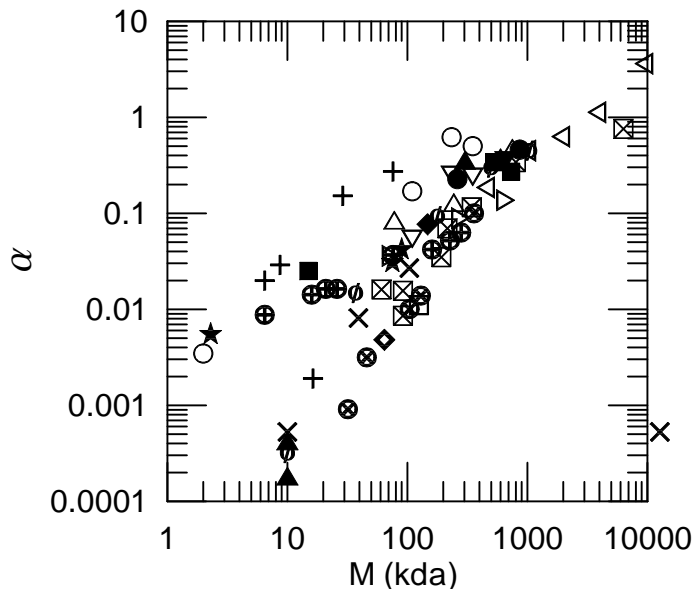


FIG. 63: Scaling pre-factor α as a function of M for data from Refs. (○)⁴³ for polymers in CCl_4 , (●)⁴⁶, (□)⁴⁷, (■)^{52,53}, (△)⁵⁶, (▲)^{62,66} with linear chains, (+)^{62,63} with $f = 3$, (×)⁶² with $f = 8$, (⊠)⁶⁶ with $f = 18$, (◇)⁴¹, (◆)⁴², (▽)⁴³ for polymers in C_6D_6 , (▼)⁴⁶, (⊗)⁶⁵, (⊙)⁶⁴, (★)⁶³ for linear polybutadiene, (⊕)⁶³ for $f = 3$ polybutadiene, (▷)⁴² for PEO in water, and (◁)⁶¹ for xanthan in water. Other details as in Fig. 61

solid lines are best fits for the data on linear chains (filled circles) to $\alpha \sim R^n$ for n of 3 or 4. If $\alpha \sim [\eta]$ as predicted by the Adler model³³, then $n = 3$ is expected. The hydrodynamic scaling model^{34,35} instead predicts $n = 4$. The fit with $n = 3$ gives a modestly better fit to the data than does the $n = 4$ fit, but neither fit is visibly inconsistent with experiment.

Figures 61 and 62 also present α of 3-, 8- and 18-armed stars. α of an 18-armed star polymer tends to be somewhat smaller than α for a representative linear chain. However, α of star polymers almost always lies within the scatter in the values for α observed for the linear chains. α for three-armed stars includes results⁶³ in which only a limited number of concentrations were studied for a given polymer.

Figures 61 and 62 emphasize polymer topology: one point style each for linear, 3-, 8-, and 18-armed chains. For some purposes, identifying the points by reference (and, hence, by chemical system and experimental method) is more useful. Figures 63 and 64 give α against M and R , respectively, with points labelled by reference, this time including results of Tinland, et al.⁶¹ on a system with a large- c phase transition. The correlation between α and molecular weight is somewhat better than the correlation between α and the inferred – in most cases, not directly measured – chain radius.

The scaling exponent ν depends on M at low M . Figure 65 shows the dependence of ν on polymer molecu-

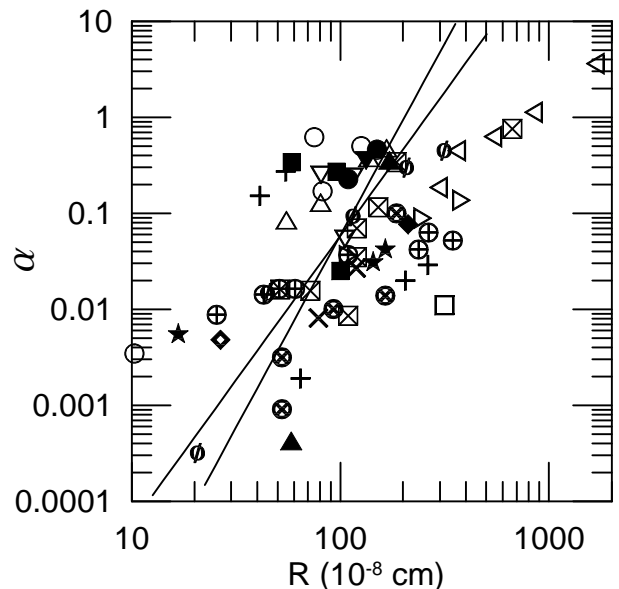


FIG. 64: Scaling pre-factor α as a function of R . Other details as in Fig. 63.

lar weight. The filled circles refer to linear polymers as studied in refs.^{41,42,43,46,47,52,53,56,62,64,65,66}, but excludes systems⁶¹ in which there is a phase transition at elevated polymer concentration. As seen from the Figure, for polymers larger than 250 kDa ν approaches very closely to 0.5. For smaller polymers, ν is substantially scattered, but increases with decreasing M .

Sixteen systems in Table I, including linear and three-armed star polymers, had ν forced to 1.00 during the fitting process. In these fits $\nu = 1$ was forced because the data would not support more free parameters, or because the fit with ν as a free parameter did not have a significantly better root mean square fractional error in the fit than did the fit with $\nu = 1$ forced. All but four of these fits refer to polymers with $M < 200$ kDa. The circumstance that successful fits with ν forced to unity are largely found with polymers of lower molecular weight is consistent with the interpretation that ν increases toward 1.0 at small M . These fits are represented in Figure 65 by the open circles.

Figure 65 also shows the molecular weight dependence of ν for star polymers in solution. The data on stars are substantially confined to smaller polymers ($M < 250$ kDa). However, a trend in ν with increasing M is apparent. At very small M , ν is substantially scattered around 1.0. For $M \geq 200$ kDa, ν for star polymers appears from the few points to be trending toward 0.5.

Third, several papers^{42,67,71,73,74,75,77,78,79,80,82,83,84,85,87,91,92} report D_s and D_p for a series of homologous polymers with different molecular weights. Each of these papers describes a study made by a given method using consistent operating conditions and data analysis procedures, thereby avoiding data scatter arising from any practical

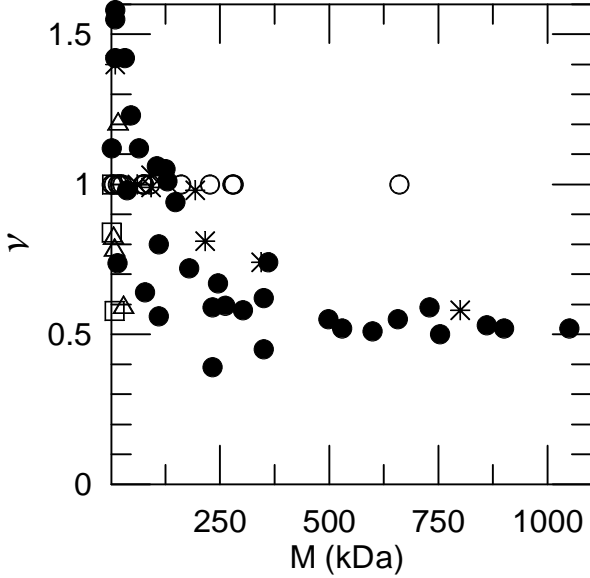


FIG. 65: Scaling exponent ν for polymers of Table 1 plotted against the polymer molecular weight M . A large-molecular-weight asymptote $\nu \approx 0.5$, and a low-molecular-weight increase in ν toward $\nu = 1$ are apparent for linear polymers (filled circles) and for 3- (triangles), 8- (squares), and 18- (asterisks) armed star polymers. Open circles refer to linear polymers in which an adequate fit was obtained with $\nu = 1$ forced during the fitting process.

experimental issues. To use these studies to obtain information about the molecular weight dependences of D_s and D_p , data from each paper were separately fit to eq 17, which is a joint stretched exponential in c , M , and P . (For D_s , P and M are the same variable.) As seen Sections III and IV, eq 17 with parameters in Table III fits most of each data set well.

Some studies were limited in the range of matrix concentrations that was explored, either by not going to very high concentration or by not making measurements at low concentration. These^{41,73,82,83,85} studies are excluded here from further consideration. Some studies are subsets of other studies, for example cases in which measurements were first made at fixed M for a range of P , and then extended to cover a range of M . To avoid double-counting experiments, data sets that are subsets of other data are not considered further here.

Section IV described fits of D_p to eq 17. Much of the probe diffusion data is represented well by this joint stretched exponential in c , P , and M . However, eq 17 is less accurate when M and P differ substantially. In particular, for $M/P > 3$ or for $P/M > 3$, eq 16 tends to overstate the decrease in D_p with increasing c . Specific results of Section IV pertaining to the range of validity of eq 17 include:

Brown, et al.⁶⁷'s data for $D_p/D_{p0} < 10^{-3}$ show an experimental D_p that is smaller than the calculated value from a fit to eq 17. Also, for $P/M \approx 80$, the measured

D_p is larger than predicted. Hanley, et al.'s data⁷³ and Kent, et al.'s⁷⁴ data (all follow well eq 17's P and M dependences. Kim, et al.'s⁷⁵ extensive results on the effects of varying P and M indicate that eq 17 generally works well for $M/P \leq 3$, but overstates the dependence of D_p on M for $M/P > 3$. From this data, it appears that as c is increased there is a narrowing of the range of values of M/P for which eq 17 works well.

For M/P never larger than 3 or so, Lodge and Wheeler⁷⁷ found that the joint stretched exponential worked well for linear polystyrene chains and also worked well for $f = 3$ polystyrene stars, both diffusing through linear-chain matrices. For large $f = 12$ polystyrene stars in a short linear polyvinylmethylether, Lodge and Markland⁷⁸'s data follow a joint stretched exponential, even for $P/M \approx 12$. If the comparison is made by arm rather than total molecular weights, Lodge and Markland's data is confined to a region $P_a/M_a < 2$. Lodge, et al.⁷⁹ examined the diffusion of small $f = 12$ stars through solutions of a large linear polyvinylmethylether. For $M/P \geq 3$ and elevated concentrations, the measured D_p is larger than expected from the joint stretched exponential. Lodge, et al.^{78,79} also studied three-armed stars diffusing through linear chains; with increasing matrix molecular weight, the joint stretched exponential predicts too small a D_p for $M/P > 3$.

Martin^{71,80} reported D_p of linear polystyrenes diffusing through linear polyvinylmethylether. Equation 17 fits well (Fig. 49) the joint data, but throughout this data $M/P < 2.2$. Nemoto, et al.⁸² studied diffusion of PMMA through polystyrene solutions; the joint fit (Fig. 50) of all data to eq 17 was more accurate for $2 \geq M/P \geq 0.5$ then it was outside this range. Numasawa, et al.'s data⁸⁵ on polystyrene in polymethylmethacrylate:benzene, Fig. 52, is described reasonably well by eq 17. However, for Numasawa, et al.'s data the joint stretched exponential clearly gives a better description of the concentration dependence of D_p than it does of the M -dependence. Wheeler, et al.^{91,92} report on linear polystyrenes diffusing through polyvinylmethylethers. Fits to their measurements (Figs. 59 and 60) show that eq 17 underestimates D_p for $M/P \geq 7$ and for $P/M \geq 3$.

The joint stretched exponential thus describes well a great number of measurements of D_p in systems with $0.3 \leq M/P \leq 3$. Outside this range, eq 17 predicts a concentration dependence for D_p that is stronger than that found experimentally. Corresponding to each set of measurements are a set of scaling exponents and pre-factors. To what extent do these parameters show universal rather than system-specific behavior? In eq 17, data were parameterized as $D_o M^{-a} \exp(-\alpha c^\nu P^\gamma M^\delta)$. For each system, the exponent ν was treated as a single constant, the dependence of ν on M at small M , discussed above, being suppressed. This suppression will reduce the quality of the fits when a very wide range of molecular weights is studied, as will be seen below in one system.

From Table III: (i) a is almost always in the range

0.5 to 0.6. (ii) ν is generally in the range 0.5-0.75. In two cases, ν was found to be larger (0.86, 0.99) than this range; in one case it was smaller (0.43). In a few cases, $\nu = 1$ was forced during the fitting process, rather than being obtained from the fit. (iii) For linear chains, γ is almost always in the range 0.25-0.3. There are outliers at 0.14, 0.19, and 0.43; each of these is associated with a system in which ν was unusually small (0.43) or unusually large (0.86, 0.99). For star polymers, γ is ≈ 0.15 . (iv) For linear polymers and three-armed stars, δ is usually in the range 0.25–0.30.

Fourth, in all of two cases, concentration and molecular weight dependences were not, or were not necessarily, described by stretched exponentials. First, Nemoto, et al.⁵⁷ studied the M -dependence of D_s at large fixed c . Their data show a transition from a stretched-exponential to a power-law molecular weight dependence for $M \geq 800$ kDa. Second, Tao, et al.⁶⁰ studied very large polymers in highly concentrated solutions. Their data are almost equally well-described by power laws and by stretched exponentials, as seen in Figs. 13 and 14. For this data, α of eq. 16 is nearly independent of M , contrary to the behavior of α in other systems. The lack of an M -dependence in α , and the ability of a power-law to describe this data, are consistent with the proposal⁶⁰ that polymer transport coefficients have different phenomenologies in the melt/near-melt domain and in the solution domain here.

Fifth, there is evidence for other correlations.

Several papers that report D_s or D_p also report the solution viscosity η . In particular, Martin^{71,80} gives not only D_p but also η of solutions of his 110 kDa polyvinyl-methylether matrix polymer. Martin reported for 50 kDa probe polystyrene that the product $D_p\eta$ increased dramatically (up to 6-fold) with increasing c . For larger probe polymers (100 kDa, 420 kDa), the increase in $D_p\eta$ was less dramatic; with 900 kDa probes, "...this product is very nearly independent of concentration." Martin⁷¹ interpreted the dramatic increase in $D_p\eta$ with increasing matrix concentration as arising from a crossover from Stokes-Einsteinian to reptational diffusion, the crossover occurring more readily for $P \leq M$ than for $P \gg M$.

D_p , η and probe radius of gyration R_g for the same set of solutions were reported by Numasawa, et al.⁸⁵, who studied polystyrene diffusing through polymethyl-methacrylate:benzene. For a range of matrix concentrations and matrix and probe molecular weights, Numasawa, et al. identified a regime in which $D_p\eta R_g$ is approximately constant. For small probe chains diffusing through larger matrix chains but not large probe chains diffusing through smaller matrix chains, the product $D_p\eta R_g$ increases markedly (up to 100-fold) with increasing c and M . Numasawa, et al.⁸⁵ interpreted their data as showing Stokes-Einstein type diffusion and a crossover with increasing matrix molecular weight to a region in which reptational motion was dominant.

Martin⁷¹ and Numasawa, et al.⁸⁵ propose that the failure of the Stokes-Einstein equation, with $D_p\eta$ in-

creasing markedly with increasing c , is associated with a transition to reptation dynamics for large polymer chains. However, the diffusion of rigid spherical probes through high-molecular-weight polymers shows a phenomenology highly similar to the phenomenology for $D\eta$ is observed⁸¹; namely $D\eta$ increases dramatically with increasing c at large M , even though there is no possibility that spheres have a transition permitting them to diffuse via reptation.

Like effects do not prove that like causes are at work. The existence of non-reptating spherical probe-polymer systems in which $D\eta$ increases markedly with increasing c does *not* prove that polymer systems showing the same phenomenology are not reptating. However, non-reptating sphere-probe systems can have a $D\eta$ that increases markedly at large matrix c . Therefore, the observation that $D_p\eta$ for probe polymers in a polymer solution increases markedly at large matrix c is not evidence that the polymer solution has had a transition to reptation dynamics.

Xuexin, et al.⁶⁶ report D_p for linear and $f = 18$ star polymers having very nearly the same D_o , i.e., very nearly the same hydrodynamic radius. For these two polymers, the scaling parameters α and ν are also very nearly the same, consistent with but not proving the interpretation that α and ν are determined by chain size and not by chain topology.

Kent, et al.⁷⁴ examined D_p for a range of probe as well as matrix concentrations. For much of their data, Kent, et al.'s probes were concentrated enough that D_p manifestly depended on the probe concentration c_p as well as on the matrix concentration c . At low c , D_p increased with increasing c_p . At elevated c , D_p decreased with increasing c_p . These results provide a specific target for theoretical investigation. Just as good hydrodynamic models¹⁹ can predict quantitatively the concentration dependence of D of hard spheres, so also a good hydrodynamic model for polymers should be able to predict the dependence of dD_p/dc_p on matrix concentration.

VII. CONCLUSIONS AND DISCUSSION

In the above, virtually the entirety of the published literature on polymer self-diffusion and on the diffusion of chain probes in polymer solutions has been reviewed. Studies that determined how D_s and D_p depend on polymer concentration and molecular weight were systematically re-analysed. Without exception the concentration dependences of D_s and D_p are described by stretched exponentials in polymer concentration. The measured molecular weight dependences also compare favorably in most cases with the elaborated stretched exponential, eq. 17. Only when $P \gg M$ or $M \gg P$ is there a deviation from eq. 17, that deviation referring only to the molecular weight dependences.

Contrarywise, almost without exception the experimental data is inconsistent with descriptions of concen-

tration or molecular weight dependences of the single-particle diffusion coefficient in terms of the power laws predicted or assumed by scaling models. The published data is sufficient to reject scaling model descriptions of polymer diffusion.

The concentration dependence $\exp(-\alpha c^\nu)$ of exponential-type models for D_s is found to be valid for all ratios of the probe and matrix molecular weights. This validity of the stretched-exponential concentration dependence over a wide range of P/M is consistent with the mathematical structure of the renormalization-group derivation³⁶ of these forms. Namely, the derivation begins with a low-concentration pseudovirial expansion

$$D_s = D_o(1 + k_2c + k_3c^2) \quad (21)$$

for the concentration dependence of D_s , c here being the matrix concentration, and then uses the Altenberger-Dahler positive-function renormalization group⁴⁰ method to extend the series from lower to larger concentration. Over a modest range of P/M around $P \approx M$, coefficients k_2 and k_3 with a simple dependence on P and M are adequate, leading to eq 17. For $P \gg M$ or $P \ll M$, the simple calculations of k_2 and k_3 of Ref. 36 are inadequate, because they do not include polymer internal modes, so the values of the k_i change. However, for $P \gg M$ or $P \ll M$ the renormalization group method still receives as input a polynomial having the form of eq 21, so it will still generate as output a stretched exponential in c for the concentration dependence of D_p .

It is sometimes argued that the success of the stretched exponential form in describing $D_s(c)$ arises from a particular flexibility of the stretched exponential, so that the successes shown in the Figures are accidental. Claims that $D_o \exp(-\alpha c^\nu)$ is 'unusually flexible', relative to other functional forms, are inconsistent with basic mathematics: The stretched exponential describes the concentration dependence with three free parameters. The function is not singular for real c and positive ν . Therefore, the region of function space spanned by the set of all stretched exponentials can be no larger than the region of function space spanned by any other function with three free parameters. Correspondingly, the functional form used here for $D_s(c)$ is no more flexible than other three-parameter forms, so its success in describing $D_s(c)$ cannot be ascribed to an unusual flexibility of the stretched exponential form.

On the other hand, there is no significant region of any set of measurements in which concentration scaling is observed, other than as tangents to smooth curves of monotonically decreasing slope. It can always be asserted that corrections to scaling, of whatever basis, mean that the predicted power-law slopes are only observed over narrow ranges of concentration, or are only true asymptotically in the limit of large molecular weight:

(A) Until the scaling models are refined sufficiently so as to predict the concentrations over which the hypothesized power-law slope should be approximately observed, it is impossible to tell whether the experimental data are

consistent with a scaling prediction. It is entirely inadequate to show that the experimental data has, in some region, the slope predicted by a particular power law model, because the observed $D_s(c)$ someplace agrees with a predicted c^{-x} behavior for every single positive x over a very wide range. If one is allowed to draw the asymptote where one chooses, the predicted x thus ceases to be falsifiable. On the other hand, a refined model might very well predict the slope for a range of concentrations in which the data did not have the predicted slope. (B) There is no indication in the experimental data that exponential models cease to be adequate as the polymer molecular weight is increased.

On the other hand, as shown by the extremely thorough experiments of Tao, et al.⁶⁰, as one moves from polymer solutions toward the melt, one encounters a region of large c in which scaling models are at least approximately correct. Scaling models therefore may very well—this review does not examine this question in detail, and there is very little data, even though it⁶⁰ is very good data—be asymptotically valid in the near-melt regime.

Acknowledgments

The partial support of this work by the National Science Foundation under Grant DMR99-85782 is gratefully acknowledged.

- * To whom inquiries should be sent phillies@wpi.edu
- ¹ Graessley, WW (1974) The Entanglement Concept in Polymer Rheology. *Adv. Polym. Sci.* **16**, 1-179.
 - ² Tirrell, M (1984) Polymer Self-Diffusion in Entangled Systems. *Rubber Chem. Tech.* **57**, 523-556.
 - ³ Pearson, DS (1987) Recent Advances in the Molecular Aspects of Polymer Viscoelasticity. *Rubber Chem. Tech.* **60**, 439-496.
 - ⁴ Skolnick, J; Kolinski, A (1989) Dynamics of Dense Polymer Systems Computer Simulations and Analytic Theories. *Adv. Chem. Phys.* **78**, 223-278.
 - ⁵ Lodge, TP; Rotstein, NA; Prager, S (1990) Dynamics of Entangled Polymer Liquids Do Entangled Chains Repeat? *Adv. Chem. Phys.* **79**, 1-132.
 - ⁶ McLeish, TCB (2002) Tube Theory of Entangled Polymer Dynamics. *Advances in Physics* **51**, 1379-1527
 - ⁷ Fuchs, M; Schweizer, KS (1997) Mode-Coupling Theory of the Slow Dynamics of Polymeric Liquids Fractal Macromolecular Architectures. *J. Chem. Phys.* **106**, 347-375.
 - ⁸ Schweizer, KS; Szamel, G (1995) Crossover to Entangled Dynamics in Polymer Solutions and Melts. *J. Chem. Phys.* **103**, 1934-1945.
 - ⁹ Schweizer, KS (1989) Microscopic Theory of the Dynamics of Polymeric Liquids General Formulation of a Mode-Mode-Coupling Approach. *J. Chem. Phys.* **91**, 5802-5821.
 - ¹⁰ Kolinski, A; Skolnick, J; Yaris, R (1987) Does Reptation Describe the Dynamics of Entangled, Finite Length Polymer Systems? A Model Simulation. *J. Chem. Phys.* **86**, 1567-1585.
 - ¹¹ Phillies, GDJ (1974) Effects of Intermacromolecular Interactions on Diffusion. I. Two-Component Solutions. *J. Chem. Phys.* **60**, 976-982.
 - ¹² Phillies, GDJ (1974) Effects of Intermacromolecular Interactions on Diffusion. II. Three-Component Solutions. *J. Chem. Phys.* **60**, 983-989.
 - ¹³ Phillies, GDJ (1975) Fluorescence Correlation Spectroscopy and Non-Ideal Solutions. *Biopolymers* **14**, 499-508.
 - ¹⁴ B. J. Berne and R. Pecora, *Dynamic Light Scattering*, John Wiley and Sons: New York (1976), especially Chapter 5.
 - ¹⁵ Altenberger, AR; Deutch, JM (1973) Light Scattering from Dilute Macromolecular Solutions *J. Chem. Phys.* **59**, 894-898.
 - ¹⁶ Phillies, GDJ (1973) Effects of Intermacromolecular Interactions on Diffusion. III. Electrophoresis in Three-Component Solutions. *J. Chem. Phys.* **59**, 2613-2617.
 - ¹⁷ Kirkwood, JG; Baldwin, RL; Dunlop, PJ; Gosting, LJ; Kegeles, G (1960) Flow Equations and Frames of Reference for Isothermal Diffusion in Liquids. *J. Chem. Phys.* **33**, 1505-1513.
 - ¹⁸ Jones, RB (1979) Diffusion of Tagged Interacting Spherically Symmetric Polymers. *Physica A* **97**, 113-126.
 - ¹⁹ Carter, JM; Phillies, GDJ (1985) Second-Order Concentration Correction to the Mutual Diffusion Coefficient of a Suspension of Hard Brownian Spheres. *J. Phys. Chem.* **89**, 5118-5124.
 - ²⁰ Phillies, GDJ (1995) Dynamics of Brownian Probes in the Presence of Mobile or Static Obstacles. *J. Phys. Chem.* **99**, 4265-4272.
 - ²¹ Benmouna, M; Benoit, H; Duval, M; Akcasu, Z (1987) Theory of Dynamic Scattering from Ternary Mixtures of Two Homopolymers and a Solvent. *Macromolecules* **20**, 1107-1112.
 - ²² Benmouna, M; Benoit, Borsali, R; Duval, M (1987) Theory of Dynamic Scattering from Copolymer Solutions Using the Random Phase Approximation. *Macromolecules* **20**, 2620-2624.
 - ²³ Benmouna, M; Duval, M; Borsali, R (1987) Dynamic Scattering from Mixtures of Homopolymers and Copolymers in Solution. *Macromolecules* **21**, 520-521.
 - ²⁴ Foley, G; Cohen, C (1987) Concentration Fluctuations in Polymer-Polymer-Solvent Systems. *Macromolecules* **20**, 1891-1896.
 - ²⁵ Roby, F; Joanny, J-F (1992) Dynamics of Concentration Fluctuations in Ternary Polymer Solutions. *Macromolecules* **25**, 4612-4618.
 - ²⁶ Hammouda, B (1993) Dynamics of Ternary Polymer Solutions. *Macromolecules* **26**, 4800-4804.
 - ²⁷ Wang, CH (1997) Theory of Quasielastic Light Scattering of a Ternary Solution Consisting of Two Homopolymers with Arbitrary Optical, Hydrodynamic, and Thermodynamic Properties. *J. Chem. Phys.* **107**, 3675-3683.
 - ²⁸ Phillies, GDJ; Streletzky, KA (2001) Microrheology of Complex Fluids Via Observation of Tracer Mesoparticles. *Recent Res. Devel. Phys. Chem.*, **5**, 269-285 .
 - ²⁹ Doob, JL (1942) The Brownian Motion and Stochastic Equations. *Annals Math.* **43**, 319.
 - ³⁰ Akcasu, AZ; Klein, R; Hammouda, B (1993) Dynamics of Multicomponent Polymer Mixtures via the Random Phase Approximation Including Hydrodynamic Interactions. *Macromolecules* **26**, 4136-4143.
 - ³¹ Akcasu, AZ; Naegele, G; Klein, R (1995) Remarks on the "Fast" and "Slow" Mode Theories of Interdiffusion. *Macromolecules* **28**, 6680-6683.
 - ³² de Gennes, P-G (1988) *Scaling Concepts in Polymer Physics*. Third Printing, Cornell UP, Ithaca.
 - ³³ Adler, RS; Freed, KF (1980) On Dynamic Scaling Theories of Polymer Solutions at Nonzero Concentrations. *J. Chem. Phys.* **72**, 4186-4193.
 - ³⁴ Phillies, GDJ (1987) Dynamics of Polymers in Concentrated Solution The Universal Scaling Equation Derived. *Macromolecules* **20**, 558-564.
 - ³⁵ Phillies, GDJ (1988) Quantitative Prediction of α in the Scaling Law for Self-Diffusion. *Macromolecules* **21**, 3101-3106.
 - ³⁶ Phillies, GDJ (1998) Derivation of the Universal Scaling Equation of the Hydrodynamic Scaling Model via Renormalization Group Analysis. *Macromolecules* **31**, 2317-2327.
 - ³⁷ Phillies, GDJ (1992) Range of Validity of the Hydrodynamic Scaling Model. *J. Phys. Chem.* **96**, 10061-10066.
 - ³⁸ Phillies, GDJ; Quinlan, CA (1995) Analytic Structure of the Solutionlike-Meltlike Transition in Polymer Solution Dynamics. *Macromolecules* **28**, 160-164.
 - ³⁹ Phillies, GDJ (1995) Hydrodynamic Scaling of Viscosity and Viscoelasticity of Polymer Solutions, Including Chain Architecture and Solvent Quality Effects. *Macromolecules* **28**, 8198-8208.
 - ⁴⁰ Altenberger, AR; Dahler, JS (1996). Application of a New Renormalization Group to the Equation of State of a Hard-Sphere Fluid. *J. Chem. Phys.* **54**, 6242-6252.

- ⁴¹ Brown, W; Stilbs, P; Johnsen, RM (1982) Self-Diffusion and Sedimentation of Dextran in Concentrated Solutions. *J. Polym. Sci. Polym. Phys.* **20**, 1771-1780.
- ⁴² Brown, W; Stilbs, P; Johnsen, RM (1983) Friction Coefficients in Self-Diffusion, Velocity Sedimentation, and Mutual Diffusion for Poly(ethylene oxide) in Aqueous Solution. *J. Polym. Sci. Polym. Phys.* **21**, 1029-1039.
- ⁴³ Callaghan, PT; Pinder, DN (1980) Dynamics of Entangled Polystyrene Solutions Studied by Pulsed Field Gradient Nuclear Magnetic Resonance. *Macromolecules* **13**, 1085-1092.
- ⁴⁴ Callaghan, PT; Pinder, DN (1981) Self-Diffusion of Random-Coil Polystyrene Determined by Pulsed Field Gradient Nuclear Magnetic Resonance Dependence on Concentration and Molar Mass. *Macromolecules* **14**, 1334-1340.
- ⁴⁵ Callaghan, PT; Pinder, DN (1984) Influence of Multiple Length Scales on the Behavior of Polymer Self-Diffusion in the Semidilute Regime. *Macromolecules* **17**, 431-437.
- ⁴⁶ Deschamps, H; Leger, L (1986) Self-Diffusion Measurements in Polymer Solutions at the Θ Temperature by Forced Rayleigh Light Scattering. *Macromolecules* **19**, 2760-2765.
- ⁴⁷ Fleischer, G (1999) Self-Diffusion in Concentrated Solutions of Polystyrene in Toluene: No Evidence for Large-Scale Heterogeneities. *Macromolecules* **32**, 2382-2383.
- ⁴⁸ Osaki, K; Nishimura, Y; Kurata, M (1985) Viscoelastic Properties of Semidilute Polystyrene Solutions. *Macromolecules* **18**, 1153-1157.
- ⁴⁹ Zero, K; Ware, BR (1984) Mobilities of Poly-L-Lysine Molecules in Low-Salt Solutions. *J. Chem. Phys.* **80**, 1610-1616.
- ⁵⁰ Johnson, G; Mel'cuk, AI; Gould, H; Klein, W; Mountain RD (1998) Molecular-Dynamics Study of Long-Lived Structures in a Fragile Glass-Forming Liquid. *Phys. Rev. E* **57**, 5707-5718.
- ⁵¹ Klein, W; Gould, H; Tobochnik, J; Alexander, FJ; Anghel, M; Johnson, G (2000) Clusters and Fluctuations at Mean-Field Critical Points and Spinodals. *Phys. Rev. Lett.* **85**, 1270-1273.
- ⁵² Giebel, L; Benmouna, M; Borsali, R; Fischer, EW (1993) Quasielastic Light Scattering from Poly(dimethylsiloxane)/Poly(methyl methacrylate)/chloroform under the Optical Theta Condition. *Macromolecules* **26**, 2433-2438.
- ⁵³ Skirda, VD; Sundukov, AI; Maklakov, AI; Zgadzai, OE; Gafrurov, IR; Vasiljev, GI (1988) *Polymer* **29**, 1294.
- ⁵⁴ Hadgraft, J; Hyde, AJ; Richards, RW (1979) Diffusion of Polystyrene in Poly(methyl methacrylate) + Benzene Solutions Measured by Photon Correlation Spectroscopy. *Far. Trans. II* **75**, 1495-1505.
- ⁵⁵ Hervet, H; Leger, L; Rondelez, F (1979) Self-Diffusion in Polymer Solutions A Test for Scaling and Reptation. *Phys. Rev. Lett.* **42**, 1681-1684.
- ⁵⁶ Leger, L; Hervet, H; Rondelez, R (1981) Reptation in Entangled Polymer Solutions by Forced Rayleigh Scattering. *Macromolecules* **14**, 1732-1738.
- ⁵⁷ Nemoto, N; Kishine, M; Inoue, T; Osaki, K (1991) Self-Diffusion and Viscoelasticity of Linear Polystyrene in Entangled Solutions. *Macromolecules* **24**, 1648-1654.
- ⁵⁸ Nemoto, N; Kojima, T; Inoue, T; Kurata, M (1988) Self Diffusion of Polymers in the Concentrated Regime I. Temperature Dependence of the Self Diffusion Coefficient and the Steady Viscosity of Polystyrene in Dibutyl Phthalate. *Polym. J.* **20**, 875-881.
- ⁵⁹ Skirda, VD; Fatkullin, NF; Sundukov, VI; Maklakov, AI (1987) Concentration Dependence of the Coefficient of Self-Diffusion of Macromolecules in Polymer Solutions. *Polym. Sci. U.S.S.R.* **29**, 2229-2236.
- ⁶⁰ Tao, H; Lodge, TP; von Meerwall, ED (2000) Diffusivity and Viscosity of Concentrated Hydrogenated Polybutadiene Solutions. *Macromolecules* **33**, 1747-1758.
- ⁶¹ Tinland, B; Maret, G; Rinaudo, M (1990) Reptation in Semidilute Solutions of Wormlike Polymers. *Macromolecules* **23**, 596-602.
- ⁶² von Meerwall, E; Tomich, DH; Hadjichristis, N; Fetters, LJ (1982) Phenomenology of Self-Diffusion in Star-Branched Polyisoprenes in Solution. *Macromolecules* **15**, 1157-1163.
- ⁶³ von Meerwall, ED; Tomich, DH; Grigsby, J; Pennisi, RW; Fetters, LJ; Hadjichristidis, N (1983) Self-Diffusion of Three-Armed Star and Linear Polybutadienes and Polystyrenes in Tetrachloromethane Solution. *Macromolecules* **16**, 1715-1722.
- ⁶⁴ von Meerwall, ED; Amis, EJ; Ferry, JD (1985) Self-Diffusion in Solutions of Polystyrene in Tetrahydrofuran Comparison of Concentration Dependences of the Diffusion Coefficients of Polymer, Solvent, and a Ternary Probe Component. *Macromolecules* **18**, 260-266.
- ⁶⁵ Wesson, JA; Noh, I; Kitano, T; Yu, H (1984) Self-Diffusion of Polystyrenes by Forced Rayleigh Scattering. *Macromolecules* **17**, 782-792.
- ⁶⁶ Xuexin, C; Zhongde, X; von Meerwall, E; Seung, N; Hadjichristidis, N; Fetters, LJ (1984) Self-Diffusion of Linear and 4- and 18-Armed Star Polyisoprenes in Tetrachloromethane Solution. *Macromolecules* **17**, 1343-1348.
- ⁶⁷ Brown, W; Rymden, R (1988) Comparison of the Translational Diffusion of Large Spheres and High Molecular Weight Coils in Polymer Solutions. *Macromolecules* **21**, 840-846.
- ⁶⁸ Brown, W; Stilbs, P (1983) Self-Diffusion of Poly(ethylene oxide) in Aqueous Dextran Solutions Measured Using FT-Pulsed Field Gradient NMR. *Polymer* **24**, 188-192.
- ⁶⁹ Daivis, P; Snook, I; van Megen, W; Preston, BN; Comper, WD (1984) Dynamic Light Scattering Measurements of Diffusion in Polymer-Polymer-Solvent Systems. *Macromolecules* **17**, 2376-2380.
- ⁷⁰ Daivis, PJ; Pinder, DN; Callaghan, PT (1992) Dynamic Light Scattering and Pulsed Gradient Spin-Echo NMR Measurements of Diffusion in Polystyrene-Poly(vinyl methyl ether)-Toluene Solutions. *Macromolecules* **25**, 170-178.
- ⁷¹ Martin, JE (1986) Polymer Self-Diffusion in Bimodal Semidilute Solutions. *Macromolecules* **19**, 922-925.
- ⁷² De Smedt, SC; Lauwers, A; DeMeester, J; Engelborghs, Y; De Mey, G; Du, M (1994) Structural Information on Hyaluronic Acid Solutions As Studied by Probe Diffusion Experiments. *Macromolecules* **27**, 141-146.
- ⁷³ Hanley, B; Tirrel, M; Lodge, TP (1985) The Behavior of the Tracer Diffusion Coefficient of Polystyrene in Isorefractive "Solvents" Composed of Poly(vinyl methyl ether) and o-Fluorotoluene. *Polym. Bull. (Berlin)* **14**, 137-142.
- ⁷⁴ Kent, MS; Tirrell, M; Lodge, TP (1992) Solution Properties of Polymer Mixtures. *Macromolecules* **25**, 5383-5397.
- ⁷⁵ Kim, H; Chang, T; Yohanan, JM; Wang, L; Yu, H (1986) Polymer Diffusion in Linear Matrices Polystyrene in Toluene. *Macromolecules* **19**, 2737-2744.
- ⁷⁶ Lodge, TP (1983) Self-Diffusion of Polymers in Concen-

- trated Ternary Solutions by Dynamic Light Scattering. *Macromolecules* **16**, 1393-1395.
- ⁷⁷ Lodge, TP; Wheeler, LM (1986) Translational Diffusion of Linear and 3-Arm-Star Polystyrenes in Semidilute Solutions of Linear Poly(vinyl methyl ether). *Macromolecules* **19**, 2983-2986.
- ⁷⁸ Lodge, TP; Markland, P (1987) Translational Diffusion of 12-Arm Star Polystyrenes in Dilute and Concentrated Poly(vinyl methyl ether) Solutions. *Polymer* **28**, 1377-1384.
- ⁷⁹ Lodge, TP; Markland, P; Wheeler, LM (1989) Tracer Diffusion of 3-Arm and 12-Arm Star Polystyrenes in Dilute, Semidilute, and Concentrated Poly(vinyl methyl ether) Solutions. *Macromolecules* **22**, 3409-3418.
- ⁸⁰ Martin, JE (1984) Polymer Self-Diffusion Dynamic Light Scattering Studies of Isorefractive Ternary Solutions. *Macromolecules* **17**, 1279-1283.
- ⁸¹ Phillies, GDJ; Ullmann, GS; Ullmann, K. Lin, TH (1985) Phenomenological Scaling Laws for 'Semidilute' Macromolecule Solutions from Light Scattering by Optical Probe Particles, *J. Chem. Phys.* **82**, 5242-5246.
- ⁸² Nemoto, N; Inoue, T; Makita, Y; Tsunashima, Y; Kurata, M (1985) Dynamics of Polymer-Polymer-Solvent Ternary Systems 2. Diffusion and Sedimentation of Polymethylmethacrylate in Semidilute Solutions of Polystyrene in Thiophenol. *Macromolecules* **18**, 2516-2522.
- ⁸³ Nemoto, N; Kojima, T; Inoue, T; Kishine, M; Hirayama, T; Kurata, M (1989) Self-Diffusion and Tracer-Diffusion Coefficient and Viscosity of Concentrated Solutions of Linear Polystyrenes in Dibutyl Phthalate. *Macromolecules* **22**, 3793-3798.
- ⁸⁴ Nemoto, N; Kishine, M; Inoue, T; Osaki, K (1990) Tracer Diffusion of Linear Polystyrene in Entanglement Networks. *Macromolecules* **23**, 659-664.
- ⁸⁵ Numasawa, N; Kuwamoto, K; Nose, T (1986) Translational Diffusion of Polystyrene Single Chains in Semidilute solutions of Poly(methyl methacrylate)/Benzene As Measured by Quasi-Elastic Light Scattering. *Macromolecules* **19**, 2593-2601.
- ⁸⁶ Nyden, M; Soederman, O; Karlstroem, G (1999) A PFG NMR Self-Diffusion Investigation of Probe Diffusion in an Ethyl(hydroxyethyl)cellulose Matrix. *Macromolecules* **32**, 127-135.
- ⁸⁷ Pinder, DN (1990) Polymer Self-Diffusion in Ternary Solutions and the Monomer and Segmental Self-Diffusion Coefficients. *Macromolecules* **23**, 1724-1729.
- ⁸⁸ Smith, BA; Mumby, SJ; Samulski, ET; Yu, LP (1986) Concentration Dependence of the Diffusion of Poly(propylene oxide) in the Melt. *Macromolecules* **19**, 470-472.
- ⁸⁹ Tead, SF; Kramer, EJ (1988) Polymer Diffusion in Melt Blends of Low and High Molecular Weight. *Macromolecules* **21**, 1513-1517.
- ⁹⁰ Tinland, B; Borsali, R (1994) Single-Chain Diffusion Coefficient of F-Dextran in Poly(vinyl pyrrolidone)/Water Fluorescence Recovery After Photobleaching Experiments. *Macromolecules* **27**, 2141-2144.
- ⁹¹ Wheeler, LM; Lodge, TP; Hanley, B; Tirrell, M (1987) Translational Diffusion of Linear Polystyrenes in Dilute and Semidilute Solutions of Poly(vinyl methyl ether). *Macromolecules* **20**, 1120-1129.
- ⁹² Wheeler, LM; Lodge, TP (1989) Tracer Diffusion of Linear Polystyrenes in Dilute, Semidilute, and Concentrated Poly(vinyl methyl ether) Solutions. *Macromolecules* **22**, 3399-3408.
- ⁹³ Aven, MR; Cohen, C (1990) Light Scattering from Dilute Polystyrene in Mixtures of Semidilute Polydimethylsiloxane and Tetrahydrofuran. *Macromolecules* **23**, 476-486.
- ⁹⁴ Borsali, R; Duval, M; Benoit, H; Benmouna, M (1987) Diffusion of Polymers in Semidilute Ternary Solutions. Investigation by Dynamic Light Scattering. *Macromolecules* **20**, 1112-1115.
- ⁹⁵ Borsali, R; Duval, M; Benmouna, M (1989) Quasi-Elastic Light Scattering from Ternary Mixtures of Polystyrene/Poly(methyl methacrylate)/Toluene. *Polymer* **30**, 610-614.
- ⁹⁶ Borsali, R; Duval, M; Benmouna, M (1989) Quasielastic Light Scattering from Ternary Mixtures of Polystyrene/Polydimethylsiloxane/Solvents. *Macromolecules* **22**, 816-821.
- ⁹⁷ Chang, T; Han, CC; Wheeler, LM; Lodge, TP (1988) Comparison of Diffusion Coefficients in Ternary Polymer Solutions Measured by Dynamic Light Scattering and Forced Rayleigh Scattering. *Macromolecules* **21**, 1870-1872.
- ⁹⁸ Smith, DE; Perkins, TT; Chu, S (1995) Self-Diffusion of an Entangled Molecule by Reptation. *Phys. Rev. Lett.* **75**, 4146-4149.
- ⁹⁹ Skolnick, J; Kolinski, A (1990) Dynamics of Dense Polymer Systems Computer Simulations and Analytic Theories. *Adv. Chemical Phys.* **78**, 223-278.
- ¹⁰⁰ Lodge, TP (1999) Reconciliation of the Molecular Weight Dependence of Diffusion and Viscosity in Entangled Polymers. *Phys. Rev. Lett.* **83**, 3218-3221.
- ¹⁰¹ Chu, B; Wu, DQ; Liang, GM (1986) Polymer Probe Dynamics. *Macromolecules* **19**, 2665-2666.
- ¹⁰² Chu, B; Wu, DQ (1987) Polymer Probe Dynamics. *Macromolecules* **20**, 1606-1619.
- ¹⁰³ Corrotto, J; Ortega, F; Vazquez, M; Freire, JJ (1996) Dynamic Light Scattering from Mixtures of Two Polystyrene Samples in Dilute and Semidilute Solutions. *Macromolecules* **29**, 5948-5954.
- ¹⁰⁴ Cosgrove, T; Griffiths, PC (1993) Diffusion in Bimodal and Polydisperse Polymer Systems. 1. Bimodal Solutions of Protonated and Deuterated Polymers. *Polymer* **36**, 3335-3342.
- ¹⁰⁵ Cotts, DB (1983) Properties of Semidilute Polymer Solutions Investigation of an Optically-Labeled Three-Component Solution. *J. Polym. Sci. Polym. Phys.* **21**, 1381-1388.
- ¹⁰⁶ Daivis, PJ; Pinder, DN (1993) Dynamic Light Scattering Experiments on PVME-Polystyrene-Toluene and PVMA-Polystyrene-Carbon Tetrachloride Solutions. *Macromolecules* **26**, 3381-3390.
- ¹⁰⁷ Desbrieres, J; Borsali, R; Rinaudo, M; Milas, M (1993) χ_f Interaction Parameter and Single-Chain Diffusion Coefficients of Dextran/Poly(vinylpyrrolidone)/Water Dynamic Light Scattering Experiments. *Macromolecules* **26**, 2592-2596.
- ¹⁰⁸ Giebel, L; Borsali, R; Fischer, EW; Meier, G (1990) Quasi-Elastic Light Scattering from Ternary Mixtures of Poly(methyl methacrylate)/ Poly(dimethylsiloxane) in Tetrahydrofuran. *Macromolecules* **23**, 4054-4060.
- ¹⁰⁹ Giebel, L; Borsali, R; Fischer, EW; Benmouna, M (1992) Dynamic Light Scattering from PDMS/PMMA/Solvent Effect of Optical Properties. *Macromolecules* **25**, 4378-4381.
- ¹¹⁰ Jamil, T; Russo, PS; Negulescu, I; Daly, WH; Schaeffer,

- DW; Beaucage, G (1994) Light Scattering from Random Coils Dispersed in Solutions of Rodlike Polymers. *Macromolecules* **27**, 171-178.
- ¹¹¹ Konak, C; Tuzar, C; Jakes, J (1990) Quasielastic Light Scattering from Polystyrene/ Poly(methyl methacrylate)/Toluene Solutions. *Polymer* **31**, 1866-1870.
- ¹¹² Marmonier, MF; Leger, L (1985) Reptation and Tube Renewal in Entangled Polymer Solutions. *Phys. Rev. Lett.* **55**, 1078-1081.
- ¹¹³ Numasawa, N; Hamada, T; Nose, T (1986) Dynamic Light Scattering of Polystyrene Single Chains in a Semidilute Solution of Poly(methyl methacrylate) and Benzene. *J. Polym. Sci. Polym. Phys.* **24**, 19-26.
- ¹¹⁴ Russo, PS; Baylis, M; Bu, Z; Stryjewski, W; Doucet, G; Temyanko, E; Tipton, D (1999) Self-Diffusion of a Semiflexible Polymer Measured Across the Lyotropic Liquid-Crystalline-Phase Boundary. *J. Chem. Phys.* **111**, 1746-1752.
- ¹¹⁵ Scalettar, BA; Hearst, JE; Klein, MP (1989) FRAP and FCS Studies of Self-Diffusion and Mutual Diffusion in Entangled DNA Solutions. *Macromolecules* **22**, 4550-4559.
- ¹¹⁶ Sun, Z; Wang, CH (1996) Quasielastic Light Scattering Study of Semidilute Ternary Polymer Solutions of Polystyrene and Poly(methyl methacrylate) in Benzene. *Macromolecules* **29**, 2011-2018.
- ¹¹⁷ Sun, Z; Wang, CH (1997) Quasielastic Light Scattering Study of Ternary Polymer Solutions of Polystyrene and Poly(methyl methacrylate) in Dioxane. *J. Chem. Phys.* **106**, 3775-3781.
- ¹¹⁸ Sun, Z; Wang, CH (1997) Light Scattering from Mixtures of Two Polystyrenes in Toluene and Self-Diffusion Coefficients. *Macromolecules* **30**, 4939-4944.

TABLE I: Fits of the concentration dependence of the self-diffusion coefficient D_s of polymers in solution to a stretched exponential $D_o \exp(-\alpha c^\nu)$. The Table gives the fitting parameters, the percent root-mean-square fractional error %RMS, the polymer:solvent system, and the reference. Square brackets “[\dots]” denote parameters that were fixed rather than floated during the least-mean-squares fitting process. D_0 is in cm^2/s or in units of D_0 . Concentrations are g/L, except * c in volume fraction units. Polymers include dex–dextran, pB–polybutadiene, HpBD–hydrogenated polybutadiene, pDMS–polydimethylsiloxane, PEO–polyethylene oxide, pI–polyisoprene, pS–polystyrene, and xanthan. Solvents include THF–tetrahydrofuran.

| D_o | α | ν | %RMS | M (kDa) | System | Refs |
|-------------------------|----------------------|-------|------|-----------|---|----------|
| $9.17 \cdot 10^{-7}$ | $4.82 \cdot 10^{-3}$ | 1.12 | 6.1 | 64.2 | dex:H ₂ O | 41 |
| $2.24 \cdot 10^{-7}$ | 0.036 | [1] | 5.2 | 73 | PEO:H ₂ O | 42 |
| $1.16 \cdot 10^{-7}$ | 0.077 | 0.94 | 7.5 | 148 | PEO:H ₂ O | 42 |
| $9.9 \cdot 10^{-8}$ | 0.089 | [1] | 5.9 | 278 | PEO:H ₂ O | 42 |
| $6.42 \cdot 10^{-8}$ | 0.137 | [1] | 3.4 | 661 | PEO:H ₂ O | 42 |
| $2.47 \cdot 10^{-6}$ | $3.47 \cdot 10^{-3}$ | 1.12 | 6.6 | 2 | pS:CCl ₄ | 43,44,45 |
| $3.08 \cdot 10^{-7}$ | 0.17 | 0.56 | 13 | 110 | pS:CCl ₄ | 43,44,45 |
| $3.38 \cdot 10^{-7}$ | 0.62 | 0.39 | 7.4 | 233 | pS:CCl ₄ | 43,44,45 |
| $2.01 \cdot 10^{-7}$ | 0.50 | 0.45 | 8.1 | 350 | pS:CCl ₄ | 43,44,45 |
| $3.62 \cdot 10^{-7}$ | 0.054 | 0.80 | 6.6 | 110 | pS:C ₆ D ₆ | 43,44,45 |
| $4.70 \cdot 10^{-7}$ | 0.25 | 0.59 | 5.8 | 233 | pS:C ₆ D ₆ | 43,44,45 |
| $3.30 \cdot 10^{-7}$ | 0.24 | 0.62 | 6.9 | 350 | pS:C ₆ D ₆ | 43,44,45 |
| $4.50 \cdot 10^{-7}$ | 0.227 | 0.595 | 11 | 262 | pS:C ₅ H ₁₀ | 46 |
| [$3.7 \cdot 10^{-7}$] | 0.355 | 0.55 | 23 | 657 | pS:C ₅ H ₁₀ | 46 |
| $3.29 \cdot 10^{-7}$ | 0.462 | 0.53 | 12 | 861 | pS:C ₅ H ₁₀ | 46 |
| $1.20 \cdot 10^{-7}$ | 0.0111 | 1.05 | 3.4 | 125 | pS:tol | 47 |
| $4.88 \cdot 10^{-6}$ | 0.025 | 0.737 | 3.4 | 15 | pDMS:tol | 52,53 |
| $8.30 \cdot 10^{-7}$ | 0.34 | 0.52 | 9.5 | 530 | pDMS:tol | 52,53 |
| $5.06 \cdot 10^{-7}$ | 0.27 | 0.59 | 1.3 | 730 | pDMS:tol | 52,53 |
| $6.21 \cdot 10^{-7}$ | 0.0848 | 0.64 | 5.1 | 78 | pS:C ₆ H ₆ | 56 |
| $7.90 \cdot 10^{-7}$ | 0.21 | 0.52 | 4.0 | 123 | pS:C ₆ H ₆ | 55 |
| $4.26 \cdot 10^{-7}$ | 0.13 | 0.67 | 24 | 245 | pS:C ₆ H ₆ | 56 |
| $2.33 \cdot 10^{-7}$ | 0.38 | 0.51 | 22 | 599 | pS:C ₆ H ₆ | 56 |
| $2.03 \cdot 10^{-7}$ | 0.48 | 0.50 | 13 | 754 | pS:C ₆ H ₆ | 56 |
| $8.15 \cdot 10^{-6}$ | 3.68^* | 0.76 | 0.7 | 2 | pEO:CHCl ₃ | 59 |
| $2.19 \cdot 10^{-6}$ | 9.07^* | 0.61 | 3.7 | 40 | pEO:CHCl ₃ | 59 |
| $2.69 \cdot 10^{-6}$ | 7.61^* | 0.78 | 12 | 20 | pEO:C ₆ H ₆ | 59 |
| $6.03 \cdot 10^{-6}$ | 4.30^* | 0.67 | 3.5 | 2 | pEO:dioxane | 59 |
| $2.05 \cdot 10^{-6}$ | 7.75^* | 0.62 | 4.9 | 20 | pEO:dioxane | 59 |
| $2.71 \cdot 10^{-6}$ | 9.72^* | 0.46 | 16 | 40 | pEO:dioxane | 59 |
| $2.30 \cdot 10^{-7}$ | 21.9^* | 0.42 | 2.3 | 3000 | pEO:dioxane | 59 |
| $5.00 \cdot 10^{-7}$ | 17.1^* | 0.81 | 5.1 | 240 | pS:C ₆ H ₆ | 59 |
| $3.30 \cdot 10^{-7}$ | 16.5^* | 0.80 | 11.2 | 240 | pS:CCl ₄ | 59 |
| $1.65 \cdot 10^{-7}$ | 23.5^* | 0.67 | 13.5 | 1300 | pS:CCl ₄ | 59 |
| $7.62 \cdot 10^{-8}$ | 0.186 | 0.79 | 17 | 450 | xanthan:H ₂ O | 61 |
| $6.24 \cdot 10^{-8}$ | 0.45 | 0.91 | 15 | 990 | xanthan:H ₂ O | 61 |
| $4.18 \cdot 10^{-8}$ | 0.63 | 1.00 | 15 | 1900 | xanthan:H ₂ O | 61 |
| $2.67 \cdot 10^{-8}$ | 1.13 | 0.88 | 15 | 3800 | xanthan:H ₂ O | 61 |
| $1.35 \cdot 10^{-8}$ | 3.63 | [1] | 27 | 9400 | xanthan:H ₂ O | 61 |
| $6.25 \cdot 10^{-7}$ | $4.25 \cdot 10^{-4}$ | 1.42 | 7.7 | 10 | $f = 2$ pI:CCl ₄ | 62 |
| $5.64 \cdot 10^{-7}$ | $1.91 \cdot 10^{-3}$ | 1.21 | 4.6 | 16.4 | $f = 3$ pI:CCl ₄ | 62 |
| $4.63 \cdot 10^{-7}$ | $8.08 \cdot 10^{-3}$ | 1.00 | 2.9 | 39 | $f = 8$ pI:CCl ₄ | 62 |
| $3.33 \cdot 10^{-7}$ | $8.61 \cdot 10^{-3}$ | 0.99 | 3.1 | 92 | $f = 18$ pI:CCl ₄ | 62 |
| $3.06 \cdot 10^{-7}$ | $2.69 \cdot 10^{-2}$ | 0.84 | 2.3 | 104 | $f = 8$ pI:CCl ₄ | 62 |
| $7.63 \cdot 10^{-7}$ | $1.83 \cdot 10^{-4}$ | 1.55 | 13.4 | 10 | $f = 2$ pI:C ₆ F ₅ Cl | 62 |
| $3.35 \cdot 10^{-7}$ | $5.3 \cdot 10^{-4}$ | 1.40 | 7.8 | 10 | $f = 8$ pI:C ₆ F ₅ Cl | 62 |

| D_o | α | ν | %RMS | M (kDa) | System | Refs |
|-----------------------|----------------------|-------|------|-----------|------------------------------|------|
| $2.18 \cdot 10^{-6}$ | $5.49 \cdot 10^{-3}$ | [1] | 3.4 | 2.3 | $f = 2$ pB:CCL ₄ | 63 |
| $1.42 \cdot 10^{-6}$ | $8.78 \cdot 10^{-3}$ | 1.00 | 8.6 | 6.5 | $f = 3$ pB:CCL ₄ | 63 |
| $8.44 \cdot 10^{-7}$ | 0.0143 | [1] | 7.8 | 16 | $f = 3$ pB:CCL ₄ | 63 |
| $7.07 \cdot 10^{-7}$ | 0.0163 | [1] | 10 | 21 | $f = 3$ pB:CCL ₄ | 63 |
| $5.98 \cdot 10^{-7}$ | 0.0163 | [1] | 7.5 | 26 | $f = 3$ pB:CCL ₄ | 63 |
| $2.53 \cdot 10^{-7}$ | 0.0308 | [1] | 8 | 75 | $f = 2$ pB:CCL ₄ | 63 |
| $3.32 \cdot 10^{-7}$ | 0.0369 | [1] | 15 | 76 | $f = 3$ pB:CCL ₄ | 63 |
| $2.22 \cdot 10^{-7}$ | 0.0421 | [1] | 1.4 | 90 | $f = 2$ pB:CCL ₄ | 63 |
| $1.53 \cdot 10^{-7}$ | 0.042 | [1] | 11 | 161 | $f = 3$ pB:CCL ₄ | 63 |
| $1.05 \cdot 10^{-7}$ | 0.052 | [1] | 13 | 227 | $f = 3$ pB:CCL ₄ | 63 |
| $1.37 \cdot 10^{-7}$ | 0.0629 | [1] | 6.8 | 281 | $f = 3$ pB:CCL ₄ | 63 |
| $1.77 \cdot 10^{-6}$ | 0.020 | 0.83 | 12 | 6.5 | $f = 3$ pB:CCL ₄ | 63 |
| $1.38 \cdot 10^{-6}$ | 0.029 | 0.79 | 9.0 | 8.7 | $f = 3$ pB:CCL ₄ | 63 |
| $8.81 \cdot 10^{-7}$ | 0.153 | 0.60 | 13 | 29 | $f = 3$ pB:CCL ₄ | 63 |
| $6.63 \cdot 10^{-7}$ | 0.273 | 0.578 | 8.5 | 87 | $f = 3$ pB:CCL ₄ | 63 |
| $2.20 \cdot 10^{-6}$ | $3.20 \cdot 10^{-4}$ | 1.58 | 22 | 10 | pS:THF | 64 |
| $1.02 \cdot 10^{-6}$ | $1.47 \cdot 10^{-2}$ | 0.98 | 5.5 | 37 | pS:THF | 64 |
| $3.97 \cdot 10^{-7}$ | $9.29 \cdot 10^{-2}$ | 0.72 | 7.4 | 179 | pS:THF | 64 |
| $2.20 \cdot 10^{-7}$ | 0.299 | 0.55 | 15 | 498 | pS:THF | 64 |
| $1.45 \cdot 10^{-7}$ | 0.452 | 0.52 | 21 | 1050 | pS:THF | 64 |
| $9.12 \cdot 10^{-7}$ | $9.07 \cdot 10^{-4}$ | 1.42 | 15 | 32 | pS:THF | 65 |
| $9.09 \cdot 10^{-7}$ | $3.17 \cdot 10^{-3}$ | 1.23 | 16 | 46 | pS:THF | 65 |
| $5.16 \cdot 10^{-7}$ | $1.01 \cdot 10^{-2}$ | 1.06 | 21 | 105 | pS:THF | 65 |
| $2.92 \cdot 10^{-7}$ | $1.39 \cdot 10^{-2}$ | 1.01 | 17 | 130 | pS:THF | 65 |
| $2.58 \cdot 10^{-7}$ | 0.100 | 0.74 | 19 | 360 | pS:THF | 65 |
| $7.04 \cdot 10^{-7}$ | 0.0161 | [1] | 4.7 | 61 | $f = 18$ pI:CCL ₄ | 66 |
| $5.05 \cdot 10^{-7}$ | 0.0156 | 1.03 | 2.0 | 92 | $f = 18$ pI:CCL ₄ | 66 |
| $3.02 \cdot 10^{-7}$ | 0.035 | 0.98 | 2.7 | 193 | $f = 18$ pI:CCL ₄ | 66 |
| $3.03 \cdot 10^{-7}$ | 0.070 | 0.81 | 2.8 | 216 | $f = 18$ pI:CCL ₄ | 66 |
| $2.38 \cdot 10^{-7}$ | 0.116 | 0.74 | 2.9 | 344 | $f = 18$ pI:CCL ₄ | 66 |
| $1.95 \cdot 10^{-7}$ | 0.341 | 0.58 | 8.1 | 800 | $f = 18$ pI:CCL ₄ | 66 |
| $5.43 \cdot 10^{-8}$ | 0.76 | [0.5] | 20 | 6300 | $f = 18$ pI:CCL ₄ | 66 |
| $2.11 \cdot 10^{-7}$ | 0.359 | 0.58 | 8.6 | 302 | $f = 2$ pI:CCL ₄ | 66 |
| 1.11 D_0 | 0.167 | 0.57 | 1.5 | 70.8 | $f = 2$ pI:CCL ₄ | 66 |
| 0.991 D_0 | 0.256 | 0.67 | 3.6 | 251 | $f = 2$ pI:CCL ₄ | 66 |
| [1.0 D_0] | 0.244 | 0.68 | 6.7 | 302 | $f = 2$ pI:CCL ₄ | 66 |
| 2.07×10^{-7} | 0.47 | 0.52 | 17 | 900 | pS:tol | 75 |

TABLE II: Concentration dependence of the probe diffusion coefficient D_p for molecular weight P probes in solutions of molecular weight M matrix polymers. The fits are to stretched exponentials $D_o \exp(-\alpha c^\nu)$ in the polymer concentration c . The Table gives the fitting parameters, the percent root-mean-square fractional fit error %RMS, the system, and the reference. Square brackets “[\dots]” denote parameters that were fixed rather than floated during the non-linear least squares fits. D_0 is in cm^2/s or in units of D_0 ; concentrations are in g/L. Abbreviations include dex–dextran, “ $f = n$ ” for an n -armed star polymer, hyal–hyaluronic acid, mr–methyl red, oFT–ortho fluorotoluene, pI–polyisoprene, PMMA–polymethylmethacrylate, PPO–polypropylene oxide, pS–polystyrene, pVME–polyvinylmethylether, PF–pulsed field gradient nuclear magnetic resonance, QE–quasielastic light scattering spectroscopy, thiop–thiophenol, and tol–toluene. Parentheses indicate parameters from fits of limited accuracy.

| D_o | α | ν | %RMS | $P(\text{kDa})$ | $M(\text{kDa})$ | System | Refs. |
|--------------------------|----------------------|--------------|------|-----------------|-----------------|---------------------------------------|-------|
| $3.35 \cdot 10^{-7}$ | 0.107 | 0.70 | 8.9 | 245 | 598 | pS:pS:C ₆ H ₆ | 56 |
| $2.19 \cdot 10^{-7}$ | 0.453 | 0.50 | 25 | 598 | 1800 | pS:pS:C ₆ H ₆ | 56 |
| 1.13 | 0.38 | 0.38 | 7.6 | 8000 | 101 | pS:pMMA:tol | 67 |
| 1.01 | 0.61 | 0.40 | 3.6 | 8000 | 163 | pS:pMMA:tol | 67 |
| 1.24 | 1.03 | 0.34 | 7.0 | 8000 | 268 | pS:pMMA:tol | 67 |
| 1.47 | 1.39 | 0.32 | 5.4 | 8000 | 445 | pS:pMMA:tol | 67 |
| 1.06 | 1.18 | 0.38 | 9.0 | 8000 | 697 | pS:pMMA:tol | 67 |
| 1.00 | 1.48 | 0.45 | 14 | 8000 | 1426 | pS:pMMA:tol | 67 |
| 0.91 | 1.19 | 0.34 | 14 | 2950 | 445 | pS:pMMA:tol | 67 |
| 0.603 | 0.62 | 0.46 | 18 | 15000 | 445 | pS:pMMA:tol | 67 |
| 0.973 | 0.0101 | ^a | 6.7 | 73 | 19 | pEO:dex:H ₂ O | 42 |
| 2.13 | 0.0169 | ^a | 1.9 | 73 | 110 | pEO:dex:H ₂ O | 42 |
| 1.05 | 0.0256 | [1] | 2.8 | 73 | 510 | pEO:dex:H ₂ O | 42 |
| 1.03 | 0.0105 | [1] | 4.1 | 278 | 19 | pEO:dex:H ₂ O | 42 |
| 0.976 | 0.0164 | [1] | 4.3 | 278 | 110 | pEO:dex:H ₂ O | 42 |
| 0.97 | 0.022 | [1] | 4.4 | 278 | 510 | pEO:dex:H ₂ O | 42 |
| 0.317 | 0.034 | [1] | 1.2 | 1200 | 110 | pEO:dex:H ₂ O | 42 |
| $1.50 \cdot 10^{-7}$ | 0.017 | [1] | 13 | 864 | 20.4 | dex:dex:H ₂ O | 69 |
| $4.97 \cdot 10^{-7}$ | 0.174 | 0.60 | 27 | 110 | 110 | pS:pVME:tol(QE) | 70 |
| $4.88 \cdot 10^{-7}$ | 0.097 | 0.71 | 21 | 110 | 110 | pS:pVME:tol(PF) | 70 |
| $4.51 \cdot 10^{-7}$ | 0.18 | 0.59 | 1.9 | 71 | 680 | dex:hyal:H ₂ O | 72 |
| $3.22 \cdot 10^{-7}$ | 0.33 | 0.59 | 5.4 | 148 | 680 | dex:hyal:H ₂ O | 72 |
| $1.75 \cdot 10^{-7}$ | 0.44 | 0.48 | 4.8 | 487 | 680 | dex:hyal:H ₂ O | 72 |
| $3.49 \cdot 10^{-7}$ | $3.58 \cdot 10^{-2}$ | 0.87 | 3.8 | 162 | 105 | pS:pMMA:C ₆ H ₆ | 54 |
| ($2.53 \cdot 10^{-7}$) | (0.142) | (0.55) | (10) | 410 | 105 | pS:pMMA:C ₆ H ₆ | 54 |
| $1.35 \cdot 10^{-7}$ | $6.35 \cdot 10^{-2}$ | 0.76 | 5.6 | 1110 | 105 | pS:pMMA:C ₆ H ₆ | 54 |
| $6.70 \cdot 10^{-8}$ | $2.89 \cdot 10^{-2}$ | 0.95 | 6.0 | 4600 | 105 | pS:pMMA:C ₆ H ₆ | 54 |
| $3.16 \cdot 10^{-7}$ | $2.26 \cdot 10^{-2}$ | 0.90 | 24 | 50 | 60 | pS:pVME:oFT | 73 |
| $2.15 \cdot 10^{-7}$ | $5.6 \cdot 10^{-2}$ | 0.80 | 17 | 179 | 60 | pS:pVME:oFT | 73 |
| $1.73 \cdot 10^{-7}$ | 0.164 | 0.65 | 9.4 | 1050 | 60 | pS:pVME:oFT | 73 |
| $6.09 \cdot 10^{-8}$ | $2.63 \cdot 10^{-2}$ | 1.01 | 19 | 1800 | 60 | pS:pVME:oFT | 73 |
| $1.33 \cdot 10^{-7}$ | $6.13 \cdot 10^{-3}$ | [1] | 3.8 | 930 | 840 | pS:pMMA:tol | 74 |
| $2.99 \cdot 10^{-7}$ | $5.05 \cdot 10^{-3}$ | [1] | 8.9 | 233 | 840 | pS:pMMA:tol | 74 |
| $2.70 \cdot 10^{-7}$ | $2.27 \cdot 10^{-3}$ | [1] | 2.2 | 233 | 66 | pS:pMMA:tol | 74 |
| $1.31 \cdot 10^{-5}$ | $4.4 \cdot 10^{-3}$ | [1] | 6 | 0 | ^a | mr:pS:tol | 75 |
| $1.26 \cdot 10^{-6}$ | $1.87 \cdot 10^{-3}$ | 1.28 | 5.6 | 10 | ^a | pS:pS:tol | 75 |
| $7.89 \cdot 10^{-7}$ | $1.82 \cdot 10^{-2}$ | 0.92 | 3.3 | 35 | ^a | pS:pS:tol | 75 |
| $4.40 \cdot 10^{-7}$ | $5.85 \cdot 10^{-2}$ | 0.80 | 4.0 | 100 | ^a | pS:pS:tol | 75 |
| $2.30 \cdot 10^{-7}$ | 0.27 | 0.60 | 18 | 390 | ^a | pS:pS:tol | 75 |
| $1.81 \cdot 10^{-7}$ | 0.70 | 0.48 | 25 | 900 | ^a | pS:pS:tol | 75 |
| $8.54 \cdot 10^{-8}$ | 0.64 | 0.55 | 17 | 1800 | 8400 | pS:pS:tol | 75 |
| $2.81 \cdot 10^{-7}$ | $5.4 \cdot 10^{-2}$ | 0.82 | 12 | 179 | 50 | pS:pVME:oFT | 76 |
| $2.94 \cdot 10^{-7}$ | 0.26 | 0.58 | 11 | 1050 | 50 | pS:pVME:oFT | 76 |
| $2.92 \cdot 10^{-7}$ | 0.368 | 0.59 | 10 | 422 | 1300 | pS:pVME:oFT | 77 |
| $2.06 \cdot 10^{-7}$ | 0.439 | 0.60 | 9.8 | 1050 | 1300 | pS:pVME:oFT | 77 |

| | | | | | | | |
|------------------------|----------------------|--------|------|------|--------------|---|-------|
| $2.97 \cdot 10^{-7}$ | 0.280 | 0.63 | 2.6 | 379 | 1300 | $f = 3$ pS:pVME:oFT | 77 |
| $1.84 \cdot 10^{-7}$ | 0.435 | 0.65 | 5.0 | 1190 | 1300 | $f = 3$ pS:pVME:oFT | 77 |
| $8.46 \cdot 10^{-7}$ | 0.085 | 0.71 | 3.7 | 55 | 140 | $f = 12$ pS:pVME:oFT | 78 |
| $3.01 \cdot 10^{-7}$ | 0.161 | 0.67 | 3.6 | 467 | 140 | $f = 12$ pS:pVME:oFT | 78 |
| $1.89 \cdot 10^{-7}$ | 0.184 | 0.66 | 1.7 | 1110 | 140 | $f = 12$ pS:pVME:oFT | 78 |
| $1.60 \cdot 10^{-7}$ | 0.196 | 0.65 | 2.0 | 1690 | 140 | $f = 12$ pS:pVME:oFT | 78 |
| $2.09 \cdot 10^{-7}$ | 0.49 | 0.56 | 5.8 | 1690 | 1300 | $f = 12$ pS:pVME:oFT | 79 |
| $2.52 \cdot 10^{-7}$ | 0.48 | 0.55 | 4.7 | 1110 | 1300 | $f = 12$ pS:pVME:oFT | 79 |
| $4.07 \cdot 10^{-7}$ | 0.49 | 0.48 | 4.9 | 467 | 1300 | $f = 12$ pS:pVME:oFT | 79 |
| $(9.41 \cdot 10^{-7})$ | (0.35) | (0.34) | 3.9 | 55 | 1300 | $f = 12$ pS:pVME:oFT | 79 |
| $1.44 \cdot 10^{-7}$ | 0.18 | 0.63 | 4.7 | 1190 | 140 | $f = 3$ pS:pVME:oFT | 79 |
| $1.58 \cdot 10^{-7}$ | 0.25 | 0.65 | 14.6 | 1190 | 630 | $f = 3$ pS:pVME:oFT | 79 |
| $2.18 \cdot 10^{-7}$ | 0.612 | 0.55 | 18 | 1190 | 1300 | $f = 3$ pS:pVME:oFT | 79 |
| $2.69 \cdot 10^{-7}$ | 0.162 | 0.63 | 3.7 | 379 | 140 | $f = 3$ pS:pVME:oFT | 79 |
| $2.57 \cdot 10^{-7}$ | 0.167 | 0.68 | 7.5 | 379 | 630 | $f = 3$ pS:pVME:oFT | 79 |
| $2.87 \cdot 10^{-7}$ | 0.288 | 0.61 | 12 | 379 | 1300 | $f = 3$ pS:pVME:oFT | 79 |
| $5.27 \cdot 10^{-7}$ | 0.061 | 0.74 | 5.9 | 50 | 110 | pS:pVME:oFT | 71,80 |
| $3.65 \cdot 10^{-7}$ | 0.054 | 0.80 | 1.6 | 100 | 110 | pS:pVME:oFT | 71,80 |
| $2.48 \cdot 10^{-7}$ | 0.145 | 0.66 | 3.6 | 420 | 110 | pS:pVME:oFT | 71,80 |
| $1.49 \cdot 10^{-7}$ | 0.116 | 0.71 | 4.6 | 900 | 110 | pS:pVME:oFT | 71,80 |
| $1.56 \cdot 10^{-7}$ | 0.32 | 0.77 | 0.9 | 342 | 43.9 | pMMA :pS:thiop | 82 |
| $1.43 \cdot 10^{-7}$ | 0.54 | 0.54 | 1.3 | 342 | 186 | pMMA :pS:thiop | 82 |
| $1.18 \cdot 10^{-7}$ | 0.79 | 0.68 | 6.1 | 342 | 775 | pMMA :pS:thiop | 82 |
| $1.23 \cdot 10^{-7}$ | 1.03 | 0.67 | 8.4 | 342 | 8420 | pMMA :pS:thiop | 82 |
| $1.51 \cdot 10^{-5}$ | $3.21 \cdot 10^{-3}$ | (1) | 5.5 | M | ^a | styrene:pS:CCl ₄ | 87 |
| $2.53 \cdot 10^{-5}$ | $3.34 \cdot 10^{-3}$ | (1) | 3.0 | M | ^a | styrene:pS:C ₆ H ₁₂ | 87 |
| $1.51 \cdot 10^{-5}$ | $3.15 \cdot 10^{-3}$ | (1) | 5.8 | M | ^a | styrene:pS:CCl ₄ | 87 |
| $4.74 \cdot 10^{-6}$ | $5.36 \cdot 10^{-3}$ | (1) | 5.0 | 0.58 | ^a | pS:pS:CCl ₄ | 87 |
| $3.31 \cdot 10^{-6}$ | $6.53 \cdot 10^{-3}$ | (1) | 4.8 | 1.2 | ^a | pS:pS:CCl ₄ | 87 |
| $2.16 \cdot 10^{-6}$ | $8.08 \cdot 10^{-3}$ | (1) | 4.1 | 2.47 | ^a | pS:pS:CCl ₄ | 87 |
| $5.13 \cdot 10^{-9}$ | 0.033 | 0.69 | 4.3 | 33.6 | 32 | PPO:PPO:PPO | 88 |
| $7.86 \cdot 10^{-11}$ | 5.23 | 0.79 | 10.8 | 255 | 93 | pS:pS:pS | 89 |
| $9.17 \cdot 10^{-11}$ | 6.29 | 0.51 | 23 | 255 | 250 | pS:pS:pS | 89 |
| $1.24 \cdot 10^{-11}$ | 4.81 | 0.47 | 8.7 | 255 | 20 000 | pS:pS:pS | 89 |
| $1.93 \cdot 10^{-7}$ | $7.3 \cdot 10^{-2}$ | 0.84 | 10.3 | 433 | 310 | dex:pVP:water | 90 |
| $7.1 \cdot 10^{-7}$ | 0.20 | 0.57 | 3.1 | 65 | 1300 | pS:pVME:oFT | 91 |
| $5.42 \cdot 10^{-7}$ | 0.21 | 0.66 | 5.4 | 179 | 1300 | pS:pVME:oFT | 91 |
| $2.87 \cdot 10^{-7}$ | 0.35 | 0.60 | 10.2 | 422 | 1300 | pS:pVME:oFT | 91 |
| $2.19 \cdot 10^{-7}$ | 0.47 | 0.59 | 10.1 | 1050 | 1300 | pS:pVME:oFT | 91 |
| $6.30 \cdot 10^{-7}$ | 0.101 | 0.62 | 3.7 | 65 | 140 | pS:pVME:oFT | 92 |
| $3.72 \cdot 10^{-7}$ | 0.150 | 0.62 | 2.3 | 179 | 140 | pS:pVME:oFT | 92 |
| $2.34 \cdot 10^{-7}$ | 0.165 | 0.63 | 4.6 | 422 | 140 | pS:pVME:oFT | 92 |
| $1.64 \cdot 10^{-7}$ | 0.194 | 0.62 | 5.5 | 1050 | 140 | pS:pVME:oFT | 92 |
| $6.32 \cdot 10^{-7}$ | 0.135 | 0.58 | 4.5 | 65 | 630 | pS:pVME:oFT | 92 |
| $3.99 \cdot 10^{-7}$ | 0.227 | 0.57 | 4.1 | 179 | 630 | pS:pVME:oFT | 92 |
| $2.60 \cdot 10^{-7}$ | 0.29 | 0.58 | 8.2 | 422 | 630 | pS:pVME:oFT | 92 |
| $1.80 \cdot 10^{-7}$ | 0.34 | 0.58 | 12.0 | 1050 | 630 | pS:pVME:oFT | 92 |

^aVarious matrix molecular weights with $M \gg P$.

TABLE III: Concentration and molecular weight dependences of D_s and D_p for molecular weight P probes in solutions of molecular weight M matrix polymers (for D_s , one has $P = M$) at concentration c . The fits are to stretched exponentials $D_o P^{-a} \exp(-\alpha c^\nu P^\gamma M^\delta)$, with the percent root-mean-square fractional fit error %R, the material, and the reference. Molecular weights are in kDa; concentrations except as noted are in g/L. Square brackets “[\dots]” denote parameters that were fixed rather than floated. Abbreviations as in other Tables.

| D_o | a | α | ν | γ | δ | %R | P | M | c | System | Refs. |
|-----------------------|--------|----------------------|-------|----------|----------|-----|---------|------|-----|----------------------------------|-------|
| 6.27×10^{-5} | [0.5] | $5.96 \cdot 10^{-5}$ | 0.93 | 0.61 | [0] | 9 | b | f | (2) | PEO:H ₂ O | 42 |
| 7.99×10^{-5} | 0.50 | $7.38 \cdot 10^{-4}$ | 0.58 | 0.46 | [0] | 17 | (2) | f | b | pS:CCl ₄ | 44 |
| 3.41×10^{-4} | 0.55 | $2.10 \cdot 10^{-3}$ | 0.64 | 0.36 | [0] | 7 | b | f | b | pS:C ₆ D ₆ | 44 |
| 2.94×10^{-4} | 0.50 | $1.53 \cdot 10^{-2}$ | 0.52 | 0.25 | [0] | 24 | b | f | b | pS:cp | 46 |
| 7.46×10^{-4} | 0.501 | $6.17 \cdot 10^{-3}$ | 0.48 | 0.33 | [0] | | b | f | b | pDMS:tol | 52 |
| 1.16×10^{-4} | [0.5] | $7.55 \cdot 10^{-7}$ | 0.95 | 0.86 | [0] | 37 | b | f | b | pS:C ₆ H ₆ | 56 |
| 1.67×10^{-4} | [0.5] | $5.08 \cdot 10^{-4}$ | 0.75 | 0.48 | [0] | 17 | b | f | b | pB:CCl ₄ | 63 |
| 1.87×10^{-4} | [0.5] | $1.93 \cdot 10^{-3}$ | 0.91 | 0.24 | [0] | 51 | b | f | b | pS:THF | 65 |
| 9.68×10^{-4} | 0.65 | $7.37 \cdot 10^{-4}$ | 0.68 | 0.42 | [0] | 5.7 | 193-800 | f | b | pI:CCl ₄ | 66 |
| 0.891 | [0] | $5.86 \cdot 10^{-4}$ | 0.43 | 0.43 | [0] | 24 | 8000 | b | b | pS:pMMA:tol | 67 |
| 1.025 | [0] | $1.53 \cdot 10^{-3}$ | 0.95 | -0.01 | 0.236 | 4.8 | b | b | b | PEO:dex:H ₂ O | 68 |
| $7.46 \cdot 10^{-6}$ | 0.36 | $2.84 \cdot 10^{-4}$ | 1.15 | 0.26 | [0] | 34 | b | 60 | b | pS:pVME:oFT | 73 |
| $8.91 \cdot 10^{-6}$ | 0.34 | $6.80 \cdot 10^{-4}$ | 1.03 | 0.25 | [0] | 24 | e | 60 | b | pS:pVME:oFT | 73 |
| $3.34 \cdot 10^{-4}$ | 0.57 | $1.82 \cdot 10^{-5}$ | 0.99 | 0.139 | 0.287 | 6.4 | b | b | b | pS:pMMA:tol | 74 |
| $1.86 \cdot 10^{-4}$ | 0.52 | $4.45 \cdot 10^{-5}$ | 0.69 | 0.30 | 0.33 | 17 | b | b | e | pS:pS:tol | 75 |
| $8.5 \cdot 10^{-4}$ | 0.61 | $2.99 \cdot 10^{-2}$ | 0.61 | 0.19 | [0] | 12 | b | 1300 | b | $f = 2$ pS:pVME:oFT | 77 |
| $3.0 \cdot 10^{-4}$ | 0.54 | $1.07 \cdot 10^{-3}$ | 0.66 | 0.42 | [0] | 6.6 | b | 1300 | b | $f = 3$ pS:pVME:oFT | 77 |
| $1.84 \cdot 10^{-4}$ | 0.50 | $1.77 \cdot 10^{-2}$ | 0.68 | 0.16 | [0] | 12 | b | 140 | b | $f = 12$ pS:pVME:oFT | 78 |
| $2.20 \cdot 10^{-4}$ | 0.52 | $5.09 \cdot 10^{-4}$ | 0.61 | 0.16 | 0.32 | 32 | b | b | b | $f = 3$ pS:pVME:oFT | 79 |
| $2.93 \cdot 10^{-4}$ | 0.53 | $2.22 \cdot 10^{-3}$ | 0.66 | 0.15 | 0.19 | 15 | b | b | b | $f = 12$ pS:pVME:oFT | 79 |
| $6.51 \cdot 10^{-4}$ | 0.67 | $9.49 \cdot 10^{-3}$ | 0.86 | 0.115 | [0] | | b | 132 | b | pS:pVME:oFT | 71,80 |
| $6.67 \cdot 10^{-5}$ | [0.5] | $4.5 \cdot 10^{-3}$ | 0.68 | [0.3] | 0.024 | 20 | 342 | a | a | pMMA:pS:thiop | 82 |
| $2.79 \cdot 10^{-5}$ | [0.52] | 0.95 | [0] | [0.16] | 0.028 | | b | b | b | pS:pS:DBP | 83 |
| $7.64 \cdot 10^{-6}$ | 0.56 | $7.61 \cdot 10^{-4}$ | a | 0.30 | 0.15 | 13 | b | b | 130 | pS:pS:DBP | 84 |
| $7.89 \cdot 10^{-6}$ | 0.63 | $1.35 \cdot 10^{-3}$ | a | 0.28 | 0.11 | 12 | b | b | 180 | pS:pS:DBP | 84 |
| $8.41 \cdot 10^{-6}$ | 0.64 | $2.31 \cdot 10^{-4}$ | 0.74 | 0.26 | 0.29 | 31 | b | b | b | pS:pS:DBP | 84 |
| $1.65 \cdot 10^{-4}$ | 0.52 | $1.56 \cdot 10^{-6}$ | 0.79 | 0.285 | 0.501 | 23 | a | a | b | pS:pMMA:tol | 85 |
| $3.98 \cdot 10^{-4}$ | 0.68 | $1.00 \cdot 10^{-3}$ | [1.0] | 0.26 | [0] | 7.9 | c | a | b | pS:pS:CCl ₄ | 87 |
| $1.31 \cdot 10^{-4}$ | 0.52 | $7.56 \cdot 10^{-4}$ | [1.0] | 0.30 | [0] | 5.1 | d | a | b | pS:pS:CCl ₄ | 87 |
| $2.01 \cdot 10^{-4}$ | 0.51 | $1.03 \cdot 10^{-2}$ | 0.64 | 0.26 | [0] | 14 | c | 1300 | b | pS:pVME:oFT | 91 |
| $4.99 \cdot 10^{-3}$ | 0.39 | $8.33 \cdot 10^{-4}$ | 0.54 | 0.25 | 0.22 | 25 | c | b | b | pS:pVME:oFT | 92 |

^aVarious, with $M/P \geq 10$

^bVarious, see text.

^cAll four probes, see text.

^dExcluding styrene monomer, see text.

^eNot all data points, see text.

^f $P = M$, self diffusion.

TABLE IV: Molecular weight dependence of the self and probe diffusion coefficients D_s and D_p for molecular weight P probes in solutions of matrix polymers at a fixed concentration c . The fits are to stretched exponentials $D_o \exp(-\alpha M^\gamma)$ in matrix molecular weight M . The Table gives the best-fit parameters, the percent root-mean-square fractional fit error %RMS, the system, and the reference. Square brackets “[\dots]” denote parameters that were fixed rather than floated. Abbreviations as per previous Tables, and DBP–dibutylphthalate.

| D_o | α | γ | %RMS | P (kDa) | c (g/L) | System | Refs. |
|----------------------|----------------------|----------|------|-----------|--------------|-----------|-------|
| $8.54 \cdot 10^{-8}$ | 0.64 | 0.55 | 17 | 1800 | ^a | pS:pS:tol | 75 |
| $2492P^{-0.5}$ | $1.37 \cdot 10^{-2}$ | 0.47 | 4.0 | P | 130 | pS:pS:dbp | 57 |
| $1771P^{-0.5}$ | $1.07 \cdot 10^{-2}$ | [0.5] | 6.9 | P | 180 | pS:pS:dbp | 57 |

^aVarious, see text.

TABLE V: Concentration and molecular weight dependences of the probe radius of gyration R_g for molecular weight P probes in solutions of molecular weight M matrix polymers as functions of matrix concentration c . The fits are to stretched exponentials $R_{g0} \exp(-\alpha c^\nu)$, with the percent root-mean-square fractional fit error %RMS, the materials, and the reference. Materials include EB–ethyl benzoate, PMMA–polymethylmethacrylate, pS–polystyrene.

| R_{g0} (Å) | α | ν | %RMS | P (kDa) | M (kDa) | System | Refs. |
|--------------|----------------------|-------|------|-----------|-----------|--------------|-------|
| 390 | $4.11 \cdot 10^{-3}$ | 0.99 | 2.2 | 930 | 1300 | pS: pMMA: EB | 74 |
| 397 | $8.06 \cdot 10^{-3}$ | 0.77 | 1.1 | 930 | 70 | pS: pMMA: EB | 74 |
| [395] | $4.49 \cdot 10^{-3}$ | 0.64 | 1.9 | 930 | 7 | pS: pMMA: EB | 74 |